

**IMPROVEMENT OF THE VEHICLE WARM-UP  
PERFORMANCE THROUGH LOW THERMAL INERTIA  
EXHAUST HEAT RECOVERY UNIT**

**IR AZMI BIN OSMAN**

**FACULTY OF ENGINEERING  
UNIVERSITY OF MALAYA  
KUALA LUMPUR**

**2021**

**IMPROVEMENT OF THE VEHICLE WARM-UP  
PERFORMANCE THROUGH LOW THERMAL  
INERTIA EXHAUST HEAT RECOVERY UNIT**

**IR AZMI BIN OSMAN**

**DISSERTATION SUBMITTED IN FULFILMENT OF  
THE REQUIREMENTS FOR THE DEGREE OF MASTER  
OF ENGINEERING SCIENCE**

**FACULTY OF ENGINEERING  
UNIVERSITY OF MALAYA  
KUALA LUMPUR**

**2021**

**UNIVERSITY OF MALAYA**  
**ORIGINAL LITERARY WORK DECLARATION**

Name of Candidate: Ir Azmi Bin Osman

Matric No: KGA180010

Name of Degree: Master of Engineering Science

Title of Dissertation: Improvement of the vehicle warm-up performance through low thermal inertia exhaust heat recovery unit

Field of Study: Heat transfer (Heat recovery)

I do solemnly and sincerely declare that:

- (1) I am the sole author/writer of this Work;
- (2) This Work is original;
- (3) Any use of any work in which copyright exists was done by way of fair dealing and for permitted purposes and any excerpt or extract from, or reference to or reproduction of any copyright work has been disclosed expressly and sufficiently and the title of the Work and its authorship have been acknowledged in this Work;
- (4) I do not have any actual knowledge, nor do I ought reasonably to know that the making of this work constitutes an infringement of any copyright work;
- (5) I hereby assign all and every right in the copyright to this Work to the University of Malaya ("UM"), who henceforth shall be owner of the copyright in this Work and that any reproduction or use in any form or by any means whatsoever is prohibited without the written consent of UM having been first had and obtained;
- (6) I am fully aware that if in the course of making this work, I have infringed any copyright whether intentionally or otherwise, I may be subject to legal action or any other action as may be determined by UM.

Candidate's Signature

Date: 21/12/2021

Subscribed and solemnly de before,

Witness's Signature Date:

Name: **Dr. Nurin Wahidah Mohd Zulkifli**  
Pensyarah Kanan  
Jabatan Kejuruteraan Mekanik  
Fakulti Kejuruteraan  
Universiti Malaya,  
Kuala Lumpur.

Designation:

# **IMPROVEMENT OF THE VEHICLE WARM-UP PERFORMANCE THROUGH LOW THERMAL INERTIA EXHAUST HEAT RECOVERY UNIT**

## **ABSTRACT**

Internal combustion engines in general waste plenty of heat to the exhaust gas and coolant for every milligram of fuel burned. Considering that daily driving consists of frequent cold start, idling and part load driving within short driving distances, the potentials to recover heat from high enthalpy exhaust gas are limited to hard acceleration, hill climbing and highway driving. These constraints limit many heat recovery technologies that rely on conversion of thermal energy into electricity or kinetic energy. In recovering precious energy from the low enthalpy exhaust gas early and sustainably, a low thermal inertia exhaust heat recovery unit (EHRU) is proposed to be integrated to the simplified split cooling circuit used in the earlier studies to expedite the powertrain warm-up. This lightweight, compact and simple EHRU concept made of machined steel plate is targeted for naturally aspirated engines that are still being widely used in motorcycles, stationary engines and small car segments worldwide. Large temperature difference between the coolant and exhaust gas was possible using cooler coolant feed from the bottom of the cylinder block's water jacket rear end. To prove its effectiveness in speeding up the recovered heat availability for reuse, a 1.3l passenger car equipped with strategically placed multiple thermocouples and flow meters was tested using idle and NEDC tests. The EHRU was later modeled using a simplified energy system (SES) to overcome the experimental limitations. From the experiments and classical analysis, the recovered thermal energy was available in just 23-25 seconds instead of 50 seconds after cold start. The improvements over the variant with no EHRU revealed during the idle and NEDC tests are in the range of 0.9-13.9% and 1.6-25.1% respectively. The study also provided a new direction in the design of EHRU and its integration into an engine.

**Keywords:** Internal combustion engine; thermal management system; exhaust heat recovery; low-grade heat; low thermal inertia; accelerated engine warm up

Universiti Malaya

**PENAMBAHBAIKAN PRESTASI PEMANASAN KENDERAAN MELALUI  
UNIT PENEBUS HABA EKZOS YANG MEMPUNYAI INERTIA HABA YANG  
RENDAH**

**ABSTRAK**

Enjin pembakaran dalam secara umumnya membazirkan banyak haba melalui gas ekzos dan jugak bendalir penyejuk untuk setiap milligram bahan api yang dibakar. Memandangkan pemanduan harian terdiri daripada permulaan sejuk yang kerap, melahu dan pemanduan sebahagian beban pada jarak panduan yang singkat, potensi untuk mendapatkan semula haba dari gas ekzos berentalpi tinggi adalah terhad kepada pecutan, pendakian bukit dan pemanduan di lebuhraya. Kekangan ini menghadkan banyak penggunaan teknologi pemulihan haba yang bergantung kepada penukaran haba kepada tenaga elektrik atau kinetik. Bagi pemulihan tenaga dari gas ekzos berentalpi rendah dengan pantas dan lestari, unit pemulihan haba ekzos (EHRU) berinersia rendah dicadangkan untuk disepadukan dengan litar penyejukan berpecah dua yang digunakan dalam kajian sebelum ini untuk mempercepatkan pemanasan powertrain. Konsep EHRU yang ringan, padat dan murah yang dimesin daripada plat keluli ini disasarkan untuk enjin bukan turbo yang masih digunakan secara meluas pada motosikal, enjin pegun dan kereta segmen kecil di seluruh dunia. Perbezaan suhu tinggi di antara gas ekzos dan cecair penyejuk yang diperolehi dari bahagian belakang jaket air blok silinder menambahkan keberkesanan pemindahan haba. Untuk membuktikan keberkesanannya dalam mempercepatkan ketersediaan haba dari pemulihan haba ekzos, kereta penumpang 1.3 liter yang telah dipasang dengan pelbagai termokopel dan meter aliran diuji dengan ujian melahu dan NEDC. Kemudian, EHRU dimodelkan menggunakan sistem tenaga mudah untuk mengatasi batasan eksperimen. Daripada eksperimen dan analisa klasik, tenaga dari haba yang dipulihkan tersedia dalam masa 23-25 saat dan bukannya 50 saat selepas

permulaan sejuk. Penambahbaikan ke atas varian yang tidak mempunyai EHRU berada dalam julat 0.9-13.9% semasa ujian melahu dan julat 1.6-25.1% semasa ujian NEDC. Kajian ini telah memberikan hala tuju baru mengenai rekabentuk EHRU dan penyepaduannya ke dalam enjin.

**Katakunci:** enjin pembakaran dalam; sistem pengurusan haba; pemulihan haba ekzos; haba gred rendah; pemanasan enjin pantas

Universiti Malaya

## ACKNOWLEDGEMENTS

Alhamdulillah for the courage and determination that have enabled me to complete my research. It has never been easy for me to juggle more than 50 hours a week of working full time during the day and to continue with my research and writings in the evening and weekend.

I am indebted to my supervisor Dr Nurin Wahidah Mohd Zulkifli for her constant guidance and supports in which many of the requests were made in the evening and weekend.

I would like to thank my parents for their continuous prayers, supports and encouragements in completing my study. Not forgetting my wife and three children who have been always by my side in supporting me to complete my research and dissertation.

To all my former staffs at Advanced Engineering Department who have supported me throughout the research project, such supports were priceless and may Allah reward all of you in the day after. Special thanks to Dr Mior Azman Bin Meor Said from Universiti Teknologi PETRONAS and Dr Tengku Nordayana Akma Binti Tuan Kamaruddin from Universiti Islam Antarabangsa who have provided valuable feedbacks and comments throughout the research project. Special thanks also to Encik Hazrin Fadzail Bin Haroon, the Director of Group Engineering at Proton for his approval to conduct such research.

## TABLE OF CONTENTS

<b>ABSTRACT.....</b>	<b>iii</b>
<b>ABSTRAK.....</b>	<b>v</b>
<b>ACKNOWLEDGEMENTS.....</b>	<b>vii</b>
<b>TABLE OF CONTENTS.....</b>	<b>viii</b>
<b>LIST OF FIGURES.....</b>	<b>x</b>
<b>LIST OF TABLES.....</b>	<b>xiv</b>
<b>LIST OF SYMBOLS AND ABBREVIATIONS.....</b>	<b>xv</b>
<b>CHAPTER 1: INTRODUCTION.....</b>	<b>19</b>
<b>1.1 Overview.....</b>	<b>19</b>
<b>1.2 Background.....</b>	<b>21</b>
<b>1.3 Problem statement.....</b>	<b>25</b>
<b>1.4 Objectives of the research.....</b>	<b>25</b>
<b>1.5 Scope of research.....</b>	<b>26</b>
<b>1.6 Outline of the dissertation.....</b>	<b>27</b>
<b>CHAPTER 2: LITERATURE REVIEW.....</b>	<b>28</b>
<b>2.1 Introduction.....</b>	<b>28</b>
<b>2.2 Heat conservation and distribution within the cooling circuit.....</b>	<b>30</b>
<b>2.3 Heat recovery and reuse of the exhaust heat.....</b>	<b>42</b>
<b>2.4 Summary.....</b>	<b>49</b>
<b>2.5 Research gaps.....</b>	<b>50</b>
<b>CHAPTER 3: METHODOLOGY.....</b>	<b>52</b>
<b>3.1 Introduction.....</b>	<b>52</b>

3.2	Comparison between the standard and the proposed cooling circuit.....	53
3.3	Modifications of the standard parts.....	58
3.4	Instrumentation of the test vehicle.....	65
3.5	Vehicle tests .....	68
3.6	Theories .....	72
3.6.1	Heat transfer classical calculations .....	72
3.6.2	Simplified energy system (SES) .....	75
<b>CHAPTER 4: RESULTS AND DISCUSSION.....</b>		<b>78</b>
4.1	Introduction.....	78
4.2	Results.....	78
4.2.1	Idle tests.....	78
4.2.2	NEDC tests .....	84
4.2.3	Summary of the warm-up performances .....	95
4.3	Discussions.....	97
4.3.1	Connecting the dots .....	97
4.3.2	Research gaps identified in the study .....	101
4.3.3	Key findings, novelties and new knowledge from the study.....	104
<b>CHAPTER 5: CONCLUSIONS AND RECOMMENDATIONS .....</b>		<b>110</b>
5.1	Conclusions.....	110
5.2	Recommendations for future work.....	111
<b>REFERENCES.....</b>		<b>113</b>
<b>LIST OF PUBLICATIONS AND PAPERS PRESENTED .....</b>		<b>118</b>
<b>APPENDIX A .....</b>		<b>119</b>

## LIST OF FIGURES

Figure 1.1: Regulated carbon dioxide discharge from passenger cars in major markets (www.theicct.org/info-tools/global-passenger-vehicle-standards, 2019).....	20
Figure 2.1: The side view (top) and isometric view (bottom) of the earliest simplified split cooling proposed by the authors (Osman, Sabrudin, Hussin & Bakri, 2003).....	35
Figure 2.2: Cooling circuit with the turbocharger as the heat recovery unit (Osman, Yusof & Rafi, 2016) .....	37
Figure 2.3: Optimized cooling circuit for reduced thermal inertia (Osman, Razali & Nurdin, 2018).....	38
Figure 2.4: Replot of the Demo1's coolant temperature exiting the cylinder head and block during NEDC test (Osman, Razali & Nurdin, 2018).....	40
Figure 2.5: Demo1's cylinder block with coolant outlet at the bottom of the water jacket's rear end .....	41
Figure 2.6: EHRU from Faurecia (Chiew, Clegg, Willats, Delplanque & Barrieu, 2011) .....	44
Figure 2.7: Heat exchanger construction to recover the exhaust gas heat (Chiew, Clegg, Willats, Delplanque & Barrieu, 2011).....	46
Figure 2.8: Vacuum actuated flap valve (Chiew, Clegg, Willats, Delplanque & Barrieu, 2011) .....	47
Figure 3.1: Flowchart of the research methodology .....	53
Figure 3.2: The standard cooling circuit of Proton Iriz .....	56
Figure 3.3: a) The proposed cooling circuit and the locations of the EHRU, thermocouples and flow meters. b) Cross section of the EHRU and locations of thermocouples adjacent to EHRU .....	57
Figure 3.4: The coolant transfer holes which were enlarged in yellow circles and the ones added to the gasket are shown in red ovals.....	59

Figure 3.5: Left photo: The two apertures at the cylinder head mating face are being filled with Devcon putty generally used for metal repair at the foundry. Right photo: The putty (red rectangular) are close to solidification and the aperture on the left is ready to be drilled to form an 8 mm diameter coolant transfer hole .....	60
Figure 3.6: Left photo: Machined coolant outlet with coolant temperature sensor mounted to it. Right photo: Machined coolant outlet after being pushed into the core plug hole at the rear end of the cylinder head.....	61
Figure 3.7: T-junction made from modified HKS coolant hose connector .....	61
Figure 3.8: Left photo: Original thermostat pipe. Centre photo: Original thermostat inside the thermostat pipe. Right photo: WTI thermostat housing with the thermostat integrated within the plastic housing.....	62
Figure 3.9: With reference to the original thermostat pipe in Figure 3.8, the pipe near the bypass outlet was lengthened to allow ample clearance to the coolant outlet at the back of the cylinder head .....	63
Figure 3.10: Left photo: The original CVT oil radiator. Right photo: Oil-to-coolant heat exchanger which replaced the original CVT oil radiator .....	63
Figure 3.11: Diagram on the left shows the bottom view of the EHRU with the cooling channel shown by the hidden lines. Diagram on the right shows the isometric view of the EHRU. The blue arrows show the direction of the coolant flow and the red arrow shows the direction of the exhaust gas .....	64
Figure 3.12: The location of the EHRU which is sandwiched in between the maniverter and downpipe .....	65
Figure 3.13: Graphtec connected to various thermocouples and flow meters .....	66
Figure 3.14: The position of the tip of the thermocouples around the EHRU .....	67
Figure 3.15: The EHRU attached to the vehicle subframe instead of mounted to the exhaust flanges. This arrangement enabled the tests to proceed without any exhaust heat recovery .....	69
Figure 3.16: Complete NEDC test cycle consisting of UDC and EUDC phases.....	70

Figure 3.17: SES to represent the EHRU and its heat sources .....	76
Figure 4.1: Comparison of temperature increase of coolant and metals during idle test for cooling circuit with and without the EHRU .....	79
Figure 4.2: Comparison of temperature increase at the CVT oil cooler during idle test for cooling circuit with and without the EHRU .....	80
Figure 4.3: Comparison of temperature increase for CVT oil and engine oil during idle test.....	81
Figure 4.4: Various heat transfers within the cooling circuit during the idle test .....	82
Figure 4.5: Comparison of various accumulated thermal energy transferred within the SES during idle test .....	83
Figure 4.6: Interactions between coolant and metals during the early part of NEDC test .....	84
Figure 4.7: Chain of events that lead to the start of exhaust heat recovery and reuse....	85
Figure 4.8: Comparison of coolant temperatures with and without the EHRU .....	86
Figure 4.9: Comparison of coolant temperatures with and without the EHRU .....	87
Figure 4.10: Comparison of temperature increase at the CVT oil cooler during NEDC test for cooling circuit with and without the EHRU .....	88
Figure 4.11: Comparison of temperature increase for CVT oil and engine oil during NEDC test.....	88
Figure 4.12: Comparison of temperature profiles for the exhaust gas during NEDC test .....	90
Figure 4.13: Comparison of temperature increase for the exhaust system and EHRU during NEDC test.....	91
Figure 4.14: Comparison of various heat transfers during NEDC test .....	93

Figure 4.15: Comparison between exhaust heat losses and recovered exhaust heat from EHRU during NEDC test.....	94
Figure 4.16: Comparison of various accumulated thermal energy transferred within the during NEDC test.....	95
Figure 4.17: Efficiency of the EHRU during NEDC.....	102

Universiti Malaya

## LIST OF TABLES

Table 3.1: Specifications of the test vehicle .....	54
Table 3.2: Technical data sheet of PETRONAS Mach 5 Plus 10W30 mineral engine oil .....	54
Table 3.3: Technical data sheet of PETRONAS Tutela Multi CVT 700 oil .....	55
Table 3.4: Comparison between NEDC and WLTP.....	71
Table 4.1: Comparison of the warm-up performances involving various fluids during idle and NEDC test .....	96

Universiti Malaya

## LIST OF SYMBOLS AND ABBREVIATIONS

NEDC	:	New European Driving Cycle
EUDC	:	Extra Urban Driving Cycle
UDC	:	Urban Driving Cycle
CVT	:	Continuously Variable Transmission
EHRU	:	Exhaust Heat Recovery Unit
WLTP	:	Worldwide Harmonised Light Vehicle Test Procedure
SES	:	Simplified Energy System
$q_{EHRU}$	:	heat quantity to the heat exchanger plate, W
$q_{conv}$	:	convective heat quantity from exhaust gas to the EHRU, W
$q_{coolant}$	:	convective heat quantity from the EHRU to coolant, W
$q_{cond1}$	:	conductive heat quantity from the upper flange to the EHRU, W
$q_{cond2}$	:	conductive heat quantity from the lower flange to the EHRU, W
$q_{ext\ cond1}$	:	conductive heat quantity from the maniverter to the system, W
$q_{ext\ cond2}$	:	conductive heat quantity from the lower pipe to the system, W
$q_{surroundings1}$	:	combined heat losses from the EHRU to the surroundings, W
$q_{surroundings2}$	:	combined heat losses from the system to the surroundings, W

$q_{block}$	:	convective heat quantity from the cylinder block to coolant, W
$q_{head}$	:	convective heat quantity from the cylinder head to coolant, W
$q_{CVT\ cooler}$	:	convective heat quantity from the coolant to CVT oil cooler, W
$q_{system}$	:	heat quantity absorbed by the SES, W
$q_{exh}$	:	heat losses from the exhaust gas to the SES, W
$Q_{EHRU}$	:	total thermal energy absorbed by the EHRU, kJ
$Q_{CVT}$	:	total thermal energy absorbed by the CVT oil cooler, kJ
$Q_{exh\ losses}$	:	total thermal energy losses from the exhaust gas, kJ
$h$	:	convection heat transfer coefficient, W/m <sup>2</sup>
$\dot{m}_{coolant}$	:	mass flow rate of coolant entering the EHRU, kg/s
$\dot{m}_{block}$	:	mass flow rate of coolant exiting the cylinder block, kg/s
$\dot{m}_{head}$	:	mass flow rate of coolant exiting the cylinder head, kg/s
$\dot{m}_{CVT\ cooler}$	:	mass flow rate of coolant exiting the CVT oil cooler, kg/s
$\dot{m}_{exh}$	:	mass flow rate of exhaust gas into the simplified system, kg/s
$m_{EHRU}$	:	mass of the heat exchanger, kg
$c_{coolant}$	:	specific heat capacity of coolant, J/(kg*K)
$c_{exh}$	:	specific heat capacity of exhaust gas, J/(kg*K)

$c$	:	specific heat capacity of the EHRU or liquid, J/(kg*K)
$k$	:	thermal conductivity, W/(m*K)
$A_{flange}$	:	surface area of the flange (upper and lower), mm <sup>2</sup>
$A_{EHRU}$	:	EHRU's surface area in contact with the exhaust gas, mm <sup>2</sup>
$L_{upper}$	:	thickness of the upper flange, mm
$L_{bottom}$	:	thickness of the lower flange, mm
$T_{upper}$	:	metal temperature of the upper flange, K
$T_{ave}$	:	average metal temperature of the EHRU, K
$T_{bottom}$	:	metal temperature of the lower flange, K
$T_{end}$	:	average metal or liquid temperature at certain point of time, K
$T_{start}$	:	average metal or liquid temperature at the beginning, K
$T_{exh in}$	:	temperature of exhaust gas at the inlet of the EHRU, K
$T_{EHRU}$	:	temperature of EHRU's surface in contact with exhaust gas, K
$T_1$	:	coolant temperature at the cylinder head outlet, K
$T_2$	:	coolant temperature at the EHRU inlet or cylinder block outlet, K
$T_3$	:	coolant temperature at the CVT oil cooler inlet, K
$T_4$	:	coolant temperature at the CVT oil cooler outlet, K

$T_5$	:	coolant temperature at the EHRU outlet, K
$T_{12}$	:	coolant temperature at the water pump inlet, K
$T_{14}$	:	metal temperature at the uncooled side of EHRU, K
$T_{18}$	:	metal temperature at the cooled side of EHRU, K
$T_{13}$	:	metal temperature at the upstream flange, K
$T_{15}$	:	metal temperature at the downstream flange, K
$T_{16}$	:	exhaust gas temperature at the SES inlet, K
$T_{17}$	:	exhaust gas temperature at the SES outlet, K
$t$	:	time from the beginning of the cold start, s

## CHAPTER 1: INTRODUCTION

### 1.1 Overview

The carbon dioxide concentration in atmosphere has increased from 330 ppm in December 1975 to 413 ppm in January 2020 (Lindsey, 2020). Such increase has been widely accepted to cause global warming. This eventually melts glaciers and icebergs to increase the sea level around the world. In particular, populated coastal areas of pacific islands like Fiji Island and countries like Bangladesh and India have high risk of being partially flooded by seawater decades from now. Understanding that the worldwide trades increase every year since the industrial revolutions, steady increases in electricity generations and mobility are unavoidable. In particular, the electricity generations and transportation sectors in the United States alone generated about 1.6 and 1.8 billion metric tonnes of carbon dioxide respectively in 2019 (Kusnetz, 2020).

In mitigating the negative impacts of the increase of carbon dioxide concentration, developed countries have taken the lead in regulating the carbon dioxide discharge from the transportations and electricity generations sectors. Considering that the global warming also affects the developing countries, large countries like India and China have also joined the bandwagon in limiting the carbon dioxide discharge.

In the context of limiting the carbon dioxide discharge, the transportation sector around the world has been required to minimize the carbon dioxide discharge to the environment. As shown in **Figure 1.1**, passenger cars in major markets are required to continuously reduce the carbon dioxide to as low as 59 g/km. Understanding that the carbon dioxide discharge is directly related to the hydrocarbon fuels oxidised during engine operations, reducing the carbon dioxide discharge necessitates the internal combustion engines powering the motor vehicles to be more efficient thus requiring lesser gasoline or diesel fuel for every kilometre travelled.

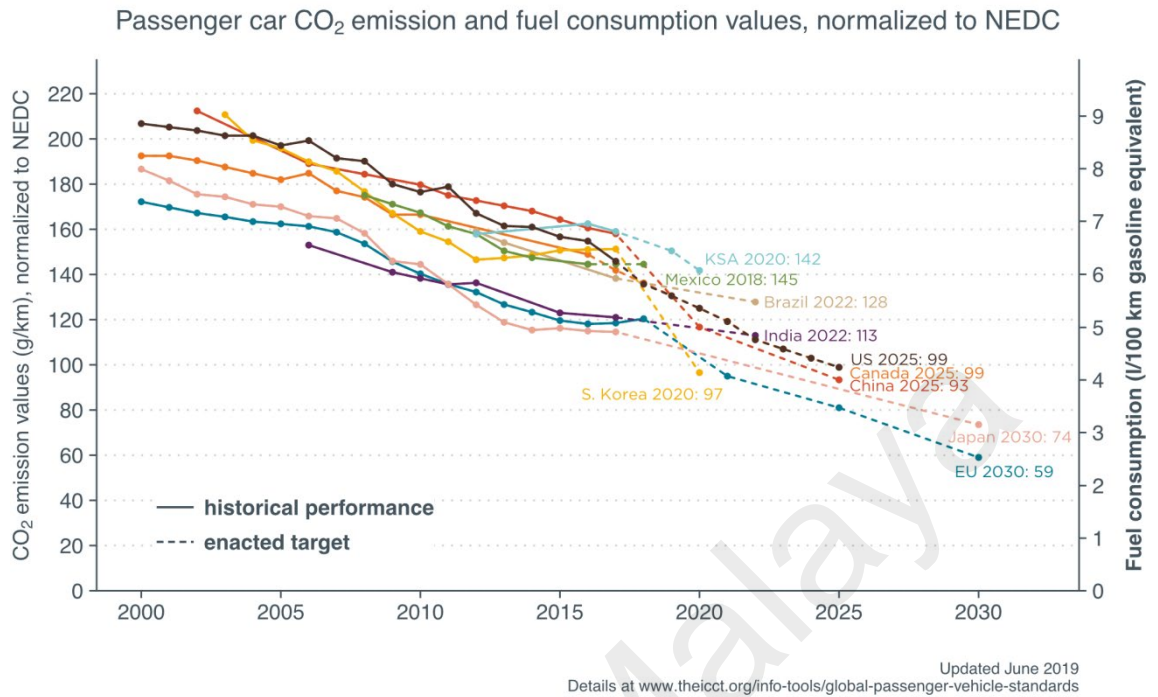


**Figure 1.1: Regulated carbon dioxide discharge from passenger cars in major markets (www.theicct.org/info-tools/global-passenger-vehicle-standards, 2019).**

In ensuring the biggest impact to the reduction of carbon dioxide worldwide, the measures or technologies to improve the fuel economy must be suitable to be applied to as many motor vehicles around the world as possible, especially in the developing countries. This necessitates the technologies to be simple, cost effective, practical, lightweight and compact.

Once these traits are achieved, quick applications to small segments passenger cars and budget motorcycles which have been dominating the total sales worldwide are likely to be easier. In 2018, the global sales volumes of passenger cars and motorcycles in general were 86 million units (Demandt, 2019) and 61.9 million units (Motorcycles data, 2019) respectively. In this context, mass applications of practical technologies to improve the fuel economy will surely make a huge impact in reducing the carbon dioxide.

## **1.2 Background**

Ever since the introduction of heat engines hundreds years ago, improvement in thermal efficiency is mostly dependent on how much heat can be prevented from being wasted through the exhaust tailpipe and coolant radiator (Osman, 2009). In view of the constantly improving thermal efficiency of internal combustion engines, such efficiency has gone up above the 50% barrier for both the spark ignition and compression ignition engines (Boretti, 2019a, Boretti, 2019b).

The high thermal efficiency generally reduces the average exhaust gas temperature, thus making it more challenging for the exhaust heat to be recovered. Considering that the conversion of thermal energy into electrical or kinetic energy is highly dependent on the enthalpy of the exhaust gas, it can be really challenging to effectively recover and reuse the thermal energy from low temperature exhaust gas. Nevertheless, the potentials for the exhaust heat to be recovered from the low enthalpy exhaust gas during cold start, idle and part load operations are still high. Even if the low-grade heat is not convertible to other form of energies, it contains precious thermal energy that shall not be wasted (Osman, 2009).

There have been plenty of research in exhaust heat recovery unit (EHRU) for conversion into electricity and kinetic energy (Neumeister, Heckenberger & Brehm, 2008; Talom & Beyene, 2009; Saidur et al., 2019; Lan et al., 2019). For the exhaust heat conversion into electricity, the efficiency of the thermoelectric generator is still low at 2-5% (Orr et al., 2016; Jouhara et al., 2018) and the complete system is still big, complicated, costly and has high exhaust backpressure. As for the conversion of such heat to kinetic energy, there have been plenty of research in Rankine cycle involving various fluids (Quolin et al., 2011). Similar to the thermoelectric generator, the system has low conversion efficiency of 3-8% during general operating conditions (Wang et al., 2013) and it shares many of the limitations of the thermoelectric generators explained earlier. In addition, there are challenges in extracting the kinetic energy because the work output may not be in sync with the primary engine throughout the engine speed and load.

From the thermodynamics standpoint, the limited availability of high enthalpy heat and exergy makes it difficult to justify the costs and complexities of using the EHRU involving either the thermoelectric generator or Rankine cycle. Considering that majority of real-world driving involving frequent cold start, idling and part load driving within short driving distances, both coolant and exhaust gas are hardly hot enough for energy conversion to take place. In this context, an excellent review paper has included many studies related to the various driving trends in major markets and how quick powertrain warm-up and high exhaust temperature availability have been lacking (Roberts, Brooks & Shipway, 2014). On the other hand, even if the vehicles fitted with the EHRU benefit from having high enthalpy exhaust gas during hard driving, the weight penalty during frequent part load driving when the exhaust temperature is low can negatively affect the fuel consumption.

In overcoming the limited exhaust gas exergy and enthalpy availability, many researchers have stepped up the research in recovering the exhaust heat to expedite the warm-up of powertrain's fluids and metals (Chiew et al., 2011; Will & Boretti, 2011; Di Battista & Cipollone, 2018; Vittorini, Battista & Cipollone, 2018; Cipollone, Di Battista & Maurello, 2015; Di Battista, Cipollone & Fatigati, 2018; Osman, Yusof & Rafi, 2016; Osman, Razali & Nurdin, 2018). These fluids consist of the engine coolant, engine oil and transmission oil. The combination of the fluids and metals present large thermal inertia and requires as much as 60-65% of engine's thermal energy to overcome the thermal inertia in the early phase of cold-start (Boam, 1986; Jarrier, Champoussin & Yu, 2000). The sooner the fluids and metals get into the optimum temperatures and stay within the recommended ranges, the lesser the intake port wall wetting, combustion heat quenching (Roberts, Brooks & Shipway, 2014; Osman, Yusof & Rafi, 2016; Osman, Razali & Nurdin, 2018) and parasitic losses (Will & Boretti, 2011; Di Battista & Cipollone, 2018; Vittorini, Battista & Cipollone, 2018; Cipollone, Di Battista & Maurello, 2015; Di Battista, Cipollone & Fatigati, 2018; Jehlik et al., 2017; Iliev & Lohse-Busch, 2018) will negatively impact the fuel consumption throughout the vehicle operations.

Without doubt, the research in this area has much greater potentials for quick applications to mass production. In particular, the EHRU from Faurecia is already in production and they have published an interesting paper about its technology (Chiew et al., 2011). Faurecia's EHRU relies on arrays of heat transfer fins to maximize the surface area for the coolant to absorb heat from the exhaust gas. These large fins require a large housing and necessitating it to be placed far away from the engine. Faurecia's EHRU weighs 5.4 kg and the big housing requires significantly large volume of coolant to continuously fill the void. The large thermal inertia and the EHRU's placement a distance away from the exhaust port negatively affect the time for the heat to be recovered and

eventually reused because the cold metals and coolant will also take time to be warmed up. In improving the warm-up performances, it is necessary for the thermal inertia to be reduced (Torregrosa et al., 2008; Agarwal, Chiara & Canova, 2012) or alternatively, the heat source must be increased to overcome the high thermal inertia (Burke et al., 2012).

In separate studies, the EHRU used was not based on conventional heat exchanger (Osman, Yusof & Rafi, 2016; Osman, Razali & Nurdin, 2018). Understanding that a typical turbocharger has coolant inlet and outlet for cooling, they proposed the use of the conventional turbocharger as an EHRU. The EHRU was optimized to work with the simplified split cooling circuit in which the circuit works differently from the conventional ones in many ways and has gone through several evolutions (Osman, Yusof & Rafi, 2016; Osman, Razali & Nurdin, 2018; Osman et al., 2013; Osman, Hussin & Abidin, 2015). In the studies, the single thermostat was used to reverse the direction of the coolant flow across the EHRU thus enabling the recovered heat to either be recirculated into the engine for reuse or be discharged to the radiator to avoid overheating the engine. Although, the proposed concept managed to make available the recovered exhaust heat at  $t = 180$  s of the NEDC test, the room for improvement is still large. For example, the complete turbocharger assembly which weighs around 5.2 kg exerts high thermal inertia that would delay the recovered heat availability. In this case, making the EHRU lighter will speed up the recovered heat availability.

As stated in the earlier paragraph, there were close to 150 million cars and motorcycles globally sold in 2018. Majority of these motor vehicles have naturally aspirated engines instead of the more expensive and complicated supercharged or turbocharged engines. Considering that naturally aspirated engines are still in high demands, it is necessary for the EHRU to be simple and cost effective that it can be applied to as many naturally aspirated engines as possible.

To sum it up, research gaps exist in terms of limited availability of high enthalpy exhaust gas in daily driving, delayed availability of the recovered exhaust heat, complicated EHRUs designs and constructions, high thermal inertia of the EHRUs and practicality of the EHRUs for mass applications to non-premium engines.

### **1.3 Problem statement**

The proposed EHRU is intended for quick application to the market and this requires the design of the proposed EHRU to be simple, durable and cost effective. In addition to that, the EHRU must also be compact to enable it to be fitted into the tight packaging space of a currently in production vehicle used for this study. The EHRU must be made lightweight to ensure that the thermal inertia is low enough for quick exhaust heat recovery process.

To ensure that the proposed solution is effective, the study must also be able to answer the question on how quick and how much thermal energy can be recovered through the EHRU from a typical cold start. The study must identify any improvements in warm-up performances affecting the coolant, CVT oil and engine oil, with the additional thermal energy added to the cooling circuit.

### **1.4 Objectives of the research**

The research focuses on evaluating the effectiveness of the proposed EHRU with the simplified split cooling circuit to quickly recover the exhaust heat and to reuse it to expedite the warm-up of powertrain fluids. The objectives of the study are as the following: -

- 1) To design, fabricate and develop the EHRU.
- 2) To measure the effectiveness of the proposed EHRU over the variant with no EHRU in reducing the warm-up time of coolant, engine oil and CVT oil.
- 3) To measure the thermal energy recoverable by the EHRU during NEDC test.

## **1.5 Scope of research**

The scope of the research covers the evaluation of the warm-up performances of the powertrain's fluids consisting of coolant, engine oil and CVT oil with the proposed EHRU and cooling circuit. In addition, the research also covers the heat transfers and recoverable thermal energy within the specific time periods as defined by the idle and NEDC tests.

Although it is desirable for the fuel consumption to also be measured, such measurement was not possible because the test vehicle was derived from currently in production Proton Iriz in which the engine and transmission electronics were tediously calibrated based on the standard cooling system with no EHRU. Ideally, with so many changes from the original setups, the electronics need to be recalibrated to match all the mechanical changes introduced. The few months long electronics recalibration activities focusing on achieving the best fuel consumption and low exhaust tailpipe emissions specific to the homologation test cycle require specialist engineers with special equipment. These costly specialised supports are normally available from the electronics supplier which in this case happens to be Bosch Germany.

Nevertheless, many studies have confirmed the improvement of fuel economy in the range of 1.6 to 10.6% due to the improvements in the warm-up performances (Will & Boretti, 2011; Cipollone, Di Battista & Maurello, 2015; Jehlik et al., 2017; Iliev & Lohse-

Busch, 2018; Torregrosa et al., 2008). In view of these evidences, the study assumed that improvement in the warm-up performances involving coolant, CVT oil and engine oil is likely to improve the fuel economy accordingly.

## **1.6 Outline of the dissertation**

This dissertation consists of five chapters and organised in the following order:

Chapter 1: This chapter provides a brief overview of the research related to energy conservation, carbon dioxide and its effect to global warming. In addition, this chapter also includes the problem statement, research objectives and scope of the research.

Chapter 2: This chapter is focused on the literature review of the current trends in engine cooling system, exhaust heat recovery and the improvements in fuel economy due to the accelerated warm-up of the powertrain's fluids.

Chapter 3: This chapter covers the detailed discussion of the preparations of the test subject. This chapter also covers the test methodology to achieve the research objectives.

Chapter 4: This chapter covers the results of the experiments together with the detailed explanations of the findings.

Chapter 5: The conclusions drawn based on the key findings are presented in this chapter. Recommendations for future work are also presented in this chapter.

## CHAPTER 2: LITERATURE REVIEW

### 2.1 Introduction

In mitigating the effects of global warming, it is necessary for cars and motorcycles manufacturers around the world to reduce the carbon dioxide discharge to the environment by reducing their products' fuel consumption. In general, there are many measures available to improve the fuel economy involving improvements to vehicle architecture, weight, aerodynamics, rolling resistance, frictions, hybridisation, transmissions and engines.

In addressing the problem at the source of the problem, the emphasis is always on the internal combustion engine where the fuel is being combusted into heat. The combustion heat expands the combustion gases to push the pistons downward to do work. Once work is obtainable from the output shaft, it is equally important to ensure that the work output can be efficiently transmitted by the transmission to the wheels to propel the vehicle forward.

From the thermodynamics perspective, it is necessary for the combustion heat losses to be minimised by ensuring the coolant, engine oil and metals adjacent or in contact with the combustion flame and hot combustion gases to be at the optimum elevated temperatures. Under ideal gas law, these hot combustion gases increase the cylinder pressure to push the piston downward during the expansion stroke. Similarly, it is also important for the wall wetting of the fuel inside the intake ports to be minimised by expediting the coolant temperature increase to 40-60°C during cold start.

From the friction reductions perspective, both engine and transmission have moving components that are rubbing against one and another causing frictions and wears. This

makes it necessary for the engine and transmission oils to be at the optimum viscosities which can only be obtained when the oils are within the optimum temperature ranges.

In improving these thermodynamics and frictions, it is important for the engine oil, transmission oil and coolant to operate within the optimum temperature ranges to reduce the fuel consumption and tailpipe emissions. This makes it necessary for these fluids to be warmed-up as soon as possible during cold-start and to sustain the optimum temperatures throughout the rest of the engine operations. By ensuring that the fluids are within the optimum temperature ranges, the parasitic losses, combustion heat losses and intake port wall wetting can be minimised to improve the fuel economy (Osman, Razali & Nurdin, 2018).

In quickly reaching the fluids' optimum temperatures, the limited combustion heat available during the cold start must be optimally distributed between the fluids, metals and catalytic converter. Understanding that the thermal efficiency of the engines is continuously improving from time to time, there will also be lower waste heat from the combustion which makes it more challenging for the exhaust and coolant heats to be recovered for reuse.

In view of these challenges, this research addresses the challenges by applying two main strategies into the vehicle's thermal management system. The first one involves the enhancements of the conventional engine cooling circuit to improve its heat conservation and distribution within the cooling circuit. Within the circuit, there are enablers like valves, electric pumps and thermostat that will further enhance the circuits to achieve better heat conservation and distribution. The second strategy involves the recovery of heat from the exhaust gas for the purpose of supplementing the limited heat availability during the cold start.

This literature review identified the existing research works done by others covering the two strategies above. Summary, limitations and research gaps are briefly discussed based on the cited references.

## **2.2 Heat conservation and distribution within the cooling circuit**

A group of researchers published a paper about the computer simulations on the “perfect cooling system” that enabled the coolant to be warmed up to the optimum temperature very quickly (Caresana, Bilancia & Bartolini, 2011). Their study compared the fuel consumption of such a perfect system based on the conventional cooling systems. From the study, the fuel economy was improved by as much as 17% in the NEDC (New European Driving Cycle) test with the fluids were warmed up prior to the cold start. The study however does not provide any specific practical design, approach or solution to achieve the perfect status but nevertheless it challenged others to come up with such solution.

A researcher from Jaguar Cars published a paper about the use of precision cooling to supply just enough coolant flow at the critical areas across all engine speed (Clough, 1993). His proposed concept involved the detailed optimisations of the cross section opening area of the water jacket to control the coolant flow rate and velocity throughout the strategic passages. This concept enabled the coolant flow rate requirement and water pump power consumption to be reduced by as much as 40% and 54% respectively. Although his study focused more on the cooling performance rather than the warm-up performance, the unique cross section area optimisation method is applicable in optimising the cooling passages for warm-up performance. Nevertheless, the paper is quite old, and it does not provide any in-depth study on how his proposed concept will improve the coolant warm-up during cold start using the widely used test cycles.

A paper from University of Bath provided a good general overview of the split cooling system (Pang & Brace, 2004). In general, the split cooling system independently control the coolant flow across the cylinder head and block using two separate partitions controlled by two separate thermostats with differing opening temperatures. The split cooling systems normally operate the cylinder head cooler than the cylinder block. Running the cylinder head cooler is important in keeping the volumetric efficiency high. By contrast, the relatively hotter cylinder block is crucial in keeping the cylinder bores hot thus ensuring low oil viscosity over the bore surfaces for low sliding frictions between the cylinder bores and piston assembly.

Another paper about the split cooling system reported the fuel economy and emissions improvements when their system was operated with cylinder head set at 50 °C and cylinder block at 150°C (Finlay, Tugwell, Biddulph & Marshall, 1988). However, similar study related to split cooling system by others has reported no fuel economy (Gardiner, Zhao, Addison & Shayler, 2013). Yet another paper has also claimed that their internal tests involving the conventional split cooling system did not show any improvement in fuel economy (Osman, Razali & Nurdin, 2018). The variations implied that the applications of split cooling system to the more recent engines and test conditions have not guaranteed improvement in fuel economy.

In addition to that, Japanese researchers operated their experimental engine with coolant temperatures at 50 °C for the cylinder head and 80°C for the cylinder block (Kobayashi, Yoshimura & Hirayama, 1984). They reported improvements in volumetric efficiency and knock resistance. In view of the improvement in knock resistance, the geometrical compression ratio could be increased from 9:1 to 12:1. As a result, the fuel consumption was improved by 5% at part load and 7% at idle. Although the improvement

in fuel consumption was significant, this paper is decades old and it is not known on how such concept will improve the more recent engines.

Another option to improve the heat conservation and distribution within the cooling circuit is by using an electric water pump. The use of electric water pump allows its speed to be controlled independently from the engine speed. This allows the water pump to be completely shut off during cold start and at its maximum speed during low-speed steep hill climb. In this context, with the maximum heat rejection fully defined and matched with the appropriate water pump speed, anything in between can be electronically interpolated or calibrated using physical tests.

The coolant flow rate for a typical mechanical water pump increases linearly with increase in engine speed. By contrast, an electric water pump can be sized differently, and therefore its capacity does not need to be as high as the mechanical water pump. Driving conditions that require prolonged high engine load at low vehicle speed often require the radiator, radiator fan capacity and overall water pump capacity to be enlarged to avoid overheating. Alternatively, such driving conditions can benefit from the use of electric water pump by maximising the water pump speed at low and medium engine speeds. The physical tests conducted have reduced the coolant flow rate by as much as 90% if compared to mechanical water pump (Allen & Lasecki, 2001).

In using the electric water pump, it was possible to get coolant operating temperature as high as 110°C if compared to 90°C for conventional cooling circuit (Chanfreau, Gessier, Farkh & Geels, 2003). Even with this high coolant temperature, the 110°C coolant temperature could be reduced by 10°C in just 2 seconds. This enables the risks of combustion knock and the low volumetric efficiency that are related to the high cylinder head's coolant temperature to be mitigated.

Understanding that the effect of having an electric water pump can also be simulated by throttling the conventional mechanical water pump, a study was published by researchers from University of Bath and Ford Motor Company (Brace, Hawley, Akehurst, Piddock & Pegg, 2008). From the study, the throttling of the water pump to reduce the coolant flow rate and consequently increased the coolant temperature. The higher coolant temperature made it possible for the fuel economy to be improved by as much as 2%.

In further controlling the coolant flow, various electronically controlled coolant valve configurations to achieve the best warm-up performance were compared and summarised (Mitchell, Salah, Wagner & Dawson, 2009). Their study concluded that the use of three-way valve was much better than the conventional thermostat and two-way valve. Their study provided some insight on how electronically controlled multi direction valve system can be used to conserve precious heat and how this heat can be directed to strategic places across the engine speed and load.

Separately, an electronically controlled valve with three different opening modes was studied for its effect on the tailpipe emissions and fuel economy (Mohamed, 2016). The valve was combined with an electric water pump to maximise the positive effects of the valve. His study which consisted of both simulations and experimental works has revealed clear improvements in NEDC warm-up performances which contributed to lower the tailpipe emissions and fuel consumption.

Reducing the coolant mass is effective in reducing the thermal inertia (Robinson, 2001). Lower thermal inertia speeds up the warm-up process because there is less mass to heat up. A precision cooling system was proposed and it focused on having just enough water jacket in which the coolant volume is reduced by up to 64% (Clough, 1993). This big reduction in water jacket cuts down the warm-up time by 18%.

A group of researchers studied a lumped capacity model to simulate the warm-up of 2.0l direct injection diesel engine (Samhaber, Wimmer & Loibner, 2001). The simulation model predicted that the oil's temperature would drop by 4°C in case the coolant flow rate is decreased by 10%. The drop in the oil's temperature is caused by less heat being transported out from the cylinder head to the oil-to-coolant heat exchanger. The paper shows that the conservation and distribution of the combustion heat must be optimally done to avoid negative consequences that may affect the fuel consumption. Although conserving the heat in the cylinder block and cylinder head is beneficial in warming up the coolant temperature, the viscous losses of the entire powertrain can be high unless the engine and transmission oils get to the optimum temperatures early. This necessitates optimum amount of heat to be diverted away from the coolant to the oils.

The optimum temperatures for the best fuel economy for the engine and CVT oils are in the range of 100-110°C and 70-80°C respectively (Osman, Razali & Nurdin, 2018). In view of roughly 4 litres each for both the CVT oil and engine oil in Proton cars, plenty of heat is needed to warm-up these oils to the optimum temperature ranges and to sustain the temperatures. Balancing the needs to optimally distribute the limited heat to the coolant, CVT oil and engine oil for the best overall fuel economy can be challenging.

As shown in Figure 2.1, a simplified split cooling circuit which is different from other conventional split cooling circuits was proposed to potentially replace the conventional ones (Osman, Sabrudin, Hussin & Bakri, 2013). The concept relies on the use of single thermostat placed after the cylinder head's coolant outlet to regulate the coolant flow across the cylinder head. Contrary to the conventional split cooling circuit, there is no thermostat to regulate the coolant flow rate across the cylinder block meaning the coolant flow in the cylinder block is permanently flowing. This also makes it possible for the coolant flowing out of the cylinder block to be regulated in accordance with the outlet

opening diameter. In this context, the targeted coolant temperature across the cylinder block at strategic engine operating points can also be regulated accordingly. The authors also claimed that the use of single thermostat instead of two is beneficial in terms of price, coolant pressure losses, response and complexity.

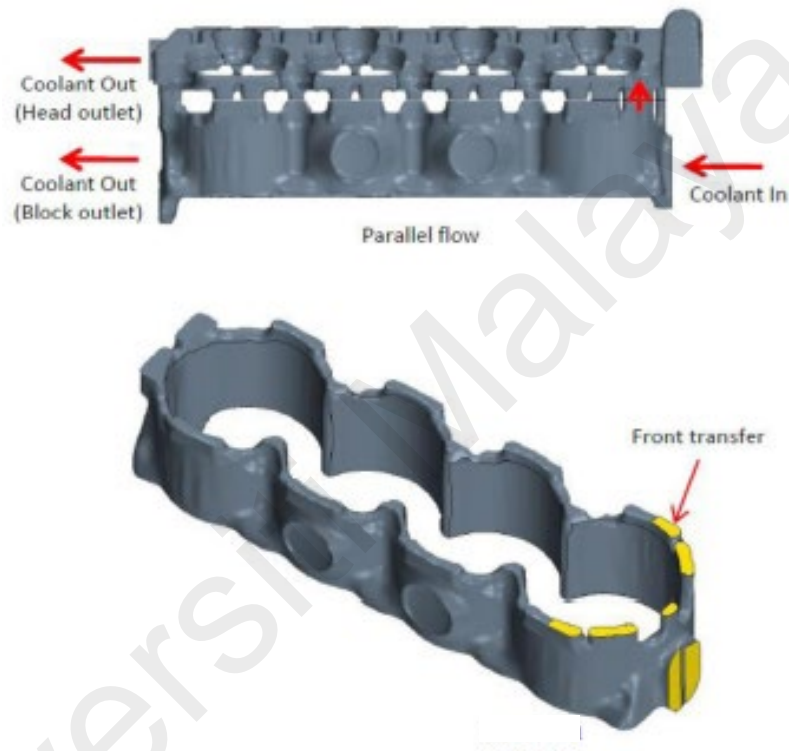


**Figure 2.1: The side view (top) and isometric view (bottom) of the earliest simplified split cooling proposed by the authors (Osman, Sabrudin, Hussin & Bakri, 2013).**

From the above-mentioned study, the authors claimed that regulating the coolant flow rate across the cylinder head affects the coolant temperature in the cylinder head. Considering that the oil jacket was placed directly above the water jacket, the authors also claimed that it was possible to heat up or cool down the engine oil above it. Placing a thermostat after the cylinder head stagnates the coolant flow during idle and part load operations to increase the coolant temperature. By contrast, when the engine is operated

at higher engine load where plenty of heat is transferred to the coolant from the combustion chamber, the thermostat will be wide open. As a result, the coolant temperature will go down when a lot of coolant flows across the radiator. The reduced coolant temperature in the cylinder head's water jacket cools off the engine oil above it as well.

The authors also claimed in the paper that the thermal inertia is expected to be low during the cold start because only the coolant in cylinder block that is circulating instead of the combined coolant volumes in both the cylinder head and cylinder block. This paper disclosed the earliest concept which was later evolved.

In 2016, the previously proposed circuit was evolved further as shown in **Figure 2.2** (Osman, Yusof & Rafi, 2016). From the diagram, the thermostat has been moved from cylinder head coolant outlet to the bypass passage coming out of the cylinder block. This change was significant in redefining the heat conservation and distribution within the cooling circuit. In particular, with the thermostat placed there, the thermostat was not affected by the coolant temperature coming out of the cylinder head. Instead, the thermostat opening depended on the relatively cooler coolant from the cylinder block flowing along the coolant bypass towards the thermostat. This arrangement enabled the heat build-up in the cylinder head to be prolonged because the thermostat would not open unless the coolant passing along the bypass passage is hot enough by the time it reaches the thermostat. In this context, heat exchangers like oil coolers and cabin heater arranged along the bypass are likely to absorb plenty of coolant heat. The more coolant heat is lost to the heat exchangers, the longer it will take for the thermostat to open.

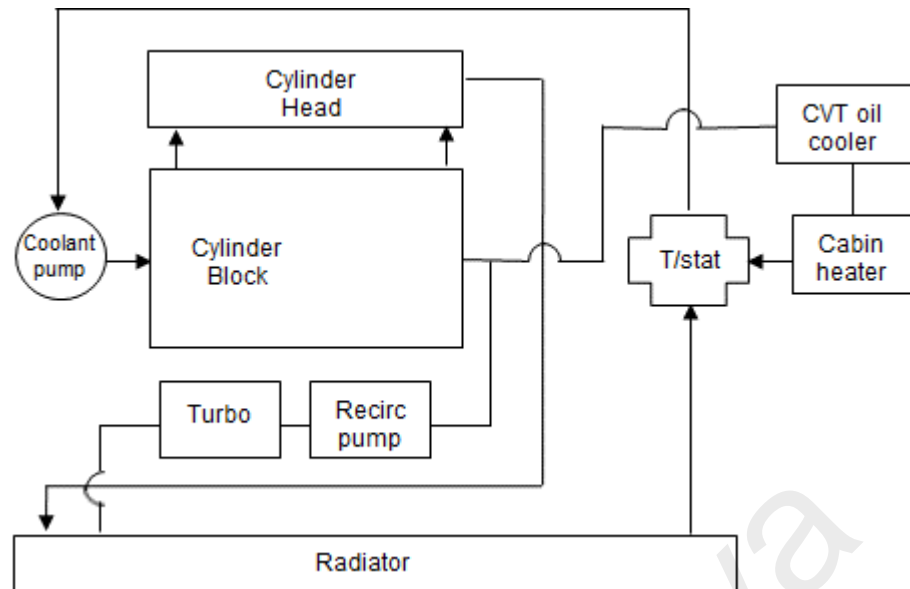


**Figure 2.2: Cooling circuit with the turbocharger as the heat recovery unit (Osman, Yusof & Rafi, 2016).**

From the tests conducted, the CVT's metals and its oil were cooler than the coolant when the engine was being warmed up. As a result, the CVT oil cooler absorbed a lot of heat from the coolant flowing across the bypass passage and this delayed the thermostat opening. This enabled the cylinder head to conserve the precious heat until all the critical fluids are warm enough for the thermostat to open.

In addressing the difference in optimum temperature ranges for both the CVT and engine oils, the CVT oil cooler is placed along the bypass passage as shown in **Figure 2.2** to make a full use of the relatively cooler coolant temperature coming out of the cylinder block. This is a stark contrast from many other automakers which normally placed the transmission oil cooler along the passage coming out of the cylinder head.

The proposed cooling circuit achieved around 4% of fuel economy improvement during the NEDC test (Osman, Yusof & Rafi, 2016). Encouraged by the fuel economy improvement that came with the improved warm-up time, the concept was further optimised to achieve even better warm-up performances (Osman, Razali & Nurdin,

2018). As shown in **Figure 2.3**, the optimisations were mostly focusing on reducing the thermal inertia by reducing the coolant volume circulations through better partitioning within the cooling circuit. In addition to that, the distributions of the heat were also improved by ensuring that the precious heat is well distributed to the strategic areas like engine and CVT oil coolers. This improved cooling circuit enabled all the critical fluids like the cylinder head coolant, engine oil and CVT oil to be warmed up faster than the earlier variant.

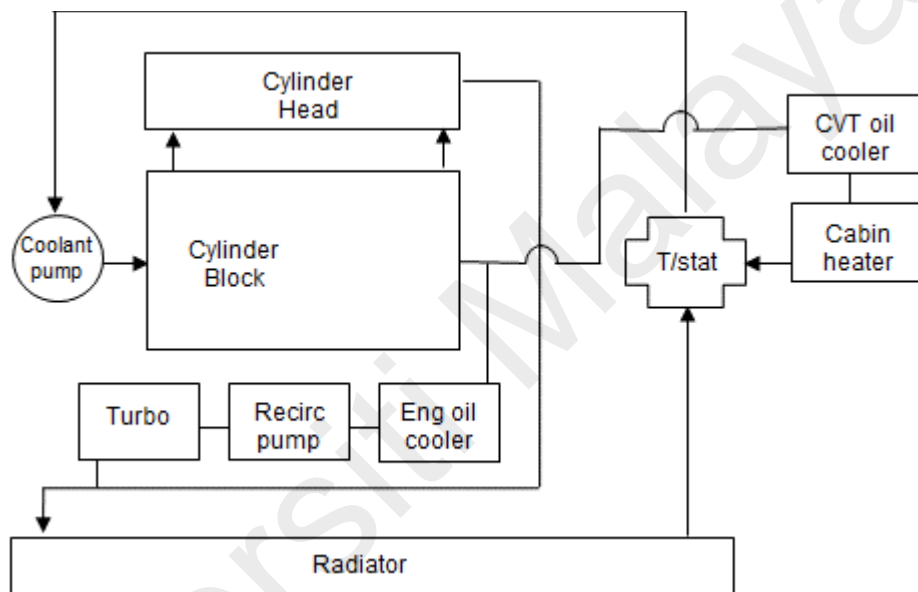


**Figure 2.3: Optimized cooling circuit for reduced thermal inertia (Osman, Razali & Nurdin, 2018).**

It is also interesting to point out that with the engine oil cooler placed in series next to the turbocharger, the recovered exhaust heat can be quickly used to heat up the engine oil during idle and part load driving. On the other hand, as the coolant flow reverses when the thermostat is fully or wide open, the excess heat from the engine oil will be discharged to the radiator together with the recovered exhaust heat. By avoiding the recovered heat from being recirculated directly into the engine, the overheating of the engine at higher load operations can be avoided.

In their paper, they discussed on the reasons why they prioritised warming up the cylinder head first instead of the cylinder block (Osman, Razali & Nurdin, 2018). In warming up the cylinder head first, they claimed that the negative impacts of the intake port wall wetting and combustion heat quenching to the cylinder head can be minimised. The authors somehow believed that minimising these two aspects were more beneficial in improving the fuel economy than trying to reduce the friction along the middle of the cylinder bore.

Improvement of the fuel economy by as much as 4% during NEDC as stated earlier is a clear evidence that prioritising the warm-up of cylinder head rather than the cylinder block is an alternative option than the widely accepted practice of warming up the cylinder block (Osman, Yusof & Rafi, 2016). A thesis by Lodi has also reported similar improvement in fuel economy through his experimental work that compared various prioritised warm-up strategies involving the cylinder head versus cylinder block (Lodi, 2008).

An important aspect on how the cooling circuit plays an important role in recovering heat from the EHRU was discussed in the earlier studies (Osman, Yusof & Rafi, 2016; Osman, Razali & Nurdin, 2018). The temperature of coolant flowing through the cylinder head became hot rapidly and it stayed hot in most of the engine operations except when the engine speed was high or when the thermostat was wide open. During a typical cold start, significant amount of precious heat is lost to heat up the relatively cooler EHRU at the early part of the cold start when the hot coolant from the cylinder head was directed to the EHRU. As the EHRU gets hotter and hotter than the coolant from the cylinder head, the resulting temperature difference is smaller than what it would be with cooler coolant feed.

As shown in **Figure 2.4**, the coolant temperature coming out of the cylinder block is uniquely cooler by as much as  $29.6^{\circ}\text{C}$  if compared to the coolant coming out of the cylinder head by the time the thermostat opens during the NEDC test (Osman, Razali & Nurdin, 2018). As shown in **Figure 2.5**, the large coolant temperature difference was possible by placing the cylinder block's coolant outlet at the bottom of the 4<sup>th</sup> cylinder water jacket which is about 107 mm from the top deck. As a reference, the engine has 86 mm stroke meaning that the outlet is located way below near the bottom of the cylinder bore.

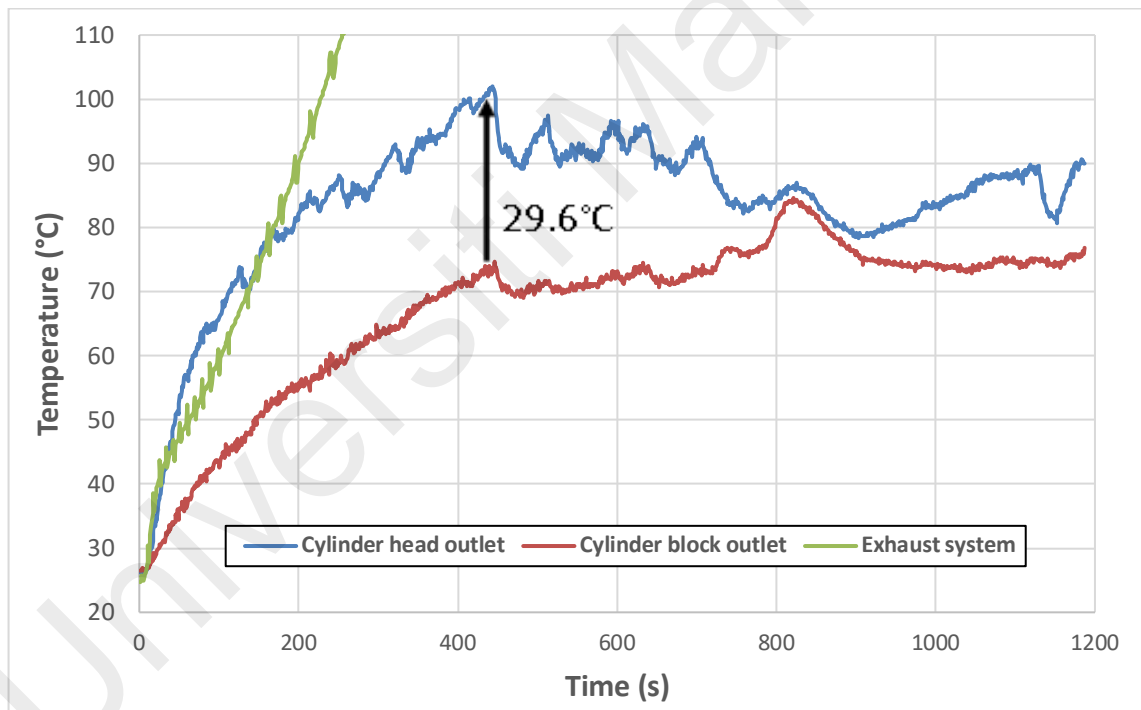


**Figure 2.4: Replot of the Demo1's coolant temperature exiting the cylinder head and block during NEDC test (Osman, Razali & Nurdin, 2018).**

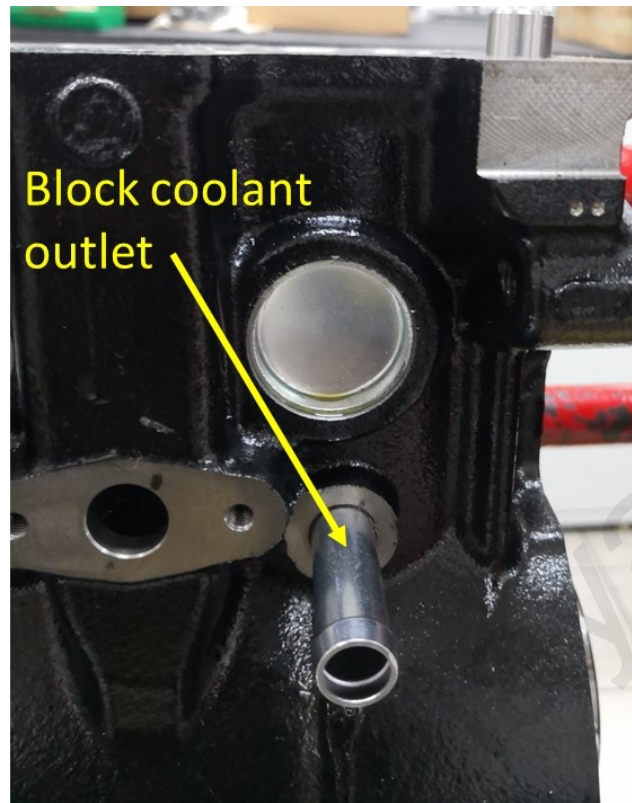


**Figure 2.5: Demo1's cylinder block with coolant outlet at the bottom of the water jacket's rear end.**

In general, combustion heat release happens mostly at the upper portion of the cylinder bore and the bore temperature plateaus below the top 40% of the piston stroke (Osman, Razali & Nurdin, 2018). A published liner temperature profile shows big temperature reduction after the top 30% of the liner height (Caresana, Bilancia & Bartolini, 2011). A CFD plot has shown that the flow velocity at the bottom portion of the cylinder block's water jacket to be far lower than the velocity at the top portion of the water jacket (Qasemian & Keshavarz, 2016).

In this context, with the hot coolant along the upper portion of cylinder block's water jacket eventually transferred to the cylinder head through the gasket apertures across the four cylinders, the cooler coolant along the bottom of the water jacket on the other hand will move from the first cylinder to the last without absorbing much of the heat from the cylinder bores. Swapping the coolant feed to the EHRU from the cylinder head to the

cylinder block is likely to enable sooner and higher recoverable energy from the exhaust gas due to larger temperature difference between the EHRU and coolant.

### **2.3 Heat recovery and reuse of the exhaust heat**

A typical 1.4l spark ignition engine wastes as much as 21% of the precious heat to the exhaust gas at 1500 rpm and quarter load and 44% at 4500 rpm and full load (Chammas & Clodic, 2005). Plenty of efforts have been invested to recover the exhaust heat and to convert it into usable kinetic or electrical energy. However, the exhaust gas needs to be hot for the enthalpy to be high enough for the conversion to take place.

Majority of daily driving consists of frequent short distance driving with plenty of idle and part load operations. In these conditions, the exhaust gas temperature will not be high enough for the conversion of thermal energy to kinetic or electrical energy to take place. Furthermore, the average exhaust gas temperature decreases from time to time with continuously improving thermal efficiency of the internal combustion engines in general. This makes it more challenging to obtain high exhaust gas temperature in everyday driving.

In general, there are many technologies being developed to recover exhaust heat (Talom & Beyenne, 2009). Another review paper highlighted the common issues in recovering the exhaust heat (Armstead & Miers, 2014). The paper highlighted the risks of increased weight, exhaust backpressure, size and cost of the EHRU. In addition to that, the paper also highlighted the challenges in recovering heat from the exhaust gas due to the engine power fluctuation. This paper listed down the common options available in reusing the recovered exhaust heat in which the energy is either converted into electricity using thermoelectric or kinetic energy using a Rankine cycle.

A published thesis stated that the energy recovery has a large potential to reduce the warm-up time (Robinson, 2001). However, he also stated that it can be challenging to design an exhaust heat recovery system that is also able to reject excess heat. In general, the recovered exhaust heat is useful to provide additional heat during cold start, idle and part load engine operations. However, once the engine is hot enough, the recovered exhaust heat can potentially overheat the engine especially during acceleration, steep hill climb and high speed driving.

Another review paper provides a good overview on the energy available from the exhaust gas (Roberts, Brooks & Shipway, 2014). The paper also provides a generic idea on how thermal energy can be recovered from the exhaust gas stream. This includes the need to avoid compromising the catalytic converter light-off due to the placement of EHRU before the catalyst. In maximising the heat recovery from the reduced exhaust gas temperature, the surface areas for the heat transfer to take place must also be maximised. The increase in surface areas reduces the exhaust gas temperature entering the catalytic converter. As a result, the catalyst will take longer time to reach its light-off temperature and it is also more difficult to sustain the light-off temperature during prolonged idle.

Researchers from South Korea have published a paper about their study in recovering heat from the exhaust gas which was later reused to heat up the CVT oil for hybrid electric vehicle (Park, Jung, Kim & Min, 2013). Their study involved both simulation and experimental validations. The proposed concept involved the use of coolant as a medium to absorb the exhaust heat and to transport the recovered heat for heating up the CVT oil. For the UDDS test cycle, the time needed to reach 50°C from 0°C was reduced from 20 to 13 minutes.

Exhaust heat recovery was also used to quickly warm-up the engine oil (Battista & Cipollone, 2016). The system relies on a thermostatic valve to divert away the engine oil

from the exhaust gas once the engine oil is already hot. In addition to that, the oil sump is also equipped with a control valve to limit the oil volume that will be circulated to the EHRU. Once the engine oil in the sump is hot enough, the control valve will release the remaining oil volume into the partition where the suction point is located. Considering that the engine oil is in direct contact with the exhaust gas heat recovery unit, there is no doubt that the oil can be warmed up rapidly. However, even if the thermostatic valve diverts most of the engine oil away from the heat recovery unit, small amount of engine oil will remain in various cavities. This small amount of oil is likely to be pyrolysed over the hot surfaces and cause oil coking. Frequent oil coking formations are likely to accumulate to cause blockage of the oil passage after certain time.

An excellent paper from Faurecia Emissions Control Technologies reported the development of an underfloor exhaust heat recovery and reuse for hybrid vehicles (Chiew, Clegg, Willats, Delplanque & Barrieu, 2011). From **Figure 2.6**, the heat recovery unit is big in size and weighs around 5.4 kg. As a result, it must be placed a distance away from the engine to provide ample clearance and rigid mounting points. Being far away from the heat source requires the heat recovery unit to be designed with large surface area to maximize the heat absorption of the exhaust gas by the coolant.

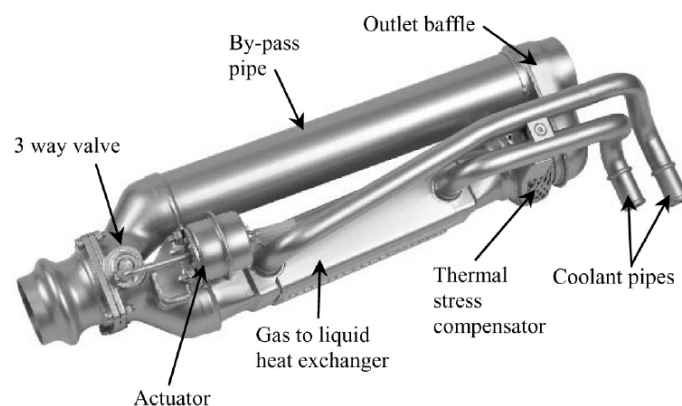


**Figure 2.6: EHRU from Faurecia (Chiew, Clegg, Willats, Delplanque & Barrieu, 2011).**

Faurecia's EHRU relies on arrays of heat transfer fins to maximize the surface area for the coolant to absorb heat from the exhaust gas. These large fins require a large housing and necessitating it to be placed far away from the engine as highlighted earlier. Faurecia's EHRU weighs 5.4 kg, and the big housing requires significantly large volume of coolant to continuously fill the void. The large thermal inertia and the EHRU's placement away from the exhaust port negatively affects the time for the heat to be recovered and eventually reused because the cold metals and additional coolant will also take time to be warmed up. In improving the warm-up performances, it is necessary for the thermal inertia to be reduced (Torregrosa et al., 2008; Agarwal, Chiara & Canova, 2012) or alternatively, the heat source must be increased to overcome the high thermal inertia (Burke et al., 2012).

**Figure 2.7** shows the construction of the heat exchanger within the EHRU to recover the exhaust gas heat (Chiew, Clegg, Willats, Delplanque & Barrieu, 2011). From the diagram, the exhaust gas has to flow across the heat exchanger and this is likely to increase the pressure losses inside the exhaust system. Considering that the exhaust gas passages are significantly reduced if compared to the main exhaust passage, carbon deposits from the exhaust gas are likely to accumulate. This will increase the pressure losses and there is also risk of blockage in the long run. Considering that there are large vibrations and extreme metal temperatures, making the delicate heat exchanger fins durable for long term usage can be challenging.

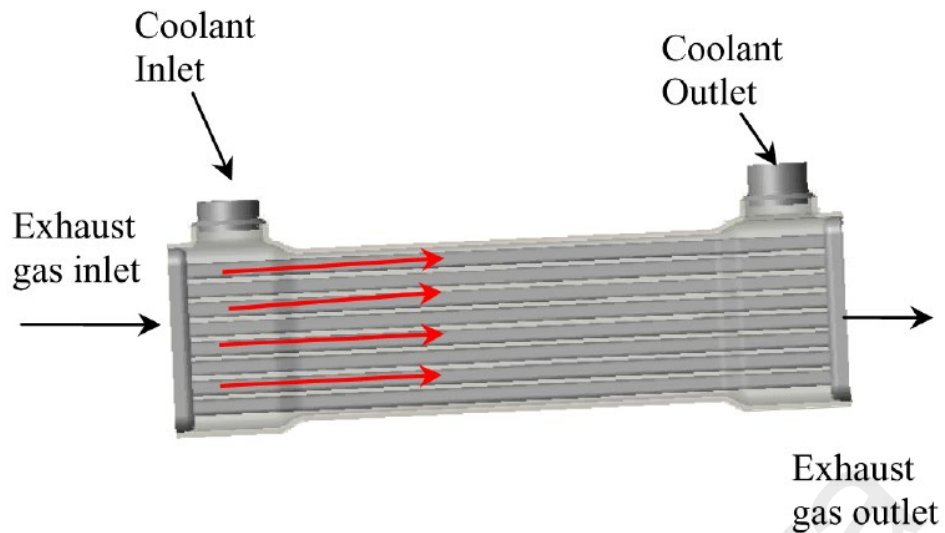


**Figure 2.7: Heat exchanger construction to recover the exhaust gas heat (Chiew, Clegg, Willats, Delplanque & Barrieu, 2011).**

The large size makes it difficult to retrofit the system to the cars on road because ample clearance is needed to fit it underneath the cabin. Ample clearance on the other hand requires a specially designed vehicle platform with dedicated tunnel where the heat recovery unit will be partially or mostly enclosed.

In ensuring that the EHRU does not continue to absorb heat when the engine is already hot, a vacuum actuated flap valve as shown in **Figure 2.8** directs the exhaust gas through the bypass passage and away from the gas-to-liquid heat exchanger. The bypass passage is crucial in preventing the recovered heat from overheating the engine when the engine is already hot. In having the bypass passage, the additional parts needed to make the assembly works are likely to affect the reliability and durability of the assembly. This additional complexity also requires relatively longer development time to get it into production.

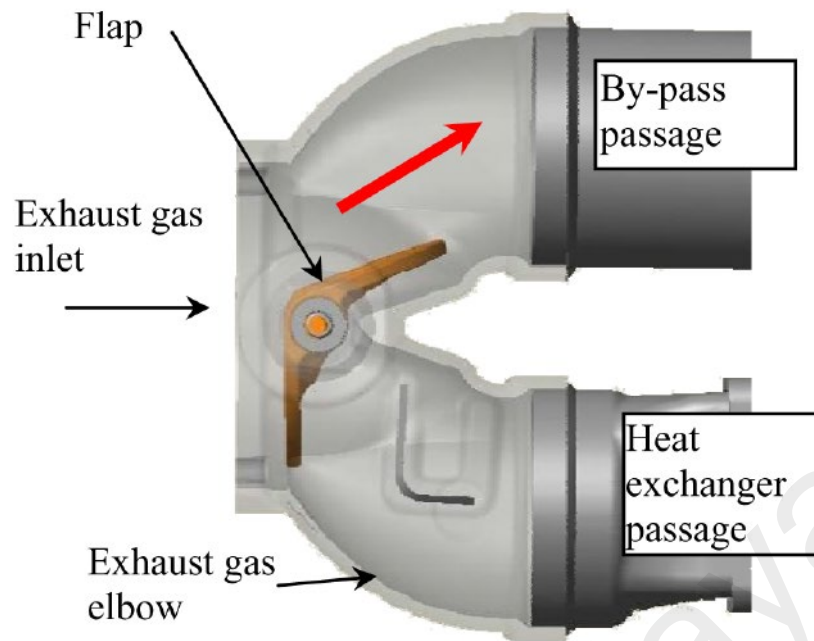


**Figure 2.8: Vacuum actuated flap valve (Chiew, Clegg, Willats, Delplanque & Barrieu, 2011).**

The paper also discussed about the reuse of the recovered heat to provide cabin heat through the cabin heater during cold winter. The paper also highlighted the improvement of the coolant warm-up and fuel economy over the baseline during the NEDC.

In making sure that the EHRU can be applied with minimum cost increase, part count and development complexity, the turbocharger housing itself was slightly modified to function as an EHRU (Osman, Yusof & Rafi, 2016; Osman, Razali & Nurdin, 2018). In a typical turbocharger system, there are coolant inlet and outlet to continuously supply coolant to cool off the plain bearing and engine oil near the bearing vicinity. The coolant coming out of the turbocharger housing is normally directed to the radiator for direct heat discharge to the environment. By contrast, the system proposed relies on the thermostat and the unique cooling circuit design to alter the coolant flow direction. For example, with the thermostat closed during cold start, idle and part load driving, the coolant across the turbocharger reverses its direction and the recovered heat from the exhaust gas will

be recirculated into the engine to provide additional heat within the cooling circuit. On the other hand, if the engine is hot enough that the thermostat opens, the coolant across the turbocharger changes direction and the coolant will flow directly to the radiator to discharge the recovered heat to the environment. Using this flow direction altering mechanism, there is no need for complicated electronically controlled vacuum actuated flap valve used by Faurecia as explained earlier. This arrangement improves the reliability of the exhaust system by not having any complicated mechanism.

Similar to the Faurecia's EHRU, the turbocharger used in the study weighs 5.2 kg and the large thermal inertia requires a lot of heat for every 1°C increase of the metal temperature. Lowering the turbocharger mass can be challenging because the turbocharger needs to be strong to withstand the harsh vibration and high metal temperature.

As discussed in **Section 2.2**, the coolant feed to the turbocharger was from the cylinder head and the coolant temperature increase inside it was faster than the coolant temperature increases inside the cylinder block. During the early part of the cold start, there will be significant amount of precious heat being absorbed by the cooler turbocharger before the coolant exiting the turbocharger can be hotter than the coolant entering it. In this context, when combined with the high thermal inertia of the 5.2 kg turbocharger, it took 180 seconds from the start of the NEDC test before the recovered exhaust heat can be reused to supply additional heat to the cooling circuit (Osman, Yusof & Rafi, 2016). As a comparison, Faurecia's EHRU was able to recover and reuse the exhaust heat as early as 50 second from the start of the NEDC test.

Importantly, a group of researchers installed an EHRU to a 3.3l spark ignition engine and investigated the coolant warm-up time and fuel consumption during highway and city driving (Goetler, Vidger & Majkrzak, 1986). The EHRU reduced the coolant warm-up

time and fuel consumption by 7% and 2.2% respectively during idle and 16% and 2.2% respectively during highway driving. In a separate study, researchers evaluated the effects of combined exhaust-to-coolant EHRU and 6 kW heater for engine oil to warm-up time and fuel consumption using Ford 1.4l spark ignition CVH engine (Andrews et al., 2007). From the study, at 35% peak load and 2000 rpm engine operation, the oil warm-up time was reduced from 10 to 3 minutes and the fuel consumption was improved by 12-15% during the first 7 minutes of cold start.

## 2.4 Summary

From the literature review conducted, certain useful and relevant trends can be established in **subchapter 2.1, 2.2 and 2.3**. From the **subchapter 2.2**, the conservation and distribution of heat within the cooling circuit are necessary to speed up the warm-up process of the powertrain's fluids to obtain better fuel economy and emissions. In supplementing the limited heat availability during warm-up, idle and part load driving, the **subchapter 2.3** is dedicated to the discussions on the use of recovery and reuse of exhaust heat.

The modifications to the cooling circuit to conserve and distribute the precious heat can be generally grouped into mechanical or electrification of the cooling system's components. The mechanical approach involves the optimisation of the coolant circuits, coolant passages cross section area and thermostat opening temperatures. By contrast, the electrifications of the components come in the form of electronically controlled flow valve and electric water pump. The electrifications provide better accuracy, precision and flexibilities but are generally more expensive and complicated.

Understanding that it is crucial to warm-up all the critical fluids simultaneously with limited heat available during cold start, it is crucial for additional heat to be introduced to supplement the deficiency. This necessitates researchers to investigate the possibility of recovering the exhaust gas that will otherwise be wasted into the environment. Among the exhaust heat recovery technologies available generally convert the thermal energy into electricity, and kinetic energy. Nevertheless, there are also papers discussing about how the recovered exhaust heat can be used to warm-up the coolant, CVT oil, engine oil and cabin heater.

Clearly, recovering the exhaust heat for the purpose of speeding up the warm-up of coolant and oils does not require the exhaust gas temperature to be high enough. This is preferable as majority of daily driving do not induce the exhaust gas temperature high enough for the thermal energy to be converted into kinetic or electrical energy.

## **2.5 Research gaps**

The simplified split cooling with integrated exhaust heat recovery and reuse was previously applied to turbocharged engine and never been tried to any naturally aspirated engine. The question on how effective the previously proposed EHRUs (Osman, Yusof & Rafi, 2016; Osman, Razali & Nurdin, 2018) can improve the warm-up and cooling performances of a naturally aspirated SI engine can be an interesting area to explore. In the absence of the turbocharger, applying the similar EHRU to a naturally aspirated engine requires a different heat exchanger to be mounted somewhere along the exhaust system. Such study also provides the opportunity to evaluate the effects of using an EHRU with lower thermal inertia if compared to the use of heavy turbocharger.

From the commercial standpoint, there have been demands for the proposed thermal management system discussed in the earlier studies (Osman, Yusof & Rafi, 2016; Osman, Razali & Nurdin, 2018) to be applied to naturally aspirated engines. This takes into consideration that there are still many motorcycles, small cars and stationary engines working optimally and economically with naturally aspirated spark ignition engines. In 2018, the global sales of cars were 86 million (Demandt, 2019) and 61.9 million for motorcycles (Motorcycles data, 2019). In this context, any cost effective and practical fuel economy improvement technology that can be massively applied to these engines can effectively reduce the global energy usage more than the limited premium technologies applied to premium vehicles. This gap necessitates a much simpler and cheaper EHRU to be designed and fitted to the limited space in the engine bay.

To sum it up, research gaps exist in terms of limited availability of high enthalpy exhaust gas in daily driving, delayed availability of the recovered exhaust heat, complicated designs and constructions of EHRUs, high thermal inertia of the EHRUs and practicality of the EHRUs for mass applications to non-premium engines. On the other hand, opportunities exist in terms of the availability of sustainable source of cooler coolant from the cylinder block and high demands of cost effective naturally aspirated engines worldwide. In view of such opportunities, knowledge gaps exist on how to redesign the existing EHRUs and how it should work in to exploit such opportunities to ultimately address all the highlighted research gaps.

## CHAPTER 3: METHODOLOGY

### 3.1 Introduction

The study focuses on the recoverable thermal energy from the proposed EHRU. In this context, the experiments were conducted based on a test vehicle fitted with the proposed cooling circuit and specially made EHRU. In evaluating the effect of the proposed EHRU to the warm-up performances, the test vehicle fitted with the proposed cooling circuit was tested with and without the proposed EHRU.

To ensure objective and focused study, Proton Iriz with 1.3l naturally aspirated SI engine was selected to be converted into the test subject. The standard production engine and the cooling passages needed to be modified before the intended cooling circuit and the EHRU can be included. This also necessitated additional vehicle parts to be designed and fabricated to replace the original parts.

No changes were made to the engine, transmission and vehicle electronics. This allowed the study to be solely focused on the mechanical system especially the proposed EHRU and to lesser degree the proposed cooling circuit. To enable repeatable and reproducible test results, the comparisons were based on idle and NEDC tests. **Figure 3.1** shows the flow chart of the research methodology outlining the activities stated in this chapter.

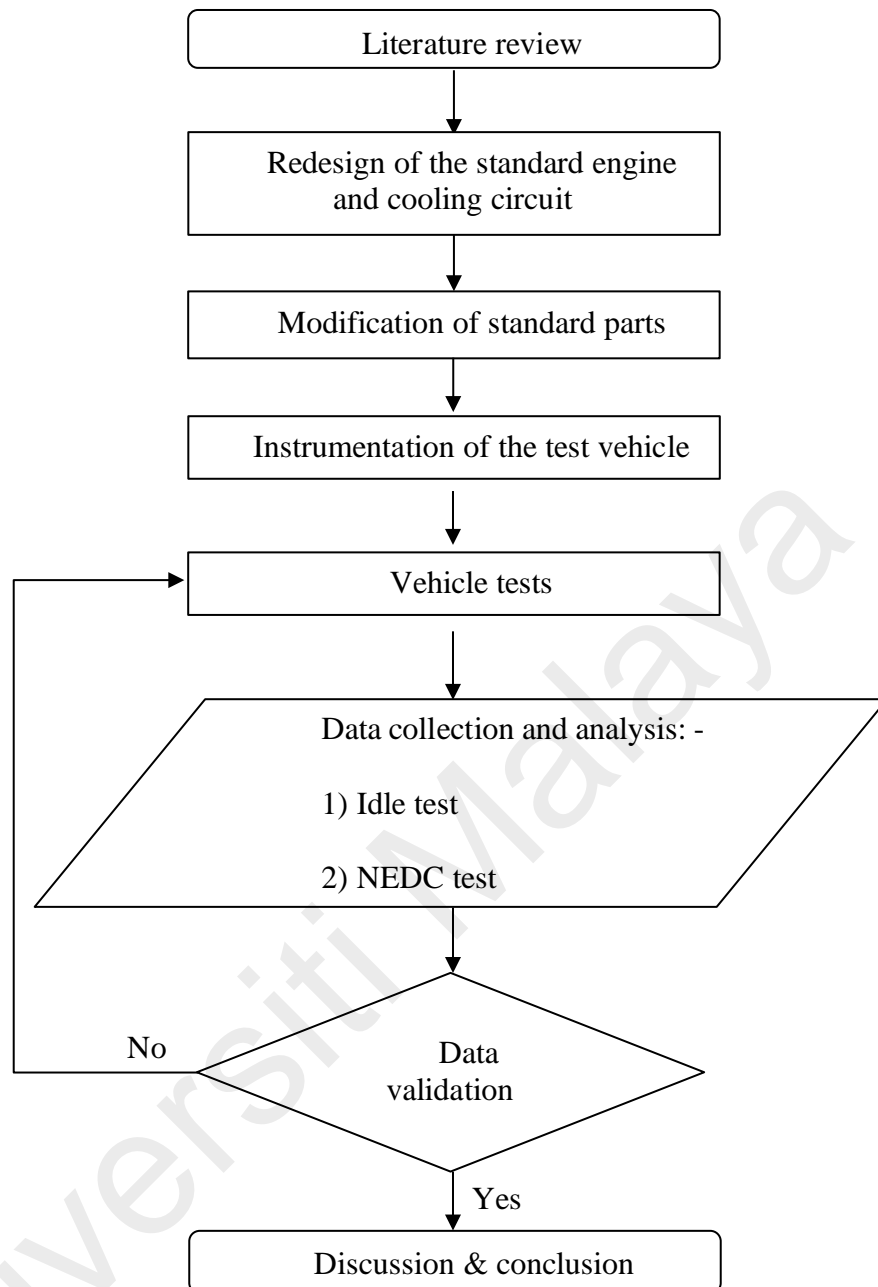


**Figure 3.1: Flowchart of the research methodology**

### 3.2 Comparison between the standard and the proposed cooling circuit

**Table 3.1** shows the specifications of the test vehicle. The 30/70 ethylene glycol to water ratio is specific to Malaysia's market in which the tropical weather ensures hot ambient all year long. The unpressurised cooling circuit typically used by Proton cars on the other hand limits the maximum coolant temperature limit of the circuit to 120°C.

**Table 3.2** shows the technical data sheet of PETRONAS Mach 5 Plus 10W30 mineral engine oil used throughout the tests. **Table 3.3** shows the technical data sheet of PETRONAS Tutela Multi CVT 700 oil.

**Table 3.1 - Specifications of the test vehicle.**

<b>Type</b>	5-seater hatchback
<b>Kerb weight</b>	1165 kg
<b>Transmission</b>	Punch CVT
<b>Displaced volume</b>	1332 cc
<b>Bore and stroke</b>	76 mm and 73.4 mm
<b>Compression ratio</b>	10:1
<b>Fuel delivery system</b>	Gasoline multipoint port injection
<b>Cooling system</b>	Unpressurized cooling circuit
<b>Coolant mix</b>	30% ethylene glycol, 70% water

**Table 3.2 – Technical data sheet of PETRONAS Mach 5 Plus 10W30 mineral engine oil.**

<b>Parameters</b>	<b>Method</b>	<b>Unit</b>	<b>Value</b>
<b>Density at 15°C</b>	ASTM D4052	g/cm <sup>3</sup>	0.875
<b>Viscosity at 100°C</b>	ASTM D445	cSt	11
<b>Viscosity index</b>	ASTM D2270	-	140
<b>Flash point</b>	ASTM D92	°C	220
<b>TBN</b>	ASTM D 2896	mg KOH/g	7.5
<b>Pour point</b>	ASTM D97	°C	-39
<b>Foaming at 24°C</b>	ASTM D892	cc/s	Trace/0

**Table 3.3 – Technical data sheet of PETRONAS Tutela Multi CVT 700 oil.**

<b>Parameters</b>	<b>Method</b>	<b>Unit</b>	<b>Value</b>
<b>Density at 15°C</b>	ASTM D4052	g/cm <sup>3</sup>	0.85
<b>Kinematic Viscosity at 100°C</b>	ASTM D445	cSt	7.4
<b>Viscosity index</b>	ASTM D2270	-	185
<b>Brookfield viscosity at -40°C</b>	ASTN D2983	cP	9500
<b>Pour point</b>	ASTM D97	°C	-45
<b>Flash point</b>	ASTM D92	°C	216

**Figure 3.2** shows the standard cooling circuit whereas **Figure 3.3(a)** shows the proposed cooling circuit which has the simplified split cooling with the EHRU. The standard engine has a serial cooling strategy, but the proposed cooling circuit splits the coolant flow from the water pump to both the cylinder block and cylinder head in a parallel manner. Each of the flow partitions exits at the rear ends of the cylinder head and cylinder block. More than 50% of the coolant from the cylinder block is transferred to the cylinder head through gasket apertures in the vicinity of first and second cylinders. A small percentage of coolant flows out from the back of the cylinder block to the cylinder head to avoid trapping of air and boiling coolant. The standard circuit has CVT oil radiator, but the proposed cooling circuit has an oil-to-coolant CVT oil cooler connected to the cooling circuit.

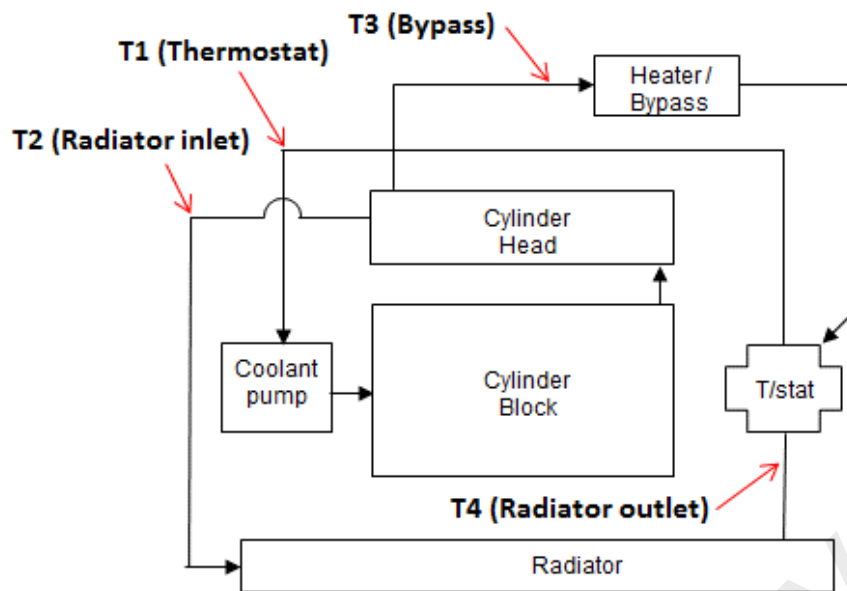


**Figure 3.2: The standard cooling circuit of Proton Iriz.**

**Figure 3.3(a)** shows the proposed cooling circuit with the EHRU located in between the cylinder block outlet and T-junction #2. The cooling circuit shares similarities with the cooling circuits used in the earlier studies (Osman, Yusof & Rafi, 2016; Osman, Razali & Nurdin, 2018) except that the coolant passage in between the two T-junctions is not connected to any heat exchanger. Like the earlier studies, the coolant flows from T-junction #1 to #2 when the thermostat is fully close or partially open (Osman, Yusof & Rafi, 2016; Osman, Razali & Nurdin, 2018). By contrast, when the thermostat is wide or fully open, the coolant flow reverses direction by flowing from T-junction #2 to #1 and certain percentage of the coolant flow coming out of EHRU will be discharged to the radiator together with excess heat recovered from the EHRU. Using this partial flow diversion mechanism, the EHRU can be sized optimally to be sufficient in quickly providing heat during warm-up, idle and part load driving without overheating the engine during full load driving.

Figure 3.3(b) shows the proposed EHRU being sandwiched in between the two flanges. 3-layer metal gaskets are placed on both sides of the EHRU to improve the heat conductivity between the EHRU and the flanges.

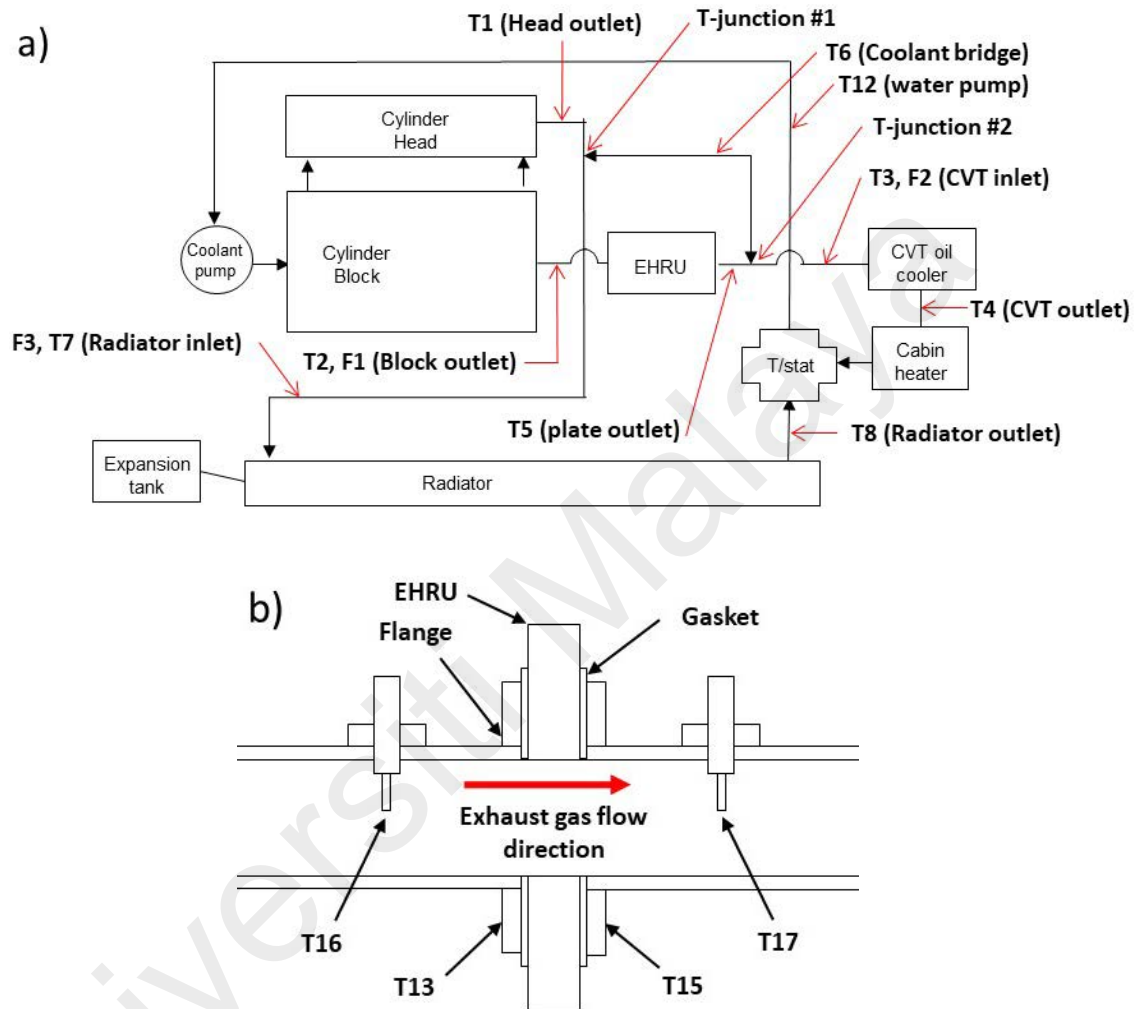


Figure 3.3: a) The proposed cooling circuit and the locations of the EHRU, thermocouples and flow meters. b) Cross section of the EHRU and locations of thermocouples adjacent to EHRU

From the earlier studies, the relatively cooler coolant exiting the cylinder block as per what shown in Figure 2.5 was necessary to sustain the optimum temperature range of 70-80°C for CVT oil instead of 100-110°C for engine oil (Osman, Yusof & Rafi, 2016; Osman, Razali & Nurdin, 2018). Unlike the Demo1 in the above-mentioned study, the

cylinder block's coolant outlet used in this study is located 67 mm from the top deck and the piston stroke is only 73.4 mm. At this location, the outlet is located outside of the top 40% of the piston stroke.

The opening temperatures of the thermostats of standard engine and the proposed cooling circuit are 78°C and 76°C respectively. As shown in **Figure 3.3(a)**, the thermostat of the proposed concept is placed along the bypass passage and it is uniquely controlled mostly by the relatively cooler coolant from the cylinder block. As demonstrated by Demo1 test vehicle in the earlier study, the cylinder head coolant temperature peaked at around 102°C when the thermostat opened at 72°C (Osman, Razali & Nurdin, 2018).

With reference to **Figure 3.3(a)**, the CVT oil cooler is placed in series after the T-junction #2 and EHRU. By placing it there, the CVT oil cooler is the main beneficiary of the heat transfer from the recovered exhaust heat and the hot coolant from the cylinder head. The cabin heater next to it also benefits from the arrangement. Similarly, an engine oil cooler can also be added if necessary either in between the two T-junction or in series with the CVT oil cooler and cabin heater.

### **3.3 Modifications of the standard parts**

In converting the serial cooling to the simplified split cooling circuit, the standard gasket needed to be modified. In **Figure 3.4**, the enlarged apertures are shown in yellow circles whereas the added apertures are shown in red ovals. The revised gasket still retains the two large transfer passages adjacent to the fourth cylinder as shown in **Figure 3.4**. Therefore, there was a need for the coolant apertures from the cylinder head to be blocked instead.

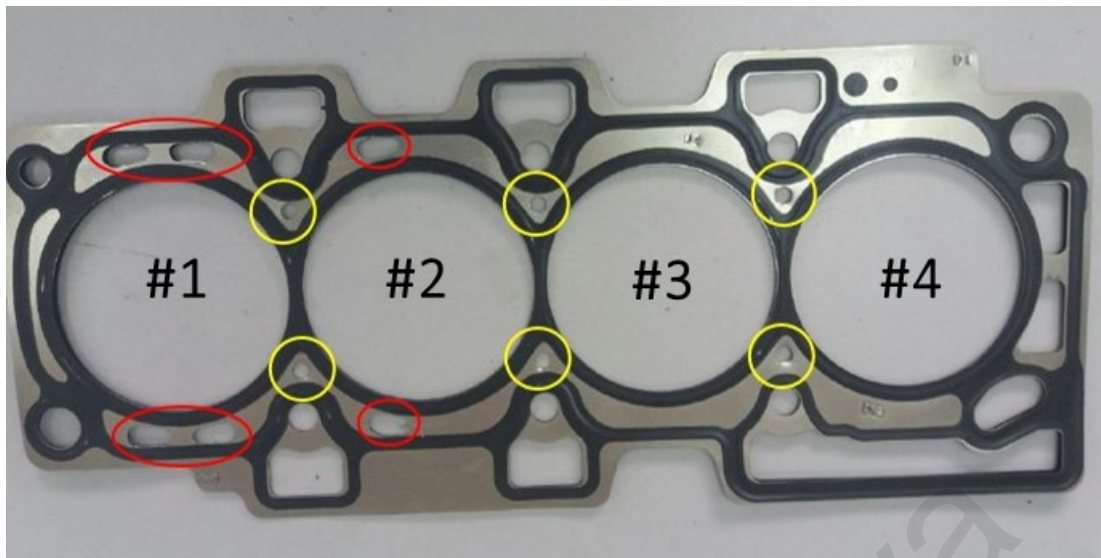


**Figure 3.4:** The coolant transfer holes which were enlarged in yellow circles and the ones added to the gasket are shown in red ovals.

As shown in **Figure 3.5**, the photo on the right shows the coolant transfer passages being sealed with Devcon putty (generally used for metal repair) before being drilled to form an 8 mm diameter coolant transfer hole. As explained earlier, this 8 mm diameter coolant transfer hole is necessary to minimize the trapping of vaporized coolant at the end of the cylinder block's water jacket.

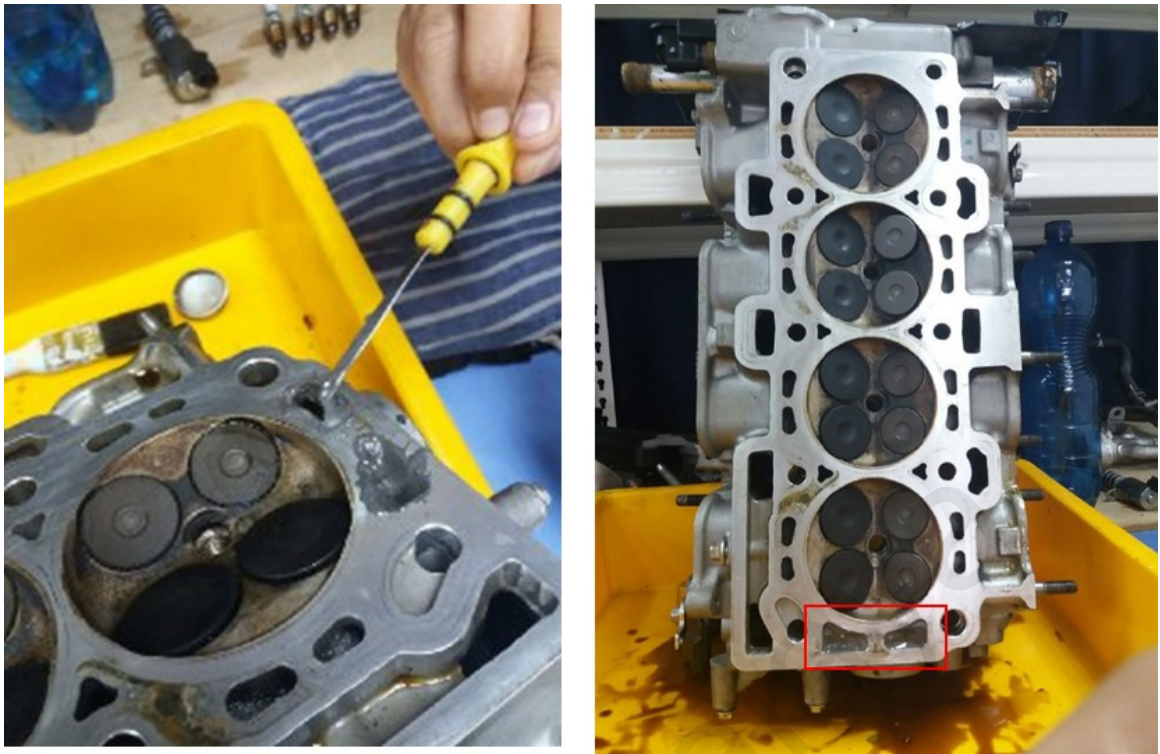


**Figure 3.5:** Left photo: The two apertures at the cylinder head mating face are being filled with Devcon putty generally used for metal repair at the foundry. Right photo: The putty (red rectangular) is close to solidification and the aperture on the left is ready to be drilled to form an 8 mm diameter coolant transfer hole.

The standard engine has the coolant temperature sensor and coolant outlet located adjacent to the front end of the cylinder head. In this context, the original coolant outlet faces the radiator whereas the coolant temperature sensor faces the firewall separating the engine bay and cabin. In ensuring that the coolant temperature sensor provides accurate temperature measurement of the coolant exiting the cylinder head, the temperature sensor was relocated to the back of the cylinder head. The left photo in **Figure 3.6** shows the coolant outlet CNC machined from 6061 aluminium block with the coolant temperature mounted to it. The right photo shows the coolant outlet assembly mounted to the cylinder head using the core plug hole. From the photo, the coolant temperature sensor is in horizontal position to make way for the airbox above it.

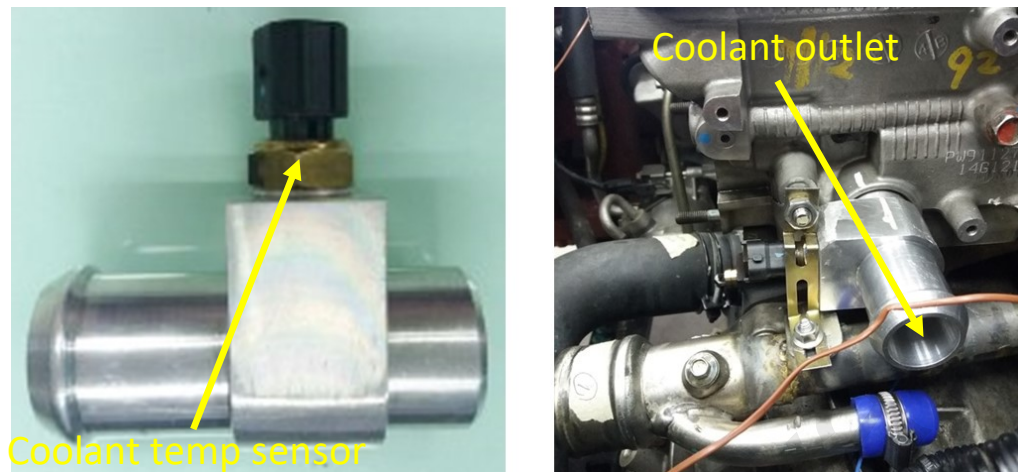


**Figure 3.6: Left photo: Machined coolant outlet with coolant temperature sensor mounted to it. Right photo: Machined coolant outlet after being pushed into the core plug hole at the rear end of the cylinder head.**

**Figure 3.7** shows T-junction being made of HKS coolant hose connector. With reference to **Figure 3.3(a)**, both T-junction #1 and #2 use the same HKS coolant hose connector. By changing the brass connectors and coolant hose diameter, the maximum coolant flow rate passing along coolant passage connecting T junction #1 and #2 can be varied accordingly.



**Figure 3.7: T-junction made from modified HKS coolant hose connector.**

**Figure 3.8** shows the original thermostat pipe with the original thermostat assembled within the pipe. The original thermostat has around 24 mm diameter opening and the small opening is likely to cause high pressure losses which will eventually limits the maximum coolant flow to the radiator. This thermostat was replaced with a thermostat with 30 mm diameter opening from WTI. The WTI thermostat comes together with plastic housing. Considering that the original thermostat was no longer needed, it was removed from the thermostat pipe. **Figure 3.9** shows the revised thermostat pipe with the pipe near the bypass outlet lengthened to allow ample clearance to the coolant outlet at the back of the cylinder head. The airbox bracket was modified to provide ample clearance between the airbox and the coolant outlet.



**Figure 3.8: Left photo: Original thermostat pipe. Centre photo: Original thermostat inside the thermostat pipe. Right photo: WTI thermostat housing with the thermostat integrated within the plastic housing.**



**Figure 3.9: With reference to the original thermostat pipe in Figure 3.8, the pipe near the bypass outlet was lengthened to allow ample clearance to the coolant outlet at the back of the cylinder head.**

**Figure 3.10** shows the original CVT oil radiator used in the Proton Iriz. This oil-to-air heat exchanger is placed in front of the condenser in Proton Iriz. Although it works well in rejecting heat from the transmission oil, such heat exchanger is not able to warm-up the oil as it is not connected with any coolant passage. To address this gap, an oil-to-coolant heat exchanger replaced the oil radiator and it was connected to cooling circuit as shown in **Figure 3.3(a)**.



**Figure 3.10: Left photo: The original CVT oil radiator. Right photo: Oil-to-coolant heat exchanger which replaced the original CVT oil radiator.**

The EHRU is made up of 20 mm thick machined plate with drilled cooling channel inside it as shown in **Figure 3.11**. The long drilled passage connecting the other two drilled passages is plugged with taper plug at both ends of the passage. The coolant flows following the drilled passages as indicated by the blue arrows. Exhaust gas flows through the 53.8 mm diameter machined hole surrounded by three M10 bolt holes.

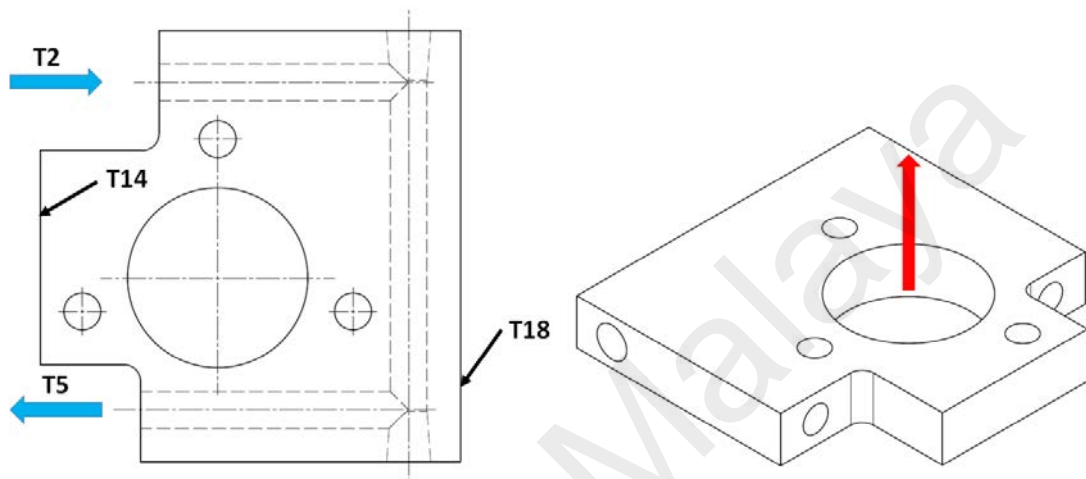


**Figure 3.11: Diagram on the left shows the bottom view of the EHRU with the cooling channel shown by the hidden lines. Diagram on the right shows the isometric view of the EHRU. The blue arrows show the direction of the coolant flow and the red arrow shows the direction of the exhaust gas.**

From **Figure 3.12**, the EHRU is placed in between the flanges of maniverter and the downpipe. 3-layer aluminum gasket (0.3mm thick each) was sandwiched on each side of the EHRU to avoid gas leak. These gaskets were necessary to ensure heat from the maniverter and downpipe can be conducted well to the EHRU.

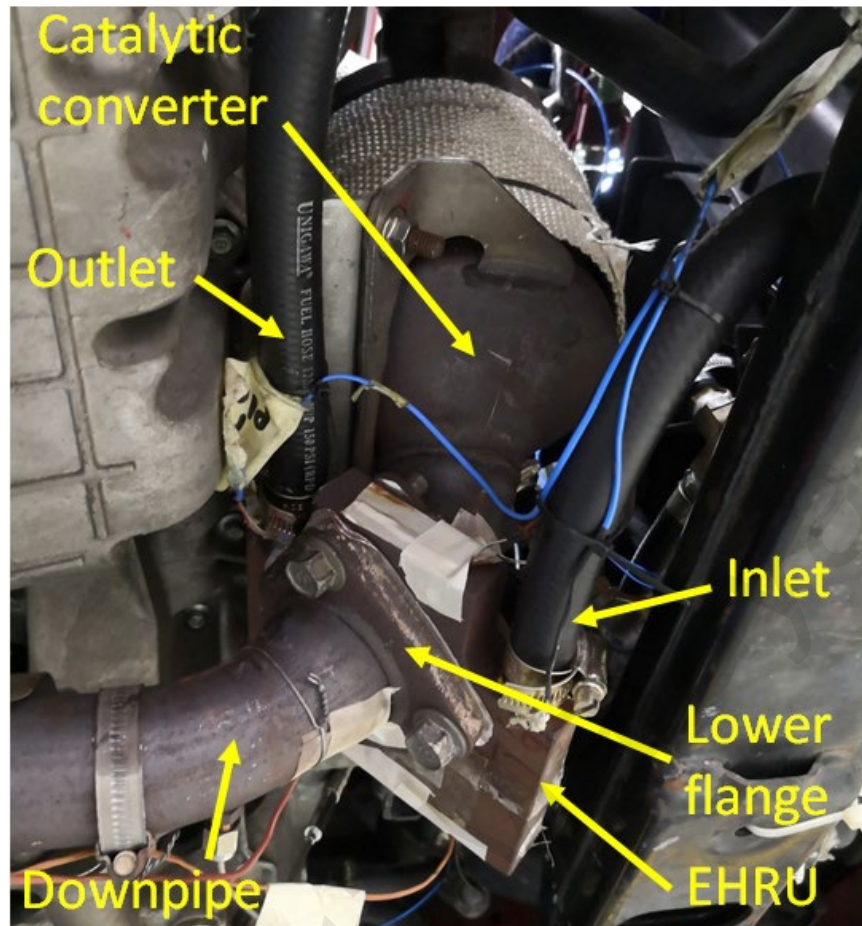


**Figure 3.12: The location of the EHRU which is sandwiched in between the catalytic converter and downpipe.**

### **3.4 Instrumentation of the test vehicle**

**Figure 3.3(a)** shows the locations of thermocouple marked with capital letter “T” and flowmeter marked with capital letter “F”. The readings from the sensors were recorded at 1 Hz to minimize fluctuations. As shown in **Figure 3.13**, Graphtec GL820 was used to record the information from the thermocouples and flowmeter. INCA 7.1 with ETAS interface module was connected to the Bosch ECU to monitor the engine operating parameters especially the engine rpm and exhaust gas mass.

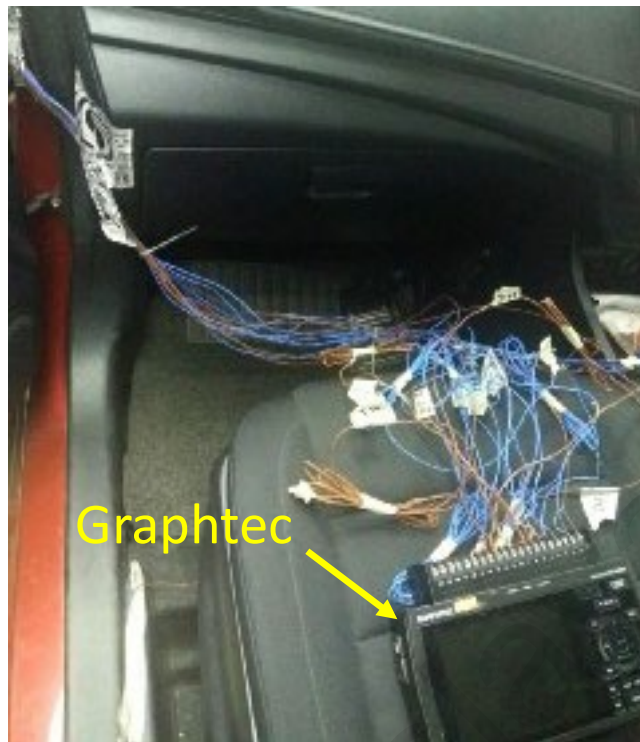


**Figure 3.13: Graphtec connected to various thermocouples and flow meters.**

Compared to the earlier studies (Osman, Yusof & Rafi, 2016; Osman, Razali & Nurdin, 2018), the study this time focuses more on the EHRU itself. Several thermocouples were attached to the EHRU and its surrounding as shown in **Figure 3.14**. As shown in **Figure 3.11**, thermocouple T14 is placed on the “uncooled” side whereas the thermocouple T18 is placed on the “cooled” side adjacent to the coolant. As a result of the temperature difference between the “cooled” and “uncooled” sides increasing during warm-up, the average temperature of the EHRU is as per equation (1). Understanding that the metal temperature of the EHRU is not uniform throughout the engine operations, averaging these two points provides rough estimate of the EHRU’s average temperature.

$$T_{ave} = (T_{14} + T_{18})/2 \quad (1)$$

As shown in **Figure 3.3(b)**, another two thermocouples were attached to the upper flange (designated as T13) and lower flange (designated as T15). Prior to the attachment

of the thermocouple, one layer of the thermal resistance tape was applied to the metal surface to insulate the thermocouple from the hot surface. This first layer of tape prevented the thermocouple insulator from melting while leaving the tip in contact with the metal surface. Once the position of the tip was fixed, another layer of tape was needed to cover the exposed tip and to secure the thermocouple assembly firmly on the surface. To measure the exhaust gas temperatures, two mounting points were welded to the upstream (designated as T16) and downstream (designated T17) exhaust pipes at roughly 50 mm from the upstream and downstream flanges as shown in **Figure 3.3(b)** and **Figure 3.14**. The tip of the thermocouples protruded about 25 to 28 mm into the exhaust pipes to enable exhaust gas temperature at the center of the pipes to be measured.

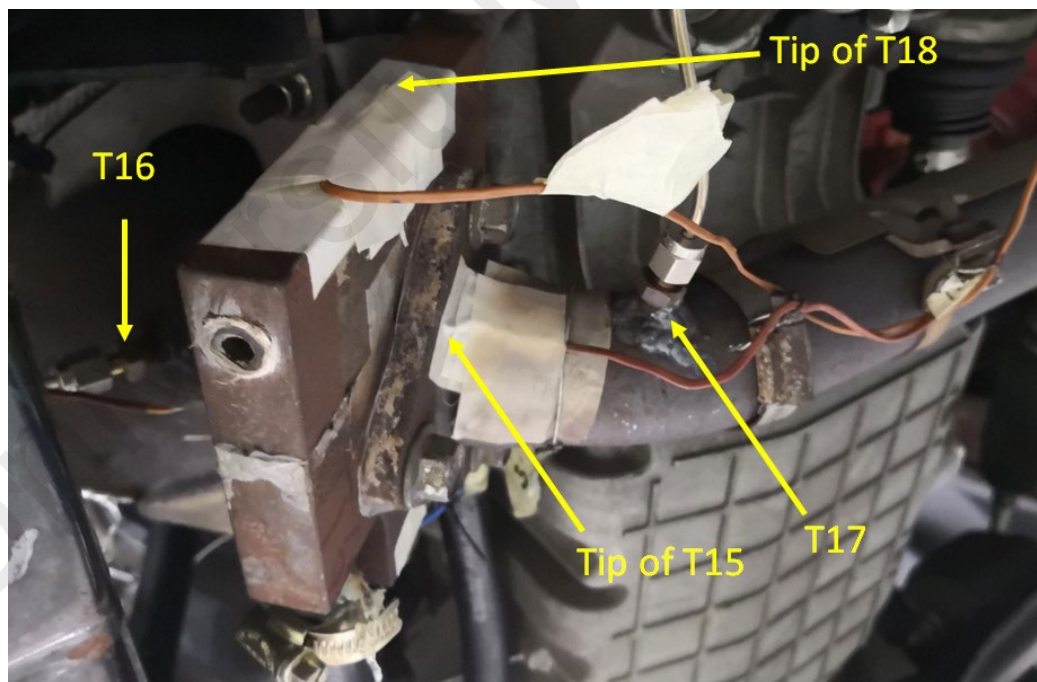


**Figure 3.14: The position of the tip of the thermocouples around the EHRU**

In addition, another two thermocouples were attached to the lower flange (shown in **Figure 3.14** as T15) and upper flange (designated as T13 but not visible in **Figure 3.14**). Prior to the attachment of the thermocouple, one layer of the thermal resistance tape was applied to the metal surface to insulate the thermocouple from the hot surface. This first layer of tape prevented the thermocouple insulator from melting while leaving the tip in contact with the metal surface. Once the position of the tip was fixed, another layer of tape was needed to cover the exposed tip and to secure the thermocouple assembly firmly on the surface.

As shown in **Figure 3.3(a)**, three flowmeters were installed strategically within the cooling circuit. F1 and F2 flowmeters were placed at the proposed locations to enable coolant flow rates to be measured even when the coolant flowing along the T-junction #1 and #2 changes direction in accordance with the thermostat opening. Understanding that the flowmeter works only in one direction, the addition or subtraction of F1 and F2 enables various coolant flow rates at various locations to be measured.

The coolant flow rate coming out of the cylinder block ( $\dot{m}_{block}$ ) can be measured directly at F1. The coolant flow rate coming out of the cylinder head ( $\dot{m}_{head}$ ) can be calculated using equation (2).

$$\dot{m}_{head} = F_2 - F_1 + F_3 \quad (2)$$

### 3.5 Vehicle tests

Since the focus of the study here is to compare the effects of having the EHRU to the warm-up performances, the test vehicle was tested with and without the EHRU. For the tests without the EHRU, the EHRU was moved away from the exhaust system and mounted to the vehicle subframe as shown in **Figure 3.15**. This ensured no heat transfer

from the exhaust system and exhaust gas to the EHRU. This arrangement also ensured no significant cooling circuit pressure difference between the two variants.

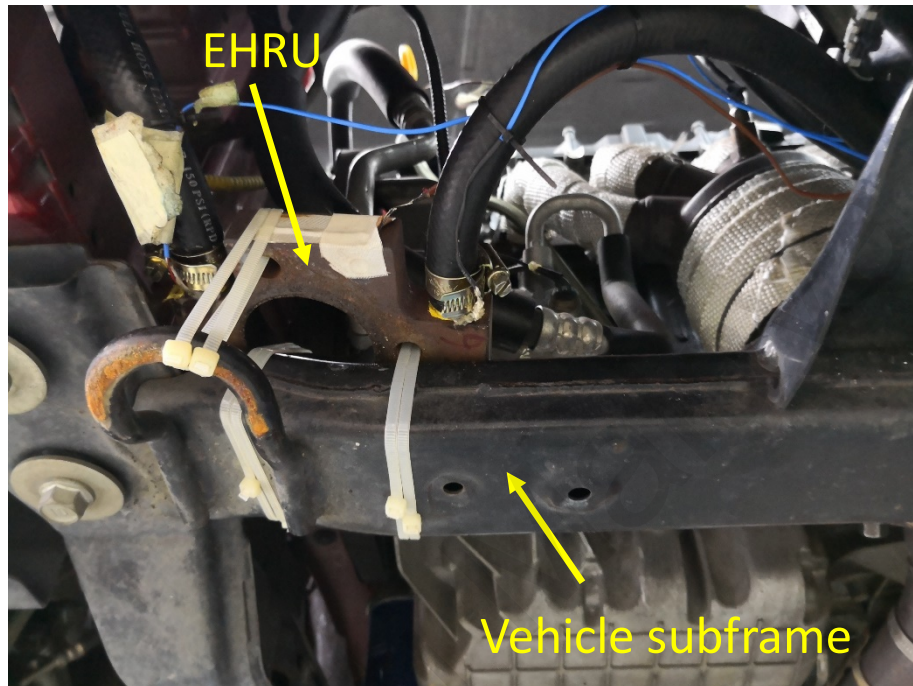


**Figure 3.15: The EHRU attached to the vehicle subframe instead of mounted to the exhaust flanges. This arrangement enabled the tests to proceed without any exhaust heat recovery.**

The first test involved the use of idle test in which the test vehicle was left overnight. The test was conducted within 60 minutes after sunrise with the ambient temperature of 24-27°C. The idle test lasted for 600 seconds and the transmission was left at “P” all the time. There was no driver input other than starting the engine. The idle test was necessary to minimize the interferences from external factors like transmission mechanical losses, test driver’s variations, rolling resistance, etc. Nevertheless, the idle test has its own limitations. For example, the thermal energy discharge is minimum, and the cycle-to-cycle variations are much higher than during the NEDC test.

The second test involved the use of NEDC test as per earlier studies (Osman, Yusof & Rafi, 2016; Osman, Razali & Nurdin, 2018). Although the WLTP is more up-to-date and more relevant to automakers, NEDC was chosen to compare the test results with internal and publicly available test data. Furthermore, the clear separation between the UDC and EUDC phases as shown in **Figure 3.16** enabled more focused data gathering of city and highway driving. **Table 3.4** provides a comparison between the WLTP and NEDC tests.

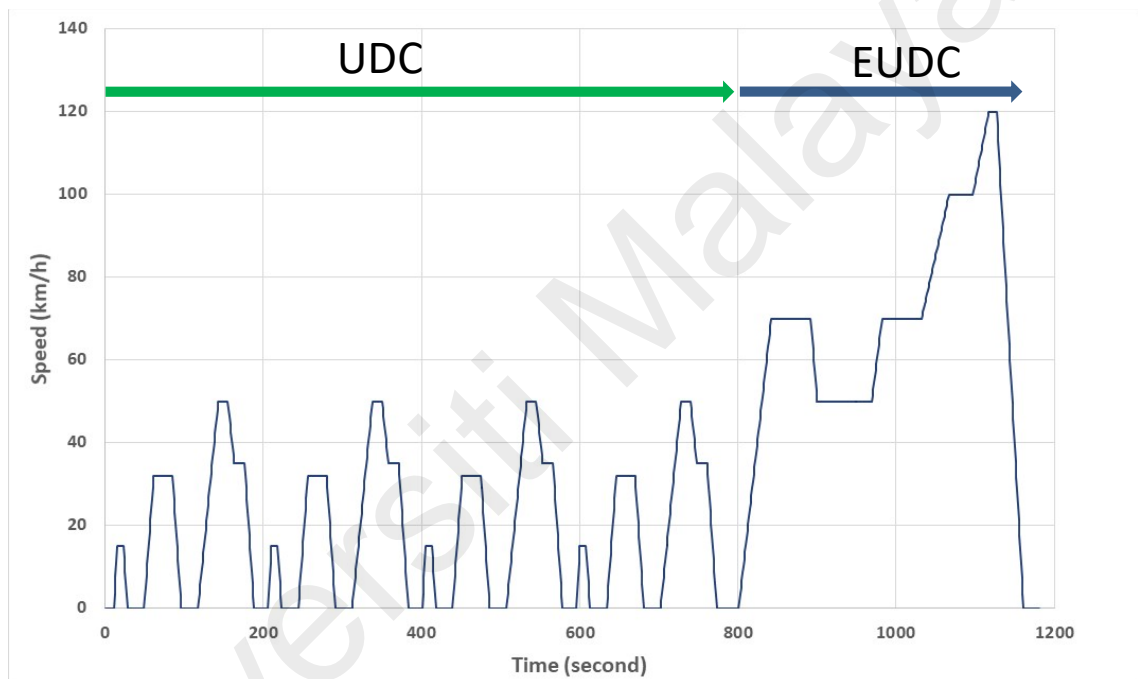


**Figure 3.16: Complete NEDC test cycle consisting of UDC and EUDC phases**

**Table 3.4: Comparison between NEDC and WLTP.**

Item	NEDC	WLTP
Test cycle	Single	Dynamic test cycle + real world validation
Cycle time	20 minutes	30 minutes
Cycle distance	11 km	23.25 km
Average speed	34 km/h	46.5 km/h
Maximum speed	120 km/h	131 km/h
Idling percentage	25%	13%
Acceleration	21%	44%
Constant speed driving	40%	4%
Build variants (test vs production car)	Loose	Fixed and monitored
Manual gear shift points	Fixed	Can be optimized to obtain best result
Test temperatures	20-30°C	23°C
Correlations with real world driving conditions	No requirement	To be measured by onboard emissions measuring equipment from September 2019

Although the earlier study has shown fuel consumption improvement as much as 4% during NEDC with improved warm-up performances (Osman, Yusof & Rafi, 2016), the test vehicle this time was equipped with more modern production powertrain's electronics. The control system requires accurate modeling of important operating parameters specific to the homologation requirements. In view of the major changes to the test vehicle's mechanical components if compared to the production variant, the fuel consumption and raw tailpipe emissions were not measured because both the engine and transmission electronics need to be tediously calibrated before the mechanical improvements in this study can be fully reflected into relevant fuel consumption and emissions improvements. In this context, extensive and time-consuming recalibrations are needed to revise the frictions, cold start and warm-up models within the control strategies. Considering that the expedited warm-up generally yielded fuel economy improvement ranging from 1.6-10.6% (Will & Boretti, 2011; Cipollone, Di Battista & Maurello, 2015; Jehlik et al., 2017; Iliev & Lohse-Busch, 2018; Torregrosa et al., 2008), it was assumed that objective improvements in coolant, engine oil and CVT oil warm-up

would generally improve the fuel consumption during NEDC test. Nevertheless, once certain mechanical targets and milestone are met in the future, the calibration activities can be outsourced to the calibration engineers at Proton.

### 3.6 Theories

#### 3.6.1 Heat transfer classical calculations involving the EHRU.

The various heat transfer to and from the EHRU can be summarized as per equation (3). From equation (3), the conduction heat transfers to EHRU are expected to be dominant throughout the engine operations. In general, the exhaust manifold gets hot quickly during a typical cold start because of the catalyst heating strategy to expedite the catalyst light off process. Since the engine does not have an exhaust VVT, the catalyst heating function is achieved by retarding the ignition timing. Once the catalyst is hot enough, the unburned substances will be oxidized with the help of the catalyst and this process will further add the thermal energy availability within the manifold.

$$q_{\text{EHRU}} = q_{\text{cond1}} + q_{\text{cond2}} + q_{\text{conv}} - q_{\text{coolant}} - q_{\text{surroundings}} \quad (3)$$

With reference to equation (4), as the bottom portion of the manifold gets hotter than the EHRU, heat will be conducted to the EHRU via the manifold flange with surface area ( $A_{\text{flange}}$ ) of 3671 mm<sup>2</sup> and 8 mm thick (L). Considering that the EHRU is continuously being cooled by the coolant exiting the cylinder block, there will be constant conduction heat transfer to the EHRU from hotter metals connected to it. Similarly, as the downpipe gets hotter than the EHRU, heat will also be conducted to the EHRU as represented by equation (5).

$$q_{\text{cond1}} = k * A_{\text{flange}} * (T_{\text{upper}} - T_{\text{ave}})/L \quad (4)$$

$$q_{\text{cond2}} = k * A_{\text{flange}} * (T_{\text{bottom}} - T_{\text{ave}})/L \quad (5)$$

The exhaust gas gets hotter than the EHRU throughout the engine operations. Therefore, convection heat transfer as represented by equation (6) can be expected from the high velocity exhaust gas passing the EHRU's 53.8 mm diameter gas passage as shown in **Figure 3.11** earlier. In using the 20 mm plate thickness, the surface area ( $A_{\text{EHRU}}$ ) of the EHRU that is in contact with the exhaust gas is 3378.6 mm<sup>2</sup>.  $T_{\text{exh in}}$  is the temperature of the exhaust gas passing the 53.8 mm diameter hole.  $T_{\text{EHRU}}$  is the temperature of the 53.8 mm diameter hole's surface in contact with the passing exhaust gas.

$$q_{\text{conv}} = h * A_{\text{EHRU}} * (T_{\text{exh in}} - T_{\text{EHRU}}) \quad (6)$$

Equation (7) represents the recoverable heat from the EHRU. In transporting out the recovered heat, the coolant coming in and out of the EHRU ( $\dot{m}_{\text{coolant}}$ ) is also the same as the coolant flow rate coming out of the cylinder block and this is measured by flow meter F1. The location of  $T_2$  and  $T_5$  thermocouples can be seen in **Figure 3.3(a)**.

$$q_{\text{coolant}} = \dot{m}_{\text{coolant}} * c_{\text{coolant}} * (T_5 - T_2) \quad (7)$$

The EHRU becomes hotter very quickly than the ambient. Therefore, the heat losses to the ambient due to convection and radiation are represented by  $q_{\text{surroundings1}}$  in equation (3). The losses are expected to be higher when the vehicle is moving especially at higher speed.

General equation (8) can be used to calculate the thermal energy absorbed by EHRU's metal. The EHRU's mass ( $m$ ) is 1.6 kg. The specific heat capacity of the AISI 1018 mild steel body ( $c$ ) is 486 J/(kg\*K) and it has thermal conductivity of 51.9 W/m-K.

The temperature of the metal is based on the average metal temperature as specified in equation (1).

$$Q_{\text{metal}} = m * c * (T_{\text{end}} - T_{\text{start}}) \quad (8)$$

Equation (9) can be used to calculate the thermal energy increase in automotive fluids. The specific heat capacities for engine and CVT oils change with changing liquid temperatures. For the engine oil, the specific heat capacity changes from 1900 to 2100 J/(kg\*K) for a temperature range of 50-100°C (Wrenick et al., 2005). By contrast, the CVT oil has its specific heat capacity ranges from 1920 to 2220 J/(kg\*K) for a temperature range of 20-100°C (Quaiyum, 2012).

$$Q_{\text{liquid}} = m(c_{\text{end}}T_{\text{end}} - c_{\text{start}}T_{\text{start}}) \quad (9)$$

The heat transfer from the cylinder block to the coolant exiting the block as measured by thermocouple T2 can be calculated using equation (10). Similarly, the heat transfer from the cylinder head to the coolant exiting the cylinder head as measured by thermocouple T1 can be calculated using equation (11) in which the temperature difference will be referenced to the coolant flowing to the water pump (as measured by thermocouple T12). The heat transfer from the coolant to the CVT oil cooler can be calculated using equation (12). CVT oil cooler absorbs heat from coolant when  $T_4 < T_3$  and this normally happens during cold-start, idle and part load driving. By contrast, when  $T_4 > T_3$ , heat is being transferred from the CVT oil cooler to the coolant and this normally happens during hard driving or right after a hard driving.

$$q_{\text{block}} = \dot{m}_{\text{block}} * c_{\text{coolant}} * (T_2 - T_{12}) \quad (10)$$

$$q_{\text{head}} = \dot{m}_{\text{head}} * c_{\text{coolant}} * (T_1 - T_{12}) \quad (11)$$

$$q_{\text{CVT cooler}} = \dot{m}_{\text{CVT cooler}} * c_{\text{coolant}} * (T_3 - T_4) \quad (12)$$

### 3.6.2 Simplified energy system (SES)

From equations (4) and (5), the existence of 3-layer aluminum gasket on both sides of the EHRU makes it difficult for the conduction heat transfer between the flanges and the EHRU to be regarded as having perfect metal contacts. This also takes into consideration that the multilayer gaskets unnecessarily hinder the perfect conduction process. In quantifying the heat losses across the gasket, it is necessary for the temperature drop to be measured in between the layers. However, the high contact pressures in between the gaskets and flanges present challenges for thermocouples to be placed there for temperature measurements. Similarly, the uneven temperature distribution on EHRU's surfaces due to multiple heat sources and cooling channels will further increase the heat transfer errors.

From equation (6), the constant  $h$  in the equation changes rapidly (Torregrosa et al., 2008) and it requires reasonably accurate Nusselt and therefore Reynolds and Prandtl numbers too (Kandylas & Stamatelos, 1999). Considering that the exhaust gas having to go through the catalyst brick and pipe bend before entering the EHRU, the exhaust gas flow modeling can be challenging. In addition, the ongoing hydrocarbon oxidations before and after the catalyst and rapidly changing engine speed and load throughout the engine operations affect the  $h$  constant from time to time. Furthermore, from equation (6), the average exhaust gas temperatures should be measured with reference to the temperatures at the inlet and outlet of the EHRU and not at the T16 and T17 thermocouple locations. Similarly, the surface temperature must be measured at the surface in contact with the exhaust gas. Unfortunately, placing thermocouples at these locations are also challenging.

In circumventing the limitations in establishing the exhaust heat availability to the EHRU, the EHRU and its surrounding can be simplified as confined by the phantom line shown in **Figure 3.17**. The system consists of the EHRU, truncated exhaust pipes upstream and downstream of the EHRU and flanges connected to the EHRU. The heat transfer to the system can be calculated using the equation (13) below.

$$q_{\text{system}} = q_{\text{exh}} + q_{\text{ext cond1}} + q_{\text{ext cond2}} - q_{\text{coolant}} - q_{\text{surroundings2}} \quad (13)$$

In this case, the thermocouple T16 is the entry point and thermocouple T17 is the exit point of the system. The heat transfer or heat losses from the exhaust gas to the SES can be calculated using equation (14).  $\dot{m}_{\text{exh}}$  can be obtained from the INCA datalogger. The specific heat capacity of the exhaust gas ranges from 1006 to 1207 J/(kg\*K) for temperature range of 280 K to 1400 K (Verem, 2016).

$$q_{\text{exh}} = \dot{m}_{\text{exh}} * c_{\text{exh}} * (T_{16} - T_{17}) \quad (14)$$

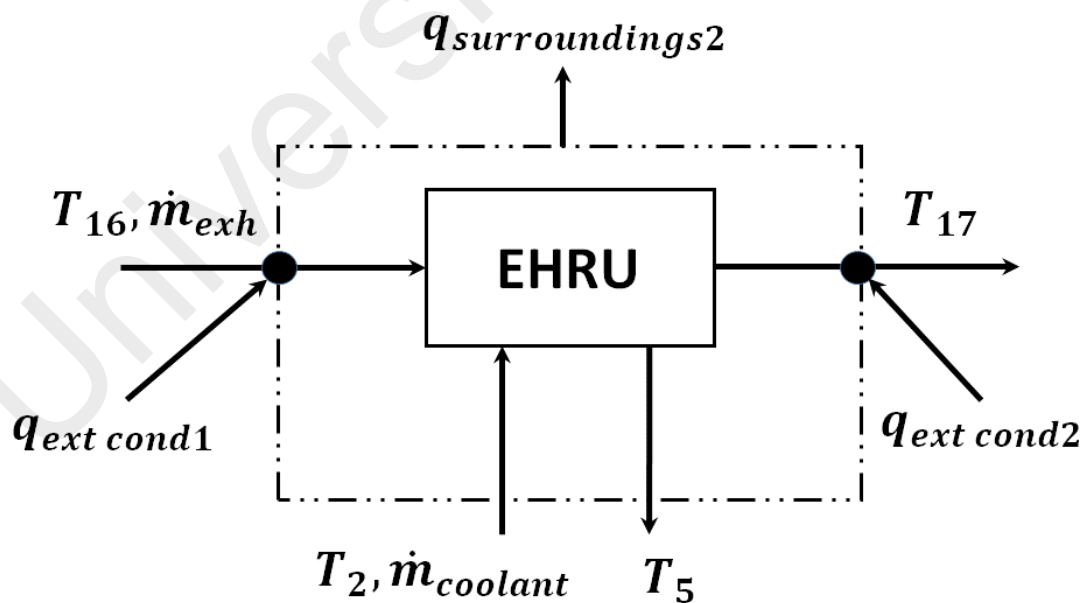


**Figure 3.17: SES to represent the EHRU and its heat sources.**

$q_{ext\ cond1}$  represents the conduction heat transfer from upstream of thermocouple T16. Similarly,  $q_{ext\ cond2}$  represents the conduction heat transfer crossing the thermocouple T17 either towards the EHRU or from the SES to the exhaust pipe downstream of thermocouple T17. In this context, the direction of the heat flow depends on the temperatures of metals, engine load and speed. Estimating the conduction heat transfer requires the temperature of the hot surfaces of the exhaust pipe to be measured. However, unlike at the placement of thermocouple T13, the thin exhaust pipe gets hot during the EUDC phase of the NEDC test. Placing a thermocouple to measure the surface temperature may cause damage to the thermocouple even when surface is insulated with the thermal tape as discussed earlier.

The  $q_{surroundings2}$  is similar to  $q_{surroundings1}$  mentioned earlier except that it represents the heat losses to the surroundings from the SES rather than just the EHRU. Lastly, the efficiency of the EHRU can be calculated using the equation (15) as per what Chiew *et al.* used in their paper (Chiew et al., 2011).

$$EHRU_{eff} = (T_{16} - T_{17}) / (T_{16} - T_2) \quad (15)$$

## CHAPTER 4: RESULTS AND DISCUSSION

### 4.1 Introduction

The experimental results are divided into 2 sections; Idle test and NEDC test. The discussions on the other hand are divided into 3 sections; Connecting the dots, Research gaps and Key findings.

### 4.2 Results

In this section, the results are mainly divided into the test results related to Idle test in Section 4.2.1 and NEDC test in Section 4.2.2.

#### 4.2.1 Idle test

From **Figure 4.1**, the coolant exiting the cylinder block and cylinder head has higher temperature increase rates for the cooling circuit with EHRU. If compared to the variant with no EHRU, the recovered exhaust heat increased the coolant temperature exiting the cylinder block more than for the coolant exiting the cylinder head.

From **Figure 4.1**, the flanges measured by T13 and T15 thermocouples show rapid increase in metal temperatures in the first 30 seconds following the increase in exhaust gas temperatures. From the graph, the cylinder head coolant temperature (as measured by thermocouple T1) at the beginning is quite close to the readings from thermocouples T13 and T15. As pointed out by point *a*, there is even a short period of time where the cylinder head coolant temperature is slightly higher than both the flanges' temperatures. As pointed out by point *b*, the temperature of the hot side of the EHRU (measured by thermocouple T14) on the other hand, stays below the coolant temperature exiting

cylinder head until the  $t = 242$  s whereas the cold side of the EHRU (thermocouple T18) stays below the coolant temperature.

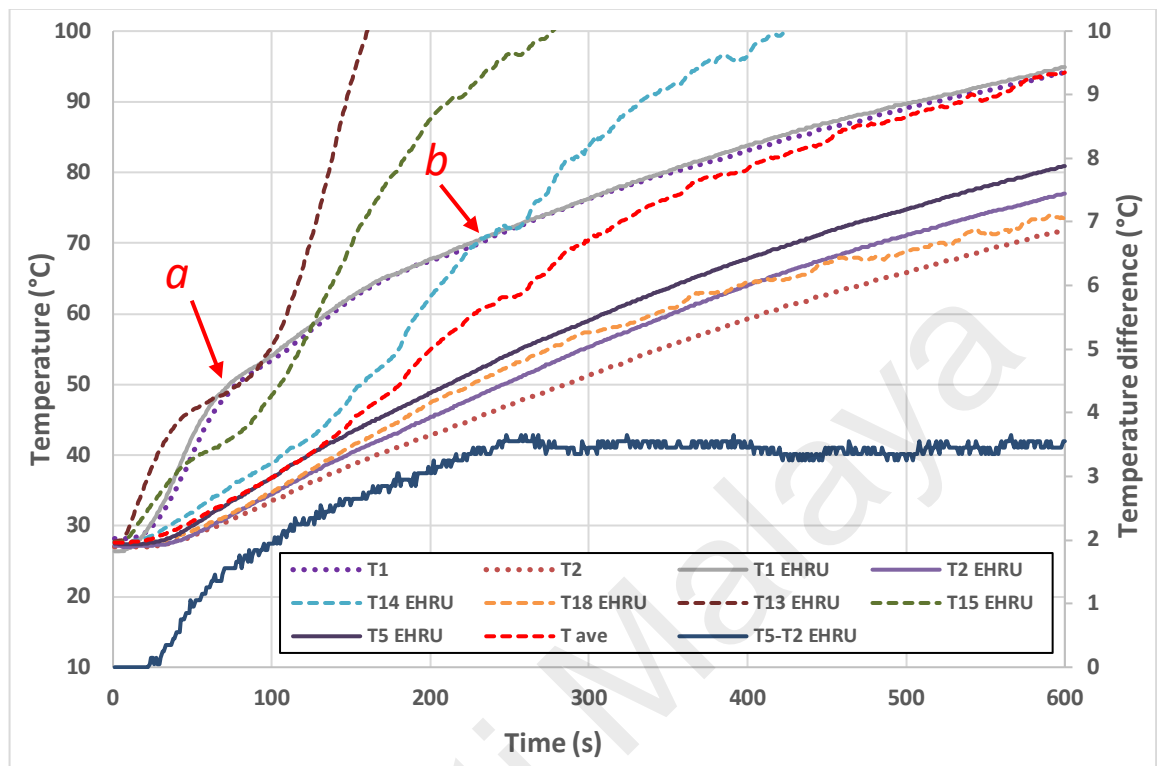


**Figure 4.1: Comparison of temperature increases of coolant and metals during idle test for cooling circuit with and without the EHRU.**

Although the flanges on both sides of the EHRU are not overlapping the coolant passage inside the EHRU, the lower flange as shown in **Figure 3.11** provides rough footprint for the conduction heat to be transferred from the flanges to the EHRU. In case the coolant feed to the EHRU comes from the cylinder head, some portion of the precious heat from the relatively hotter coolant will be wastefully absorbed by the EHRU and both the flanges.

By contrast, the upper and lower flanges together with EHRU surfaces as measured by thermocouples T14 and even T18 as shown in **Figure 4.1** are hotter than the coolant exiting the cylinder block (measured by thermocouple T2) right after the cold start and

the differences rapidly increase afterwards. These temperature differences induced rapid heat movement from the hotter metals to the coolant. Consequently, the temperature difference between the coolant entering and exiting the EHRU ( $T_5 - T_2$ ) increases from the  $t = 23$  s of the idle test.

From **Figure 4.2**, the coolant temperature entering and leaving the CVT oil cooler are both higher for the variant with EHRU. The increasing temperature difference between the coolant and oil increased the heat exchanger efficiency. In this context, the cooling circuit with EHRU has higher coolant temperature difference between the inlet and outlet of the CVT oil cooler after certain time. From **Figure 4.2**, the EHRU variant is slightly hotter from the  $t = 94$  s and the gap widened after the  $t = 125$  s (point *c*). Therefore, the CVT oil for the EHRU variant as shown in **Figure 4.3** is hotter but only after the  $t = 210$  s (point *d*) onwards. The delay was likely to be caused by the large thermal inertia of the 4 litre CVT oil and 55 kg (measured) of gearbox metals.

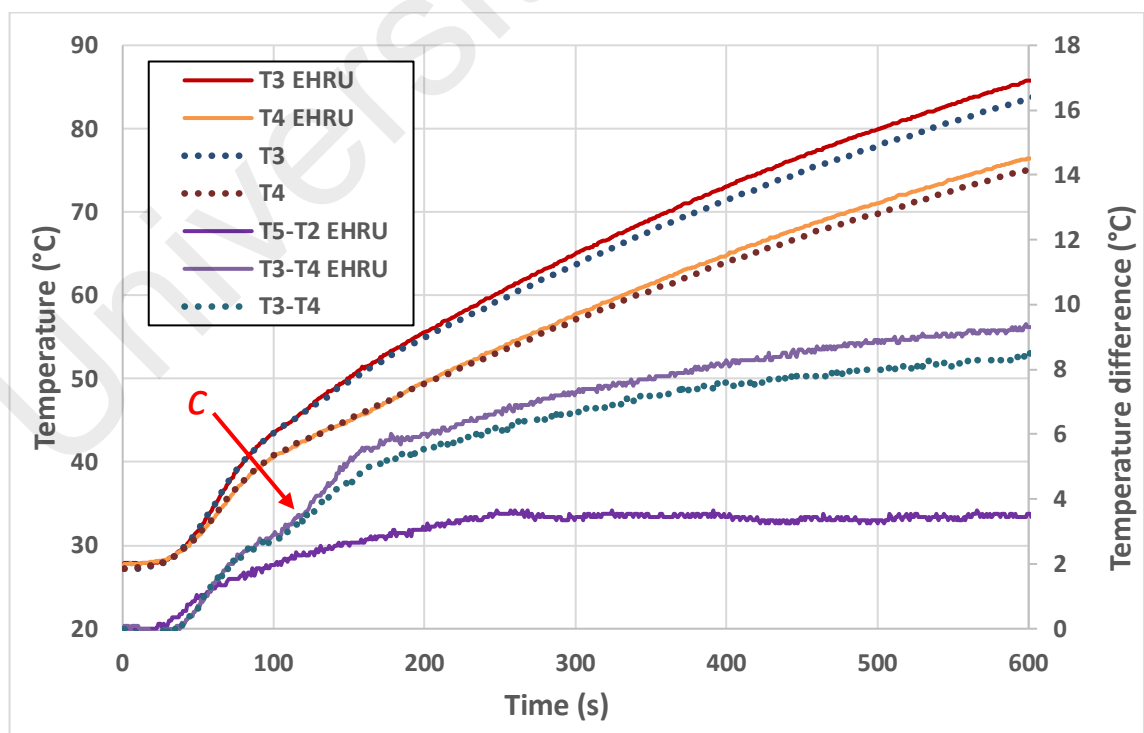


**Figure 4.2: Comparison of temperature increase at the CVT oil cooler during idle test for cooling circuit with and without the EHRU.**

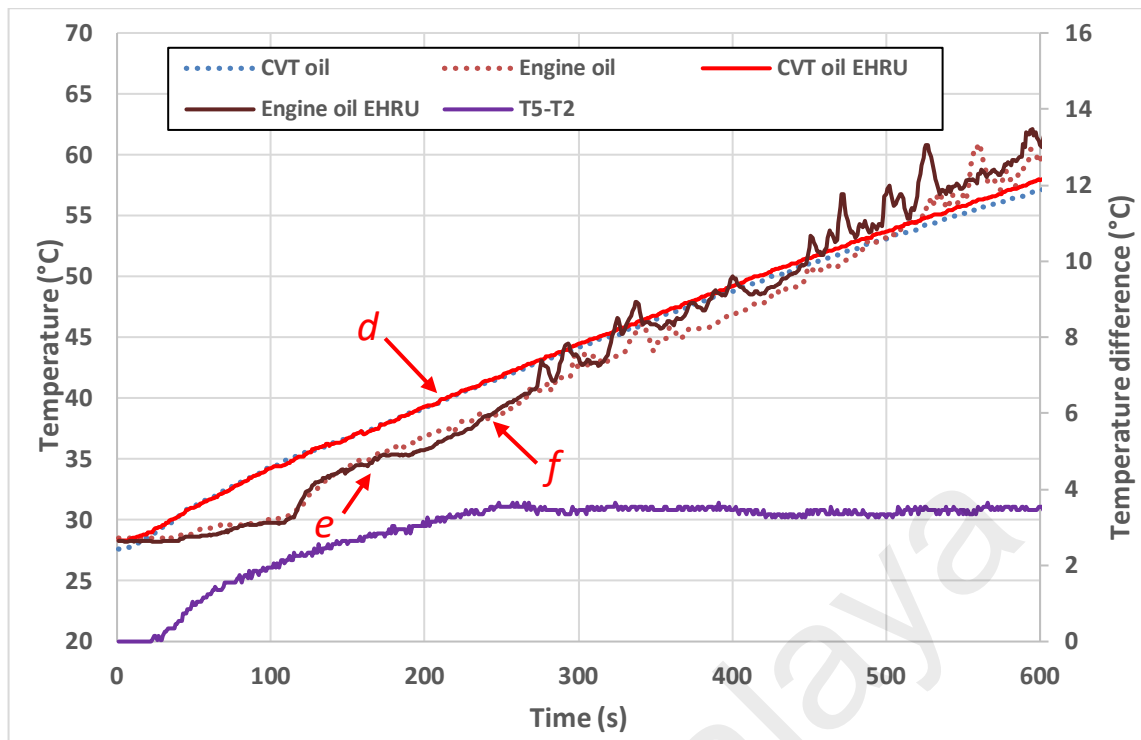


**Figure 4.3: Comparison of temperature increase for CVT oil and engine oil during idle test.**

From **Figure 4.3**, engine oil temperature increase is lower for the EHRU variant from the  $t = 170$  s (point *e*) to  $t = 240$  s (point *f*). However, the trend reverses after the  $t = 240$  s. In the absence of engine oil cooler, the higher coolant temperatures in the cylinder head and cylinder block of the EHRU variant contributed to make the engine oil hotter.

From **Figure 4.4**, the heat transfer from the cylinder head to the coolant is much higher than from the cylinder block throughout the test. In fact, the coolant flowing into the engine was losing heat to the cylinder block from the early part of the test right until  $t = 425$  s (range *y*). The hot coolant from the water pump flowed into the cylinder block and the cooler metals of the bottom half of the cylinder bores absorbed as much as 200 W of heat from the coolant. Considering that the coolant was losing heat to the cold metals, the

coolant exiting the cylinder block was cooler than the coolant entering the water pump (as measured by thermocouple T12).

From **Figure 4.4**, the CVT oil cooler absorbed close to 1000 W of heat from the coolant. Most of the heat came from the coolant exiting the cylinder head and smaller percentages came from the EHRU and cylinder block.

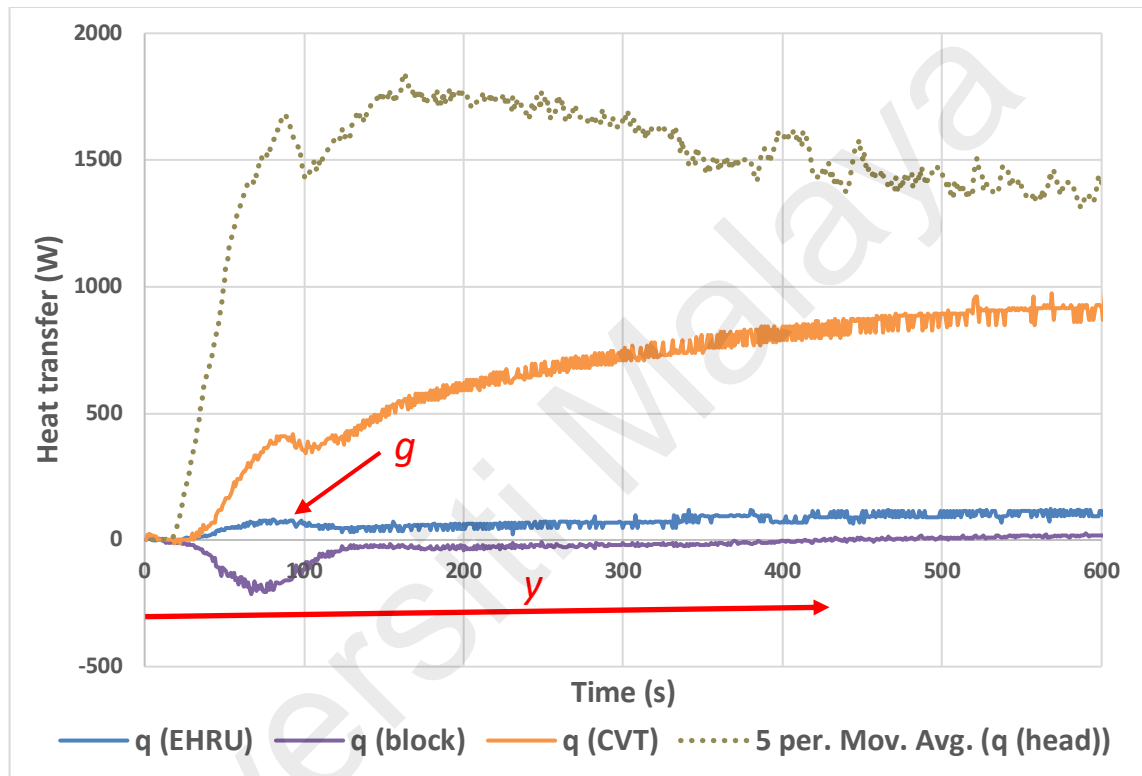


**Figure 4.4:** Various heat transfers within the cooling circuit during the idle test.

From **Figure 4.4**, the heat transfer to the EHRU is responding rapidly to the catalyst heating function at the beginning of the cold start. Once the catalyst heating intensity was decreased, the amount of the heat absorbed by the EHRU also dropped accordingly starting from  $t = 80$  s onwards as pointed out by point *g*. Similar drops can be seen to the heat transfers involving CVT oil cooler and cylinder head as well. Throughout the test,

120 W was the highest heat absorbed by the EHRU. The heat recovered during idle was small but still significant especially for an engine with just 1.3l displacement.

From **Figure 4.5**, the accumulated thermal energy profiles between the exhaust heat losses and EHRU confirmed that the thermal energy accumulated by the EHRU was lower than the exhaust heat losses during idle. As much as 43 kJ of heat was recovered by the EHRU compared to 94 kJ of exhaust heat losses. By contrast, as much as 386 kJ of heat was absorbed by the CVT oil cooler.

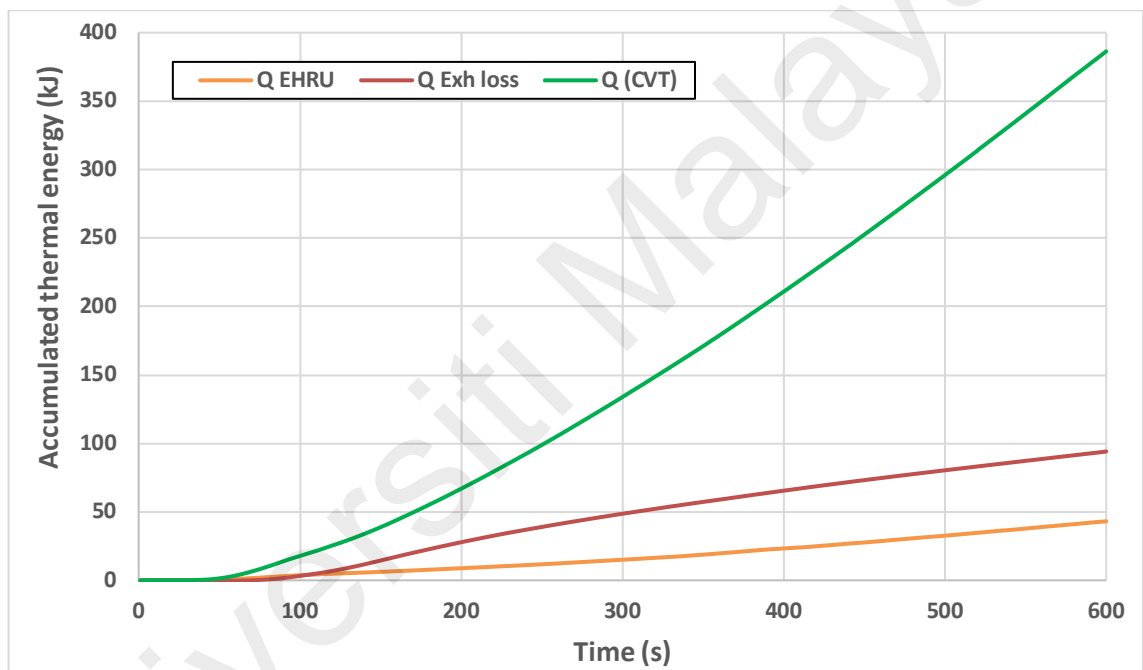


**Figure 4.5: Comparison of various accumulated thermal energy transferred within the SES during idle test.**

#### 4.2.2 NEDC test

From **Figure 4.6**, metal surfaces as measured by thermocouples T13, T14 and T15 are clearly hotter than the coolant exiting the cylinder block as measured by thermocouple T2. Even the thermocouple T18 which was located adjacent to the coolant passage of the EHRU detected higher temperature than the coolant exiting the cylinder block from  $t = 133$  s (point *h*) onwards. By contrast, the coolant exiting the cylinder head measured by thermocouple T1 is hotter than the EHRU until  $t = 205$  s (point *i*) of the test. Furthermore, the coolant temperature is also hotter than the lower flange (measured by thermocouple T15) from  $t = 49$  s until  $t = 114$  s second.

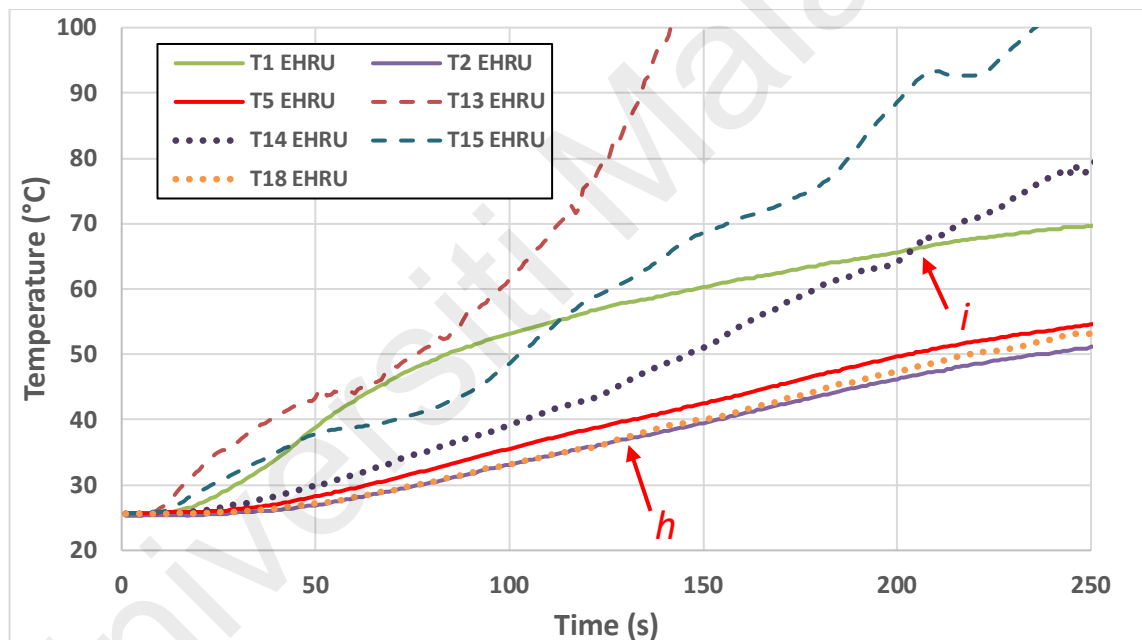


**Figure 4.6 – Interactions between coolant and metals during the early part of NEDC test.**

From **Figure 4.7**, the exhaust gas temperature difference between the upstream and downstream of the EHRU as measured by thermocouples T16 and T17 increases from  $t = 15$  s for the variant with EHRU and  $t = 52$  s for the variant without EHRU. The 37 seconds difference shows the significance of the EHRU in absorbing exhaust heat.

Consequently, the coolant temperature difference between the inlet and outlet of EHRU gradually increases from the  $t = 25$  s onwards indicating the initiation of the exhaust heat recovery and reuse that would eventually affect the warm-up process. As shown in **Figure 4.8**, the temperature difference between the coolant entering and exiting the EHRU somewhat stabilizes at around  $3\text{--}4.2^\circ\text{C}$  from  $t = 197$  s to  $t = 1134$  s. After this period, the number climbs up to  $6.1^\circ\text{C}$  especially when the EHRU and its surrounding were still hot, but the water pump speed dropped nearing the end of the test.

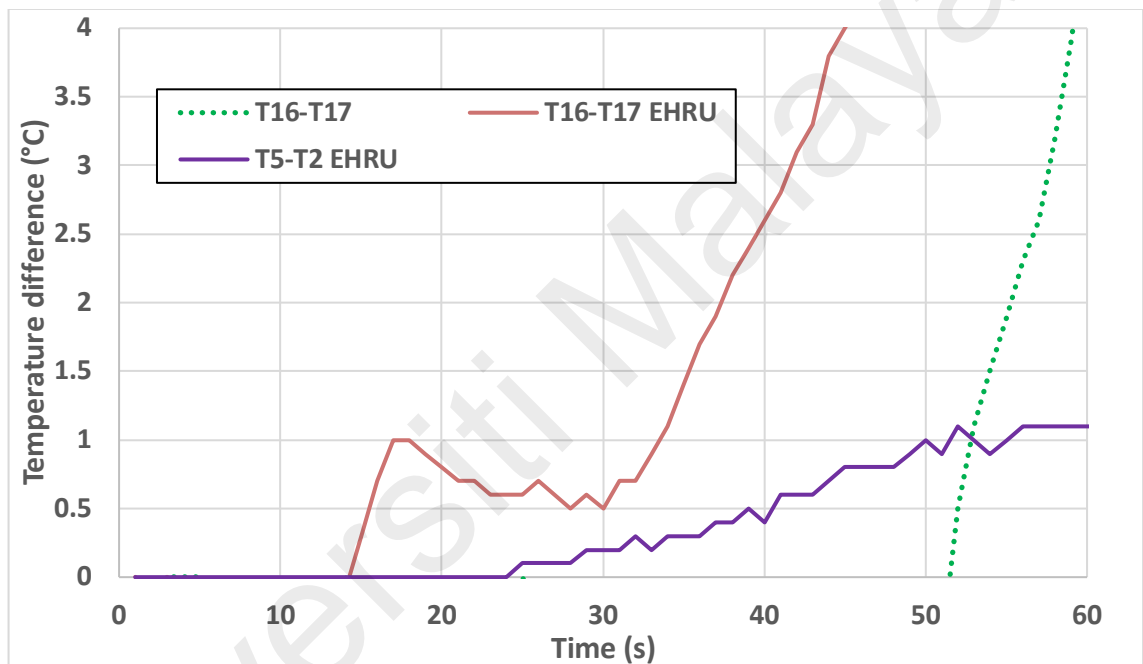


**Figure 4.7 – Chain of events that lead to the start of exhaust heat recovery and reuse.**

From **Figure 4.8**, the coolant exiting the cylinder head for the EHRU variant becomes hotter than the other variant from  $t = 58$  s (point *j*) onwards and this is 33 seconds after the exhaust heat recovery and reuse starts. Consequently, the thermostat opens earlier at the  $t = 714$  s (point *k*) followed by  $t = 812$  s (point *l*) for the non-EHRU variant.

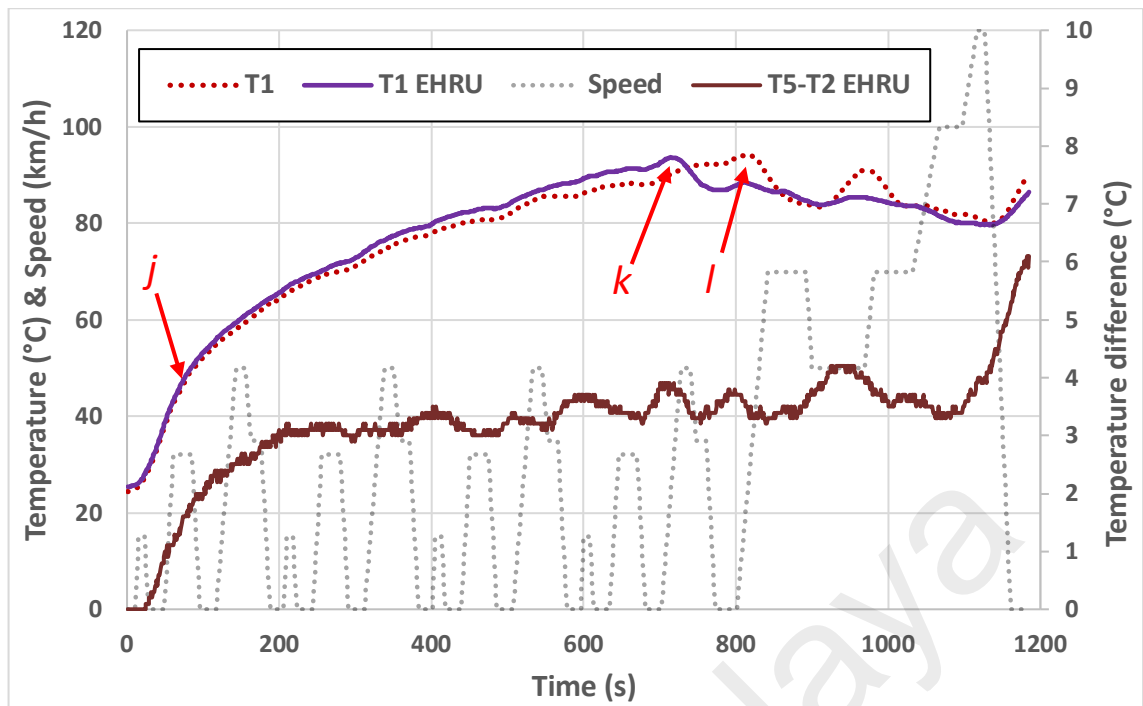


**Figure 4.8 – Comparison of coolant temperatures with and without the EHRU.**

Similarly, the coolant exiting the cylinder block (measured by thermocouple T2) becomes hotter but at higher rate as shown in **Figure 4.9**. In addition, the coolant entering the water pump (measured by thermocouple T12) is also hotter for the variant with EHRU. Interestingly, the coolant entering the water pump is hotter than the coolant exiting the cylinder block until  $t = 187$  s (point *m*) for the variant with EHRU compared to until  $t = 380$  s (point *n*) for variant without EHRU. The drop in temperature as the coolant exits the cylinder block indicated significant heat loss to the cylinder block.

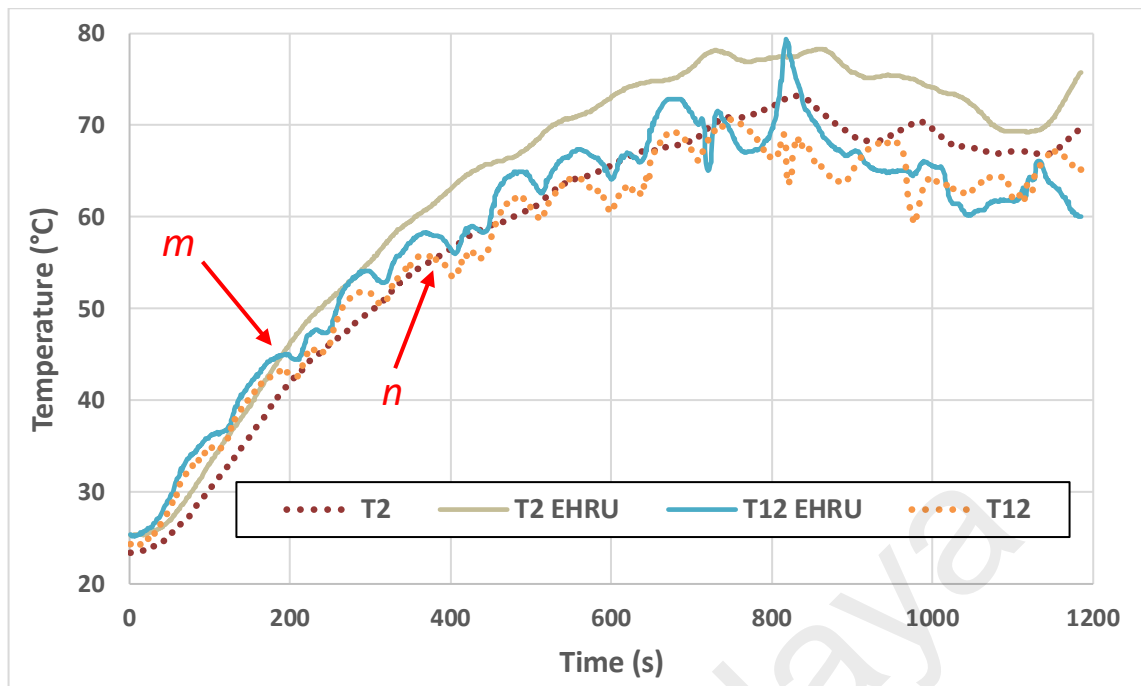


**Figure 4.9 – Comparison of coolant temperatures with and without the EHRU**

From **Figure 4.10**, the temperatures of the coolant entering and exiting the CVT oil cooler are higher for variant with EHRU. These relatively higher coolant temperatures increase the temperature difference between the coolant and CVT oil in the CVT oil cooler. In addition, the coolant temperature difference between the inlet and outlet of the oil cooler is also higher than the variant without EHRU from  $t = 120$  s onwards (point  $p$ ) until the thermostat opens at  $t = 714$  s. Both these phenomena improved the heat transfer to the CVT oil and its temperature increases at a much higher rate than the variant without EHRU as shown in **Figure 4.11**. The engine oil for variant with EHRU also has relatively higher temperature increase rate throughout most of the test duration.

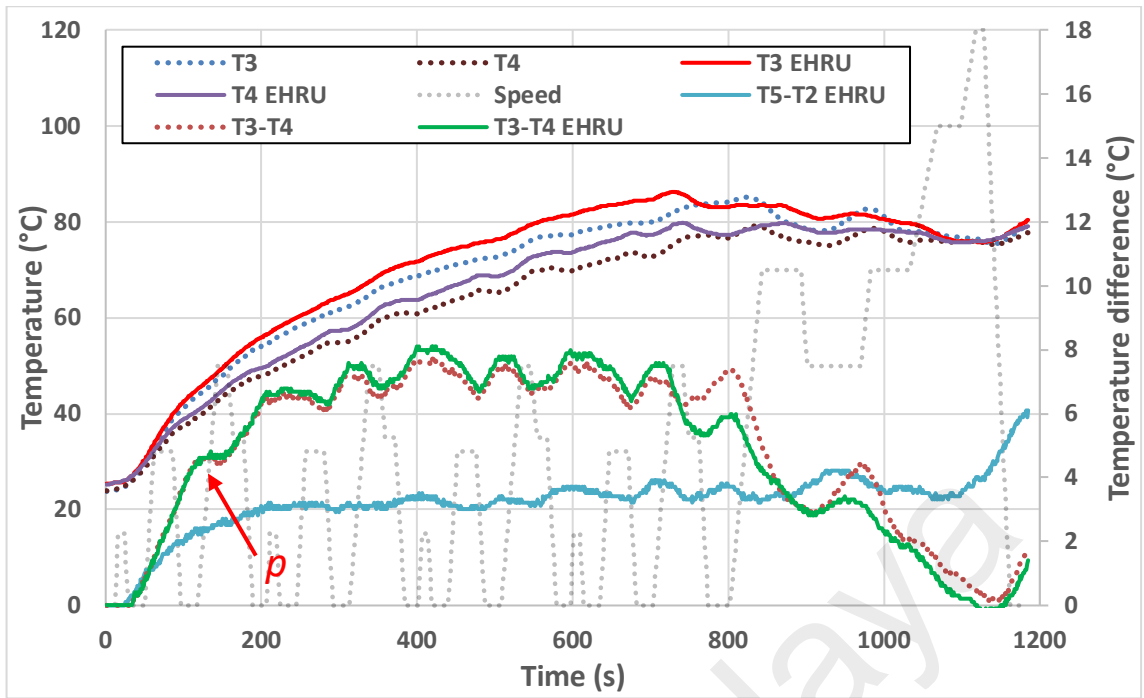


Figure 4.10 – Comparison of temperature increase at the CVT oil cooler during NEDC test for cooling circuit with and without the EHRU.

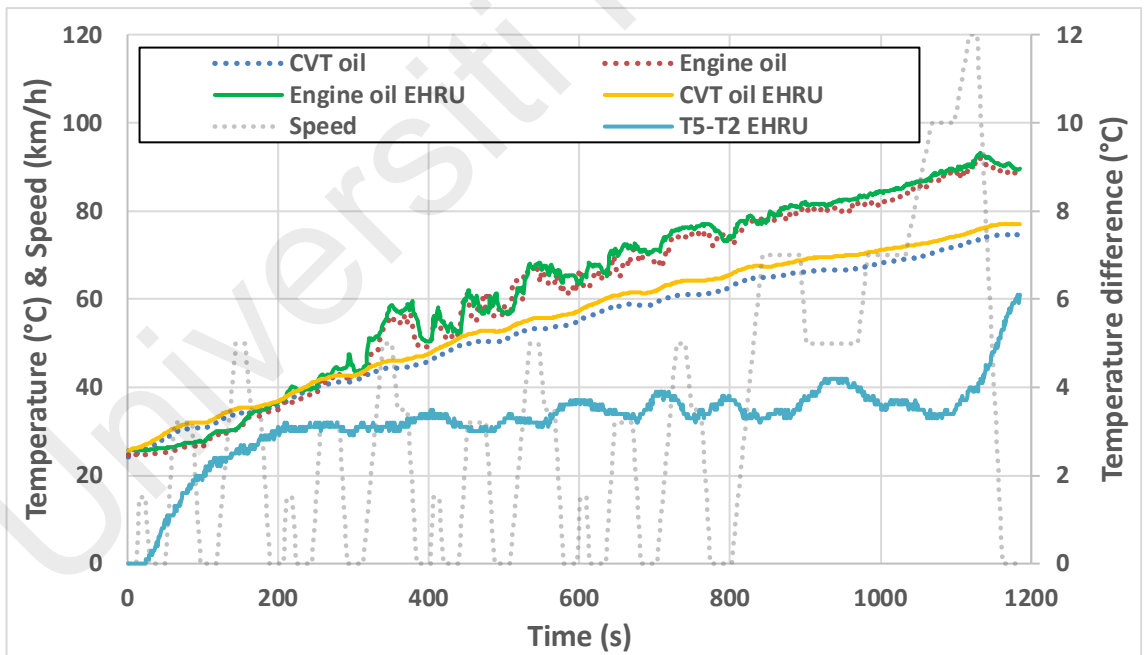
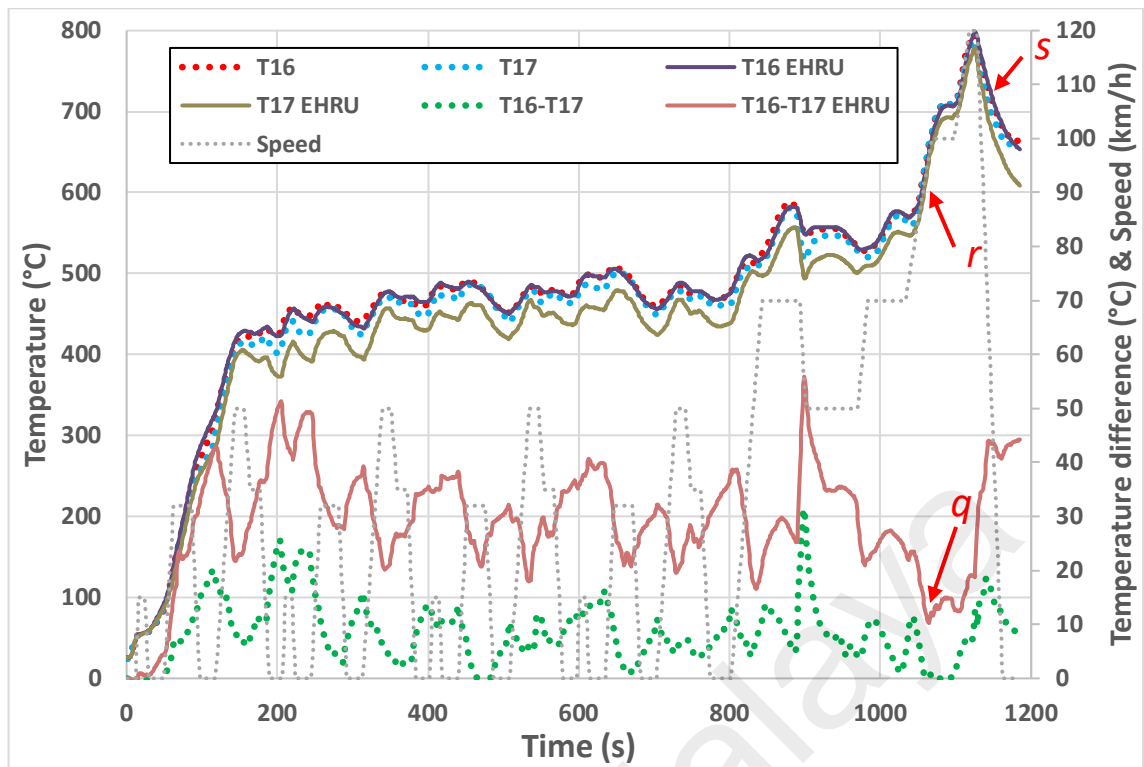


Figure 4.11 – Comparison of temperature increase for CVT oil and engine oil during NEDC test.

From **Figure 4.12**, the exhaust gas temperatures measured by thermocouple T16 for both variants are not much different. However, the exhaust gas temperature measured by thermocouple T17 for the variant with EHRU is up to 55°C cooler meaning that the heat losses between the two thermocouples were higher. The difference once again shows the significance of the EHRU in absorbing heat from the exhaust gas within the SES. The exhaust gas temperature difference as measured by thermocouples T16 and T17 for the EHRU variant drastically dropped to below 15°C from  $t = 1057$  s to  $t = 1111$  s (point *q*). The sudden drop happened when the test vehicle was accelerating hard (point *r*) and the engine speed, load and exhaust gas temperature were high. Interestingly, as the test vehicle decelerates (point *s*), the exhaust heat losses increase rapidly once again. Simultaneously as shown in **Figure 4.13**, the temperature of the upper flange (measured by thermocouple T13) rapidly drops although there is not much temperature change for the lower flange (measured by thermocouple T15). This indicated that the large heat transfer to the upper flange was no longer sustainable during the deceleration.



**Figure 4.12 – Comparison of temperature profiles for the exhaust gas during NEDC test.**

From **Figure 4.13**, both the metal temperatures for upstream and downstream flanges for the EHRU variant increase rapidly from 200 to 291.8°C and 140.2 to 196.4°C respectively from  $t = 1037$  s to  $t = 1128$  s. These rapid metal temperatures increase started 20 seconds earlier before the rapid drop in exhaust gas heat losses marked as point  $q$ . The delay suggested that as the metal temperatures of the flanges measured by thermocouples T13 and T15 increased above 210°C and 147.2°C respectively, the hot metal surfaces within the SES were hot enough that the heat transfer from the exhaust gas was minimum. Although the measured temperatures are not accurately representing the surface temperatures in contact with the exhaust gas at temperature above 550°C, it can be assumed that the actual temperatures of the metal surfaces were far higher than the flanges' temperatures.

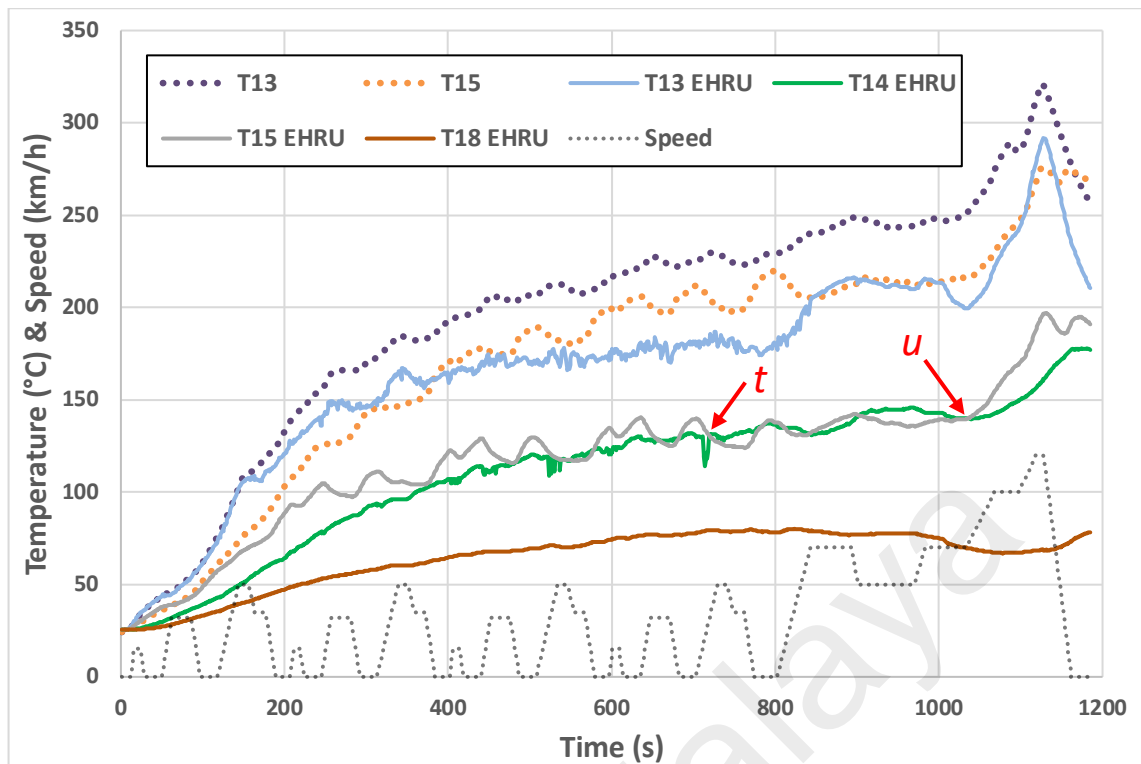


**Figure 4.13 – Comparison of temperature increase for the exhaust system and EHRU during NEDC test.**

From **Figure 4.13**, the variant without the EHRU has hotter upper and lower flanges if compared to the variant with EHRU. By contrast, the cooling effect of the EHRU has reduced the temperatures of the upper and lower flanges for the variant with EHRU. In addition, with the EHRU placed in between these flanges, the temperature difference between the upper and lower flanges is larger. The upper flange is much hotter than both the cooled and uncooled (measured by thermocouples T18 and T14 respectively) sides of EHRU. This suggested that there was a continuous heat transfer from the upper flange to the entire EHRU. The lower flange is also hotter than the cooled side of the EHRU throughout the test suggesting there was a continuous heat transfer from the lower flange to the cooled side of EHRU and the coolant flowing in the coolant passage. However, the graph also shows that the lower flange is only hotter than the uncooled side in the first half of the test. This indicated that the bulky uncooled side of the EHRU had thermal

inertia high enough that it needed enough time for the temperature to be roughly equilibrium with the lower flange from around  $t = 720$  s (point  $t$ ) onwards. Nevertheless, the lower flange's temperature increases rapidly from  $t = 1050$  s (point  $u$ ) suggesting that the conduction heat transfer to the uncooled side of the EHRU happened once again during the high speed phase of the EUDC.

From **Figure 4.14**, the coolant exiting the cylinder head has the highest heat transfer of up to 6.4 kW. By contrast, the coolant exiting the cylinder block has the highest heat transfer of 2.14 kW. The CVT oil cooler has the highest heat transfer of 2 kW. As shown in **Figure 4.15**, the maximum heat transferred out of the EHRU is 1.24 kW. By contrast, the maximum exhaust heat losses to the SES is lower at 1.06 kW. Interestingly, as the test vehicle enters the EUDC phase, the heat transferred from the coolant to the CVT oil drops from the  $t = 968$  s (point  $v$ ) due to the increase in CVT oil temperature from the transmission's mechanical losses. The high mechanical losses during the 120 km/h drive caused the CVT oil cooler to switch its function by briefly cooling the CVT oil until the end of the 120 km/h drive. It once again supplied heat to the CVT oil when the test vehicle idled as it approached the end of the cycle.

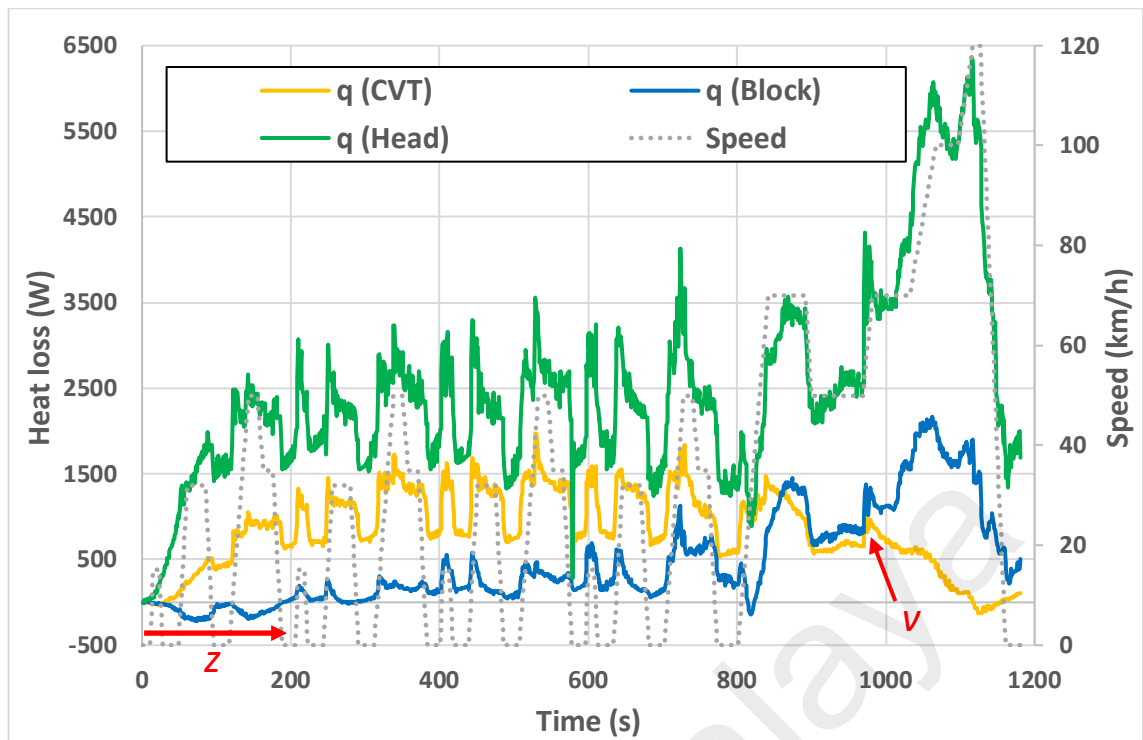


**Figure 4.14 – Comparison of various heat transfers during NEDC test.**

From **Figure 4.15**, the exhaust heat losses are generally higher than the heat transfer from the EHRU to the coolant during the UDC phase. However, the trend reverses during the EUDC phase. As shown in **Figure 4.13**, the temperatures of both the upper and lower flanges spike after point *u* resulting in large temperature differences between the flanges and the cooled side of the EHRU. These large temperature differences indicated large conduction heat transfers from the flanges to the EHRU that would eventually reach the coolant flowing inside the EHRU through convection heat transfer.

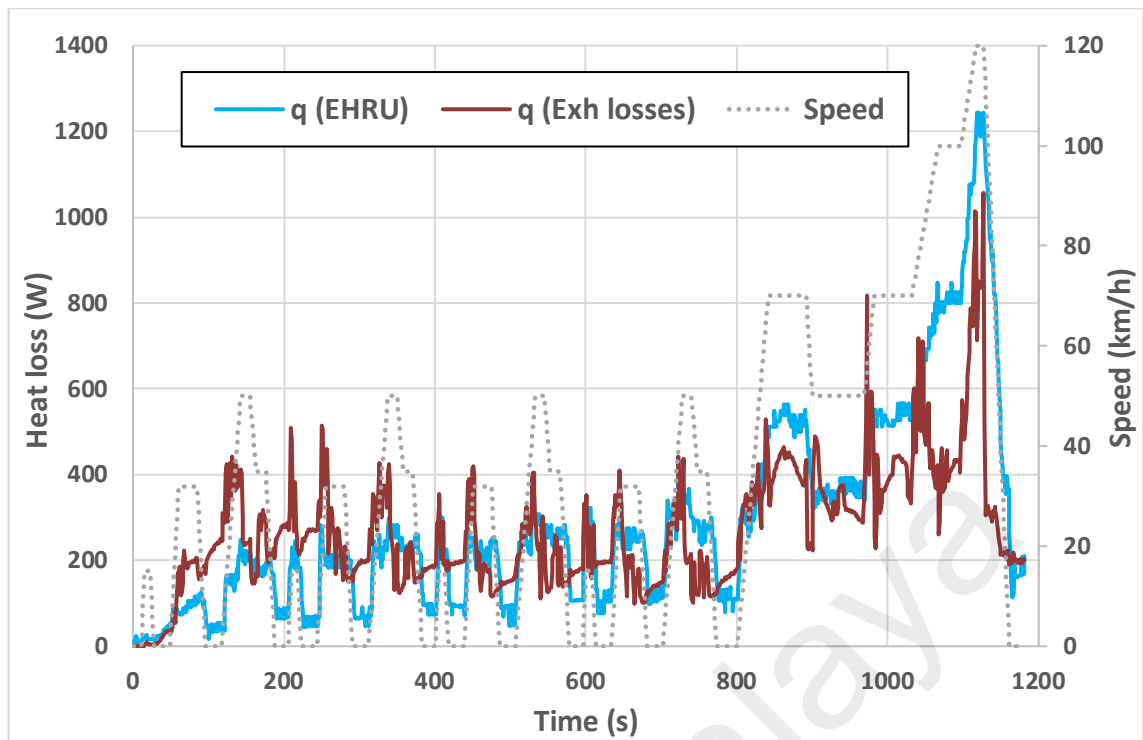


**Figure 4.15 – Comparison between exhaust heat losses and recovered exhaust heat from EHRU during NEDC test.**

From **Figure 4.16**, the accumulated thermal energy profiles between the exhaust heat losses and EHRU confirmed that the thermal energy accumulated by the EHRU was lower than the exhaust heat losses during the UDC phase. However, as the test vehicle moved to the EUDC phase, both the exhaust heat losses and the heat transfer from the EHRU to the coolant increased simultaneously from point *w* but at different rates. In particular, the heat transfer from the EHRU to the coolant is higher as shown by the steeper curve. The two curves finally crossed at  $t = 1088$  s (point *x*) and the gap widened afterwards. From **Figure 4.16**, as much as 998 kJ of thermal energy was discharged by the coolant to the CVT oil cooler. There was also thermal energy originated from the mechanical losses within the transmission assembly itself (Garcia-Contreras et al., 2018) but not included in this graph. Nevertheless, the CVT oil temperature was only  $77^{\circ}\text{C}$  at

the end of the test and this suggested that the bulk of the thermal energy must have also been absorbed by the metals within the CVT assembly and some was also lost to the surroundings.

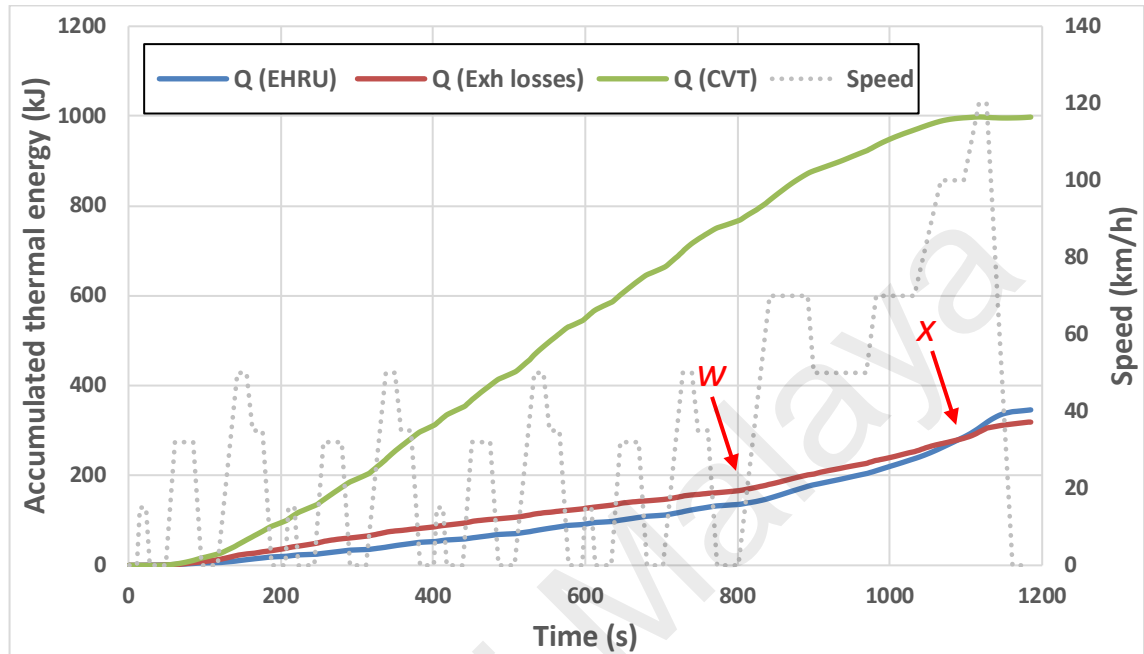


**Figure 4.16 – Comparison of various accumulated thermal energy transferred within the during NEDC test.**

#### 4.2.3 Summary of the warm-up performances

The warm-up performances of various fluids of both variants during idle and NEDC tests are summarized in **Table 4.1**. Improvements that are deemed to be significant are shaded in green. From **Table 4.1**, the maximum temperatures of the cylinder head coolant for the cooling circuit with and without the EHRU are not much different in both idle and NEDC tests. By contrast, the maximum temperatures of the cylinder block coolant are clearly higher during idle and NEDC tests for the EHRU variant.

**Table 4.1 – Comparison of the warm-up performances involving various fluids during idle and NEDC test.**

		Idle			NEDC		
		No EHRU	EHRU	%	No EHRU	EHRU	%
Cylinder head (T1 thermocouple)	40°C	50 s	45 s	-10.0	55 s	52 s	-5.5
	60°C	138 s	135 s	-2.2	159 s	148 s	-6.9
	Max temp	94.2°C	94.9°C		94.3°C	93.7°C	
Cylinder block (T2 thermocouple)	40°C	166 s	148 s	-10.8	181 s	154 s	-14.9
	60°C	409 s	352 s	-13.9	474 s	355 s	-25.1
	Max temp	71.9°C	77°C	6.6	73.2°C	78.3°C	6.5
Thermostat	Open				812 s	714 s	-12.1
CVT oil	40°C	216 s	214 s	-0.9	249 s	235 s	-5.6
	60°C				713 s	633 s	-11.2
	Max temp	57.1°C	58°C		74.6°C	77°C	3.1
Engine oil	40°C	266 s	261 s	-1.9	255 s	251 s	-1.6
	60°C	593 s	588 s	-0.8	448 s	378 s	-15.6
	Max temp	60.4°C	62.1°C	2.7	92.1°C	93.2°C	1.2

From **Table 4.1**, the cylinder head and cylinder block coolant reach 40°C and 60°C temperatures earlier for cooling circuit fitted with EHRU. Similarly, the thermostat opens 98 seconds earlier for cooling circuit fitted with EHRU during the NEDC test. As for the idle test, the thermostats for both variants did not open by the time the idle test was completed after the 600 seconds.

As explained in the earlier studies, the thermostat opening does not rely directly on the hot coolant coming out of the cylinder head (Osman, Yusof & Rafi, 2016; Osman, Razali & Nurdin, 2018). Instead, it relies on the relatively cooler coolant after the CVT oil cooler and cabin heater as shown in **Figure 3.3(a)**. In this context, even when the cylinder head coolant is more than 90°C, the thermostat will not open unless the coolant passing through thermostat reaches the opening temperature of 76°C.

From **Table 4.1**, the improvement of CVT oil warm-up during idle test for the EHRU variant is only marginal. By contrast, the improvements during the NEDC were decisive

in which the CVT oil reach the 40°C and 60°C temperatures much earlier for the EHRU variant. Nevertheless, the maximum CVT oil temperature is only 2.4°C higher than the variant without EHRU.

From **Table 4.1**, the engine oil reaches the 40°C and 60°C temperatures significantly earlier for the EHRU variant during both the idle and NEDC tests. Similar like the CVT oil, the maximum temperatures of engine oil are only slightly higher for the EHRU variant during both the idle and NEDC tests.

From **Table 4.1**, the improvements of EHRU over the no EHRU variant throughout the idle and NEDC tests in terms of warm-up times are in the range of 2-57 seconds and 3-119 seconds, respectively. The percentage improvements in warm-up times for idle and NEDC tests are in the range of 0.9-13.9% and 1.6-25.1% respectively. The maximum fluids' temperatures achievable during the idle and NEDC tests are in the range of 1.7-5.1°C and 1.1-5.1°C respectively. Percentage wise, the improvements are in the range of 2.7-6.6% and 1.2-6.5% respectively.

### **4.3 Discussions**

#### **4.3.1 Connecting the dots**

In the early part of idle and NEDC tests as shown in **Figures 4.1** and **Figure 4.5**, the coolant from the cylinder block was continuously cooler than the entire EHRU and the rest of the metals within the SES. By contrast, the cylinder head coolant temperature increased rapidly and became hotter than the average temperature of the EHRU. By not feeding the cylinder head coolant through the EHRU, no heat was being wasted to heat up the cold EHRU during the early part of the tests. Instead, the cylinder head coolant was directed to the CVT oil cooler to expedite the CVT oil warm-up. By contrast, the

coolant feed to the EHRU was much cooler as it came in from the cylinder block. This arrangement rapidly increased the temperature gap between the coolant and the EHRU and eventually caused the coolant to exit the EHRU hotter.

The large temperature difference between the coolant exiting the cylinder head and cylinder block have similarities with the earlier studies (Osman, Yusof & Rafi, 2016; Osman, Razali & Nurdin, 2018). Nevertheless, the authors have not discussed in detail on how such distinctiveness was achieved. In this context, **Figure 4.4** and **Figure 4.14** show significant amount of coolant heat being absorbed by the lower portion of the cylinder bores across all 4 cylinders in the first 425 seconds (range *y*) of the idle test and 187 seconds (range *z*) of the NEDC test. It was calculated that 17.5 kJ of thermal energy was absorbed by the cylinder block during both idle and NEDC tests within the stated time periods.

Considering that the combustion heat is mostly affecting the top 40% of the piston stroke as explained in Chapter 2 and 3, the cooler bottom portion of the cylinder bores have the tendency to absorb the heat from the warmer coolant flowing along the bottom of the water jacket. Understanding that there are plenty of engine oil splashes from the rotating components over the bottom portion of the cylinder bores and upper portion of the crankcase skirts (Roberts, Brooks & Shipway, 2014; Osman, 2012; Osman, 2014), it was also likely that the absorbed coolant heat heated up the engine oil. The large thermal inertia from both the engine oil and metals ensured continuous coolant heat absorption and this explains why it took a few minutes before the coolant exiting the cylinder block would have the same temperature as the coolant entering the water pump.

As shown in **Figure 4.7**, significant exhaust heat losses were detected by thermocouples T16 and T17 as early as  $t = 15$  s but the coolant temperature difference of the EHRU started only at the  $t = 25$  s. This delay was caused by the thermal inertia from

the combined exhaust pipes, flanges, connectors and EHRU within the SES. Considering that the EHRU is only 1.6 kg and the delay was a matter of 10 seconds, such delay could have been longer in case heavier EHRU was used. Heavier EHRU like the one used by Faurecia weighs 5.4 kg (Chiew et al., 2011) and the big void inside it requires a lot of coolant to fill the gap. Although the large surface area of the heat transfer fins is highly effective in transferring the exhaust heat to the coolant, the coolant and metals have high specific heat capacities. In this context, there was no recovered exhaust heat extracted from the Faurecia's EHRU before  $t = 50$  s (Chiew et al., 2011). As a reference, authors of this particular paper repeatedly mentioned about their exhaust-to-oil heat recovery unit requiring at least 200 seconds before heat recovery process could take place (Vittorini, Di Battista & Cipollone, 2018). The authors also briefly discussed about reducing the delay down to  $t = 120$  s but achieving it would induce higher exhaust backpressure from the increased heat transfer surface areas.

The increase in temperature difference for the coolant entering and exiting the EHRU as early as the  $t = 23$  s during idle test and  $t = 25$  s during NEDC test marked the beginning of exhaust heat recovery and reuse process from the EHRU. Although the coolant temperature differences were less than  $0.5^{\circ}\text{C}$  at the starting point, the values gradually reached  $3^{\circ}\text{C}$  in just  $t = 190$  s for idle test and  $t = 192$  s for the NEDC test. For the idle and NEDC tests, 8.3 kJ and 19 kJ of thermal energy was recovered and reused for warm-up within those time periods.

In the earlier study, the exhaust heat recovery and reuse during the NEDC test started only after the  $t = 170$  s for the idle test and  $t = 180$  s for NEDC test. By contrast, as much as 7.2 kJ of thermal energy was recovered and reused between  $t = 23$  s and  $t = 169$  s during the idle test. As for the NEDC test, as much as 17.1 kJ of thermal energy was recovered from the  $t = 25$  s and  $t = 179$  s. The thermal energy recovered in both tests have

shown the advantage of starting the exhaust heat recovery process early if compared to minutes later. The additions of the thermal energy to the cooling circuit have also accelerated the engine warm up process for the variant with EHRU.

From **Table 4.1**, **Figure 4.1-4.3** and **Figure 4.8-4.11**, the presence of the EHRU has significantly improved warm-up performances for the coolant, engine oil and CVT oil during idle and NEDC test. The clear improvement in cylinder block coolant warm-up is desirable in quickly heating the engine oil on the bore surface and to thermally expand the bottom portion of the cylinder bores to achieve optimal bore-to-piston clearance for efficient piston reversal process. The improvement in cylinder head coolant warm-up was relatively smaller at the beginning. Nevertheless, the EHRU variant reached the 40°C and 60°C marks earlier and this is significant enough to minimize the intake port wall wetting. By contrast, the increase in coolant temperature at the later stage was relatively higher and this is likely to benefit in minimizing the combustion gas quenching. Similarly, such increase was likely to contribute to heat up the engine oil inside the oil jacket above the cylinder head's water jacket. The increase in engine oil temperature as shown in **Figure 4.3** and **Figure 4.11** was significant and with no oil cooler installed, the relatively higher engine oil temperature was caused by the quicker increase in cylinder block's and cylinder head's coolant temperatures.

From the practicality standpoint, the proposed EHRU was purposely designed to speed up the recovered exhaust heat availability as the main priority. Considering that heat exchangers in general have slow response due to the mass and size (Agarwal, Chiara & Canova, 2012; Burke et al., 2012), the proposed EHRU is lightweight and compact to lower the thermal inertia. Although the delay in making the recovered heat available was minimum, the minimum surface area for heat transfer to take place has limited the amount of recoverable heat. Nevertheless, it was still able to absorb 346 kJ of thermal energy and

as much as 1.24 kW of post catalyst low-grade heat which would otherwise be wasted during the NEDC test. Throughout the test, as much as 114.7 kJ of thermal energy was recovered and reused by the time thermostat opened at  $t = 714$  s. This added energy has significantly improved the warm-up performances as shown in Table 2.

In case the test vehicle equipped with the EHRU is pushed at higher engine speed and load than the highest engine speed and load experienced during NEDC, the limited surface area also limits the amount of recoverable heat in which it will not be far higher than 1.24 kW. In this context, the hard driving is likely to open the thermostat wide and more than half of the recovered heat will be directed from T-junction #2 to T-junction #1 and eventually to the radiator instead of being wholly recirculated into the engine. This mechanism prevents overheating without the need to adopt the pneumatic flap to divert the exhaust gas (Chiew et al., 2011) or to enlarge the radiator size.

#### **4.3.2 Research gaps identified in this study.**

As shown in **Figure 4.17**, the efficiency of the EHRU is at its lowest at point *aa*. From equation (15), such low efficiency happens when the temperature difference between the upstream and downstream exhaust gas temperature as measured by thermocouples T16 and T17 is low. Interestingly, even when the efficiency is low at point *aa*, the heat transfer from the EHRU to the cooling circuit as shown in **Figure 4.15** is still higher than the exhaust heat losses between the two measured points. In this context, the rapid increase in flanges' metal temperatures during the EUDC phase in **Figure 4.13** suggested considerable conduction heat transfers from the upstream and downstream of the SES moving toward the EHRU.

From **Figure 4.17**, the average and maximum efficiency of the EHRU throughout the NEDC are 7.2% and 16.5% respectively. By contrast, Faurecia's EHRU has 85% average efficiency (Chiew et al., 2011). Such low efficiency is a big trade-off to primarily achieve low thermal inertia crucial for better response. In addition, the trade-off positively addresses the complexity, high exhaust backpressure, size, weight and overheating at high load operations that generally come with conventional EHRUs. Nevertheless, the low efficiency is a research gap to be preliminarily addressed with better EHRU design in **Section 5.2**.

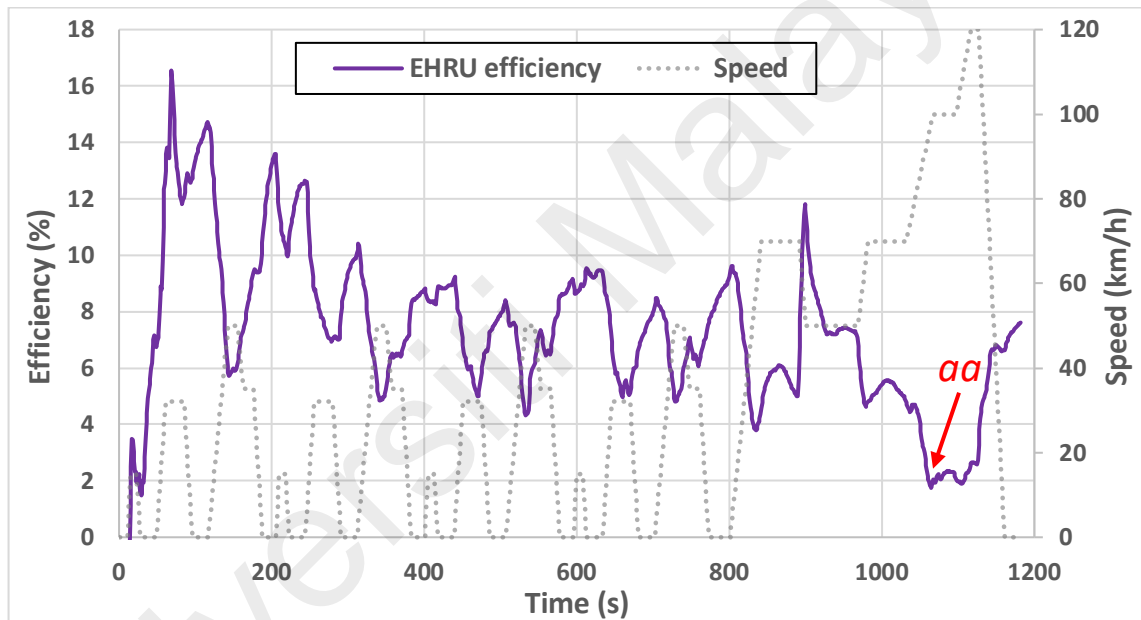


**Figure 4.17 – Efficiency of the EHRU during NEDC.**

As shown in **Figure 4.16**, the thermal energy accumulated by EHRU stays below the accumulated energy losses from the exhaust gas to the SES throughout the entire UDC phase. However, as the test vehicle entered the EUDC phase, the increase in overall thermal energy dissipations from the engine increased the thermal energy content in the exhaust gas. Such increase can also be seen in **Figure 4.16** in which the slopes for the accumulated EHRU and exhaust gas thermal energy transfers become steeper until the

vehicle decelerates at the end of the 120 km/h run. In this context, the hotter exhaust gas increased the metal temperatures starting from cylinder bores, combustion chambers, valves, exhaust ports, manifold pipes, catalytic converter assembly, flanges, downpipe and EHRU at differing magnitudes. In particular, the catalytic converter assembly in general can be hotter than the exhaust gas and the continuous oxidations of unburned hydrocarbons provide additional heat release inside the catalyst brick (Lee et al., 2002) up to the manifold flange and possibly beyond that.

In linking the paragraph before with hotter metals adjacent to the EHRU, the thermocouples T13 and T15 provided the early evidence of rapid conduction heat transfer from the flanges to the EHRU. From  $t = 1057$  s to  $t = 1111$  s, the exhaust gas temperature as measured by thermocouple T16 was 618.9-747.7°C and yet there were minimum exhaust heat losses to the hot metals within the SES. It was highly likely that the temperature gaps between the exhaust gas and metal surfaces in contact with the exhaust gas were close that the exhaust gas heat losses were rapidly decreasing. Considering that the temperature of both flanges rapidly increasing while the exhaust heat losses rapidly reducing to the lowest point, the likelihood for external heat sources to supply heat to the SES was high.

From **Figure 3.17** and equation (13), the external heat sources might be coming from the conduction heat transfer upstream and downstream of the SES. In view of the exhaust pipes and catalytic converter housing being constructed from 1.2-1.5 mm thick steel sheet metal, the thin cross section has high surface-to-volume ratio that was prone to large temperature increase within short period of time. Considering that the thin sections became hot during the EUDC phase, the conduction heat transfer to the flanges and eventually to the EHRU and coolant was unstoppable.

From the SES standpoint, the heat transferred to the EHRU during UDC phase came mostly from the exhaust gas heat losses to the SES. This suggested that that the SES can be useful in transient modeling and improving the design of EHRU and its connecting metals for better warm-up performances. However, as the external heat sources in the form of  $q_{ext\ cond1}$  and  $q_{ext\ cond2}$  becoming larger during the EUDC phase, it is no longer accurate to assume that the heat recovered by the EHRU came mostly from the exhaust heat losses within the SES. Nevertheless, modelling the external conduction heat transfer upstream and downstream of the SES can be challenging as it needs additional temperature points to be measured.

In moving forward, calculations of the heat transfers from external sources to the SES could not be covered in this study due to the difficulties in getting the temperature measurements. It is a research gap that is yet to be addressed to enable the SES to be useful in modelling and improving the design of EHRU and exhaust system for higher engine load operations. Considering that the proposed EHRU has lower heat exchanger efficiency if compared to the more conventional ones like Faurecia's, it can only be assumed based on the flanges' temperatures in **Figure 4.13** that the conduction heat transfer from the upstream of the SES to be significant during idle and city driving but dominant during highway driving. Similar assumption is also applicable to the heat transfer downstream of the SES except that the magnitude of the heat transfer is smaller.

### **4.3.3 Key findings, novelties and new knowledge established in the study**

Taking just 23-25 seconds after the cold starts for the coolant exiting the EHRU to become hotter is a reasonable benchmark for researchers looking for ways to speed up the warm-up process under the bigger picture of lowering the fuel consumption, greenhouse gases and tailpipe emissions. In particular, the very rapid exhaust heat

recovery process can be beneficial for everyday driving which requires frequent stopping, idling within short driving distances. In addition to that, this rapid process is also useful for engines with the engine start-stop technology. The rapid availability of recovered exhaust heat is much faster than any other known EHRU technologies that are based either on thermoelectric, Rankine cycle or even the existing ones intended to speed up the powertrain warm-up process. As proven during the idle test, the early starting point for the recovered exhaust heat availability was even possible during cold start idle without the need to increase the engine speed and load. This highly responsive mechanism enables rapid, effective, efficient and sustainable exhaust heat recovery and reuse applicable even to future gasoline and diesel engines with low overall exhaust gas temperature.

The study has also proven that low enthalpy and low exergy exhaust gas energy can be recovered and reused in just 23-25 seconds after engine firing. Considering that the recovered sensible heat was used directly and exhaustively to heat up the fluids and metals, there was no concern in terms of energy conversion losses and entropy formation which may exist in thermoelectric and Rankine cycle based EHRUs. The additional energy rapidly added to the coolant after the EHRU was significant and can be reused for many measures that can improve the fuel economy.

Unlike other EHRUs, the proposed EHRU is made of simple, cost effective, reliable and durable heat exchanger plate that relies mostly on conduction heat transfers from its hotter metal surroundings. Instead of integrating the EHRU with heat transfer fins to increase the heat transfer surface areas, the proposed EHRU uniquely relies on its metal surroundings that already have large surface areas on both the upstream and downstream of the EHRU. Doing so avoids the proposed EHRU from becoming complicated, delicate, heavy, bulky and costly. By not being heavy and bulky, the thermal inertia of both the metals and excess coolant within the EHRU are being kept low and this is another key

enabler in speeding up the recovered heat availability. In particular, the EHRU relies on the early exhaust heat recovery and reuse to start accumulating the thermal energy early to make up for the limited heat recovery ceiling of the EHRU at the later stage.

Even though many conventional EHRUs rely on the convective heat transfer from the exhaust gas to the heat transfer fins, this study has also revealed the significance of the conduction heat transfer making its way to the EHRU and eventually to the coolant flowing in it through convection heat transfer. Even if the conventional EHRUs are equipped with pneumatic flap to divert the exhaust gas away from the heat transfer fins, there will still be significant conduction heat transfer making its way to the metals adjacent to the cooling passage at high engine load. This excess heat is expected to require relatively bigger radiator capacity to avoid overheating the engine at higher engine load. By contrast, the proposed cooling circuit is purposely designed to divert more than half of recovered exhaust heat to the radiator when the thermostat is wide or fully open. This measure minimizes the recovered heat from being recirculated into the engine and it minimizes the risk of engine overheating at high load operations.

In general, other EHRUs have high exhaust backpressure due to the use of highly restrictive heat transfer fins. Furthermore, the use of more restrictive aftertreatments to meet the future tailpipe emissions regulations when combined with these restrictive EHRUs may negatively affect the specific outputs of these future engines. By contrast, the proposed EHRU as shown in **Figure 3.11** exerted no significant increase in exhaust backpressure. As a result, no recalibrations of the production engine and transmission electronics were required during the early part of the development because no significant drivability or cycle-to-cycle variations were detected during low and medium load driving. This opens the possibility for the proposed EHRU to be retrofitted to the existing engines currently in use. Furthermore, with no known restriction to the exhaust flow, there

was no fouling or stain on the metal surfaces in contact with the exhaust gas pointed out even after big mileage accumulation (Jouhara et al., 2018).

In sourcing the cooler coolant feed to the EHRU, this study has also revealed another important finding. Powertrain designers in general, obtain cooler coolant few centimeters after the water pump outlet. This guarantees coolant temperature that is close to the temperature of the coolant passing the water pump. This approach is effective in ensuring continuous cooler coolant supply to engine oil and transmission oil coolers at higher engine load. However, such approach does not provide relatively cooler coolant than the coolant entering the water pump during the early phase of the cold start as per what discussed in **Section 4.3.1**. Having no cool coolant to the EHRU affects the start of the coolant temperature difference between the inlet and outlet of the EHRU and this will delay the start of the exhaust heat recovery.

Alternatively, researchers from University of Bath used separate cooling circuit and water pump independent of the main cooling system (Burke et al., 2012). They were also able to recover the exhaust heat and to reuse it to heat up the engine oil reasonably fast. However, the separate cooling circuit will need its own radiator and dedicated air flow to reject heat at higher load operations. By contrast, the proposed EHRU works optimally with a single cooling circuit that is optimised for both warm-up and cooling (Osman, Yusof & Rafi, 2016; Osman, Razali & Nurdin, 2018; Osman et al., 2013; Osman, Hussin & Abidin, 2015). In keeping the cost low, the alternative from Burke et al. may not be suitable for the non-research applications intended for the proposed EHRU.

In the absence of coolant outlet at the bottom of the water jacket's rear end, the coolant flow along the bottom of the water jacket is generally weak especially during engine idle. This negativity is obvious for deep water jacket normally used for turbocharged engines. Consequently, there will be minimum heat transfer to the bottom

of the cylinder bores which is likely to affect warm-up of the bottom portion of the cylinder bores during cold start.

By contrast, the proposed concept sources the coolant from the bottom of the 4<sup>th</sup> cylinder water jacket. This arrangement directs certain percentage of the coolant into the cylinder block coolant outlet while at the same time leaving an optimal amount of hotter coolant from the upper portion of the cylinder bores to exit through the cylinder head. This measure enables relatively cooler coolant to the EHRU without compromising the quick warm-up of the cylinder head and the upper and middle portions of the cylinder bores. The increased coolant velocity along the bottom of the water jacket is also beneficial to the cold engine oil in contact with the bottom of the cylinder bore surfaces. In particular, the oil absorbs plenty of heat from the warmer coolant at the beginning of the cold start. By the time this stream of coolant exits the cylinder block, it is much cooler than the coolant entering the cylinder block during the critical first few minutes of the cold start.

In expanding the applications, this unique coolant sourcing method for EHRU is applicable to other heat engines running with closed loop coolant or oil circuit. Understanding that the coolant and oil temperature distributions are not uniform throughout the circuit, it is possible to source cooler fluid from spots with minimum contact with heat sources and has minimum flow velocity. This measure not only improves the heat recovery response, but it also eliminates coolant dead spot.

Finally, the study also provided detailed interactions on how a heat recovery device, metals and fluids responded to various heat sources from a heat engine. The interactions established through experimental, and SES provided basis for the strengths of the proposed EHRU to be benchmarked and the weaknesses to be improved in the future. In

particular, the designers of heat exchangers and EHRUs can use some of the unique findings to improve their established design guidelines and common beliefs.

Universiti Malaya

## CHAPTER 5: CONCLUSIONS AND RECOMMENDATIONS

### 5.1 Conclusions

In this study, the 1.3l Proton Iriz was fitted with simplified split cooling circuit and low thermal inertia EHRU. In order to compare the effectiveness of the EHRU in recovering the exhaust heat, the test subject was tested with and without the exhaust heat recovery. Based on the test results derived from the idle and NEDC tests, conclusions are drawn in the following paragraphs.

The baseline engine's cooling circuit has been successfully converted from serial cooling to the optimised simplified split cooling through various changes to the cylinder head, cylinder block, gaskets, brackets, thermostat and coolant passages. The proposed EHRU on the other hand was designed from scratch, fabricated, and installed in between the maniverter and exhaust downpipe. Both the simplified split cooling and the proposed EHRU were simultaneously optimized and developed to ensure synergy.

The combination of the simplified split cooling with the proposed EHRU has successfully improved the warm-up performances involving coolant (across the cylinder block and cylinder head), CVT oil and engine oil during the idle and NEDC tests. The improvements revealed during the idle and NEDC tests are in the range of 0.9-13.9% and 1.6-25.1% respectively. With clear improvements over the variant with no EHRU, the proposed EHRU was effective in reducing the time needed for the fluids to reach the intended temperatures.

The heat transfer to the EHRU peaked at 120 W and as much as 43 kJ of thermal energy was recovered throughout the idle test. By contrast, the heat transfer to the EHRU peaked at 1.24 kW and as much as 346 kJ of thermal energy was recovered throughout the NEDC test. In particular, 114.7 kJ of thermal energy was recovered and reused by the time the

thermostat opened at  $t = 714$  s. This amount was significant enough to make the difference in warm-up performances if compared to the variant without EHRU.

Throughout the NEDC test, the average and maximum EHRU efficiency were 7.2% and 16.5% respectively. Nevertheless, the additions of conduction heat transfer from upstream and downstream of the EHRU on top of the convection heat transfer were able to make up for the low EHRU efficiency.

In general, it can be concluded that the EHRU was effective in rapidly recovering the exhaust heat. The recovered exhaust heat was significant enough in improving the warm-up performances. The key in achieving the fast warm up using the EHRU was in feeding the EHRU's coolant inlet with relatively cooler coolant feed from the bottom of the cylinder block's water jacket. This has enabled the temperature gap between the EHRU and the coolant flowing in it to rapidly increase thus triggering the start of the exhaust heat recovery and reuse. Together with the low thermal inertia design of the EHRU, the coolant exiting the EHRU became hotter as early as  $t = 23$  s during idle test and  $t = 25$  s during the NEDC test. Such early starts of the exhaust heat recovery and reuse are decisively faster than the  $t = 50$  s achieved by conventional EHRU design by Faurecia.

## **5.2 Recommendations for future works**

It is obvious that the study relies on certain assumptions and SES to overcome the limitations in measuring temperatures at critical but high-risk spots. At the time of writing, there have been plans to model the convection and conduction heat transfers to the SES and the EHRU using CFD simulations. This will answer the questions on the magnitude of conduction heat transfers to the EHRU and SES. By having better understanding of the contributions, it is possible for EHRU and exhaust system of the

future to be evolved to rely less on the heat transfer fins within the EHRU and to rely more on the metal parts that are connected to the EHRU. Understanding that there is not much use of exhaust heat after the catalytic converter, among the future improvements that can be added to the exhaust system is in enlarging the surface area of pipe connection to the flange and the flange's surface area to the EHRU to enable more conduction heat transfer to the EHRU.

The much cheaper and simpler production variant of the EHRU is currently being designed and will be made from cast iron instead of machined steel block. In particular, the main body where the flanges are connected will have its thickness reduced from 20 mm to 6-8 mm. This thin mating faces is closely surrounded by relatively thicker sections to house cast water jacket for the coolant to flow in and out. The cast water jacket surrounding the mating faces will provide meandering water passage uniformly close to the mating faces for better heat transfer and more uniform temperature distribution. The production EHRU is expected to be few hundred grams lighter than the proposed EHRU in this study. This will likely lower the thermal inertia further to speed up the recovered heat availability.

Ferrous metals like iron and steel do not have thermal conductivity as high as aluminium, magnesium, copper and even brass. Understanding that the EHRU is tightly sandwiched rather than hanging or supporting other structures, it is possible to use these metals provided that the mating faces do not deform over time. The effectiveness of these metals can be simulated or even tested in the future.

## REFERENCES

- Agarwal, N., Chiara, F., & Canova, M. (2012). Control-Oriented Modeling of an Automotive Thermal Management System. *IFAC Proceedings Volumes*, 45(30), 392–399. doi: 10.3182/20121023-3-fr-4025.00051
- Allen, D. J., & Lasecki, M. P. (2001). Thermal Management Evolution and Controlled Coolant Flow. *SAE Technical Paper Series*. doi:10.4271/2001-01-1732
- Andrews, G. E., Ounzain, A. M., Li, H., Bell, M., Tate, J., & Ropkins, K. (2007). The Use of a Water/Lube Oil Heat Exchanger and Enhanced Cooling Water Heating to Increase Water and Lube Oil Heating Rates in Passenger Cars for Reduced Fuel Consumption and CO<sub>2</sub> Emissions During Cold Start. *SAE Technical Paper Series*. doi: 10.4271/2007-01-2067
- Armstead, J. R., & Miers, S. A. (2010). Review of Waste Heat Recovery Mechanisms for Internal Combustion Engines. *ASME 2010 Internal Combustion Engine Division Fall Technical Conference*. doi:10.1115/icef2010-35142
- Battista, D. D., & Cipollone, R. (2016). Experimental and numerical assessment of methods to reduce warm up time of engine lubricant oil. *Applied Energy*, 162, 570-580. doi:10.1016/j.apenergy.2015.10.127
- Battista, D.D., Cipollone, R. & Fatigati, F. (2018). Engine oil Thermal Management: Oil Sump Volume Modification and Heating by Exhaust Heat During ICE Warm Up. *SAE Technical Paper Series*. doi: 10.4271/2018-01-1366
- Boam, D.J. (1986). Energy Audit on a Two-Litre Saloon Car Driving an ECE 15 Cycle from a Cold Start. *Proceedings of the Institution of Mechanical Engineers, Part D: Transport Engineering*, 200 (1), 61-67 doi: 10.1243/pime\_proc\_1986\_200\_164\_02
- Boretti, A. (2019a). Transient positive ignition engines have now surpassed the 50% fuel conversion efficiency barrier. *International Journal of Hydrogen Energy*, 44(14), 7051–7052. doi: 10.1016/j.ijhydene.2019.01.237
- Boretti, A. (2019b). *Advances in Turbocharged Racing Engines*, SAE International, Product Code PT-199, ISBN 978-0-7680-0014-6, 236 pages.
- Brace, C. J., Hawley, G., Akehurst, S., Piddock, M., & Pegg, I. (2008). Cooling system improvements — assessing the effects on emissions and fuel economy. *Proceedings of the Institution of Mechanical Engineers, Part D: Journal of Automobile Engineering*, 222(4), 579-591. doi:10.1243/09544070jauto685
- Burke, R., Brace, C., Akehurst, S., Pegg, I. & Stark, R. (2012). Study of the behaviour of an exhaust gas heat exchanger for improved engine warm-up. Paper presented at SIA International Diesel Engine Conference 2012, Rouen, France, 6/06/12 - 6/06/12
- Caresana, F., Bilancia, M., & Bartolini, C. (2011). Numerical method for assessing the potential of smart engine thermal management: Application to a medium-upper

segment passenger car. *Applied Thermal Engineering*, 31(16), 3559-3568. doi:10.1016/j.applthermaleng.2011.07.017

Chammas, R. E., & Clodic, D. (2005). Combined Cycle for Hybrid Vehicles. *SAE Technical Paper Series*. doi:10.4271/2005-01-1171

Chanfreau, M., Gessier, B., Farkh, A., & Geels, P. Y. (2003). The Need for an Electrical Water Valve in a THERmal Management Intelligent System (THEMIS™). *SAE Technical Paper Series*. doi:10.4271/2003-01-0274

Chiew, L., Clegg, M. W., Willats, R. H., Delplanque, G., & Barrieu, E. (2011). Waste Heat Energy Harvesting for Improving Vehicle Efficiency. *SAE International Journal of Materials and Manufacturing*, 4(1), 1211–1220. doi: 10.4271/2011-01-1167

Cipollone, R., Di Battista, D. and Mauriello, M. (2015). Effects of oil warm up acceleration on the fuel consumption of reciprocating internal combustion engines. *Energy Procedia*, 82:1-8.

Clough, M. J. (1993). Precision Cooling of a Four Valve per Cylinder Engine. *SAE Technical Paper Series*. doi:10.4271/931123

Demandt, B. (2019). Global car sales analysis 2018. [carsalesbase.com/global-car-sales-2018/](https://carsalesbase.com/global-car-sales-2018/)

Di Battista, D., Cipollone, R. (2018). Improving engine oil warm up through waste heat recovery, *Energies*, 11:1-10.

Finlay, I. C., Gallacher, G. R., Biddulph, T. W., & Marshall, R. A. (1988). The Application of Precision Cooling to the Cylinder-Head of a Small, Automotive, Petrol Engine. *SAE Technical Paper Series*. doi:10.4271/880263

García-Contreras, R., Gómez, A., Fernández-Yáñez, P., & Armas, O. (2018). Estimation of thermal loads in a climatic chamber for vehicle testing. *Transportation Research Part D: Transport and Environment*, 65, 761–771. doi: 10.1016/j.trd.2017.11.010

Gardiner, R., Zhao, C., Addison, J., & Shayler, P. (2013). The effects of thermal state changes on friction during the warm up of a spark ignition engine. *Vehicle Thermal Management Systems Conference Proceedings (VTMS11)*, 307-317. doi:10.1533/9780857094735.7.307

Goettler, H. J., Vidger, L. J., & Majkrzak, D. S. (1986). The Effect of Exhaust-to-Coolant Heat Transfer on Warm-up Time and Fuel Consumption of Two Automobile Engines. *SAE Technical Paper Series*. doi: 10.4271/860363

Iliev, S., & Lohse-Busch, H. (2018). Energy Efficiency Benefits of Active Transmission Warm-up under Real-World Operating Conditions. *SAE Technical Paper Series*. doi: 10.4271/2018-01-0385

- Jarrier, L., Champoussin, J. C., Yu, R., & Gentile, D. (2000). Warm-Up of a D.I. Diesel Engine: Experiment and Modeling. *SAE Technical Paper Series*. doi: 10.4271/2000-01-0299
- Jehlik, F., Iliev, S., Wood, E., & Gonder, J. (2017). Investigation of Transmission Warming Technologies at Various Ambient Conditions. *SAE Technical Paper Series*. doi:10.4271/2017-01-0157
- Jouhara, H., Khordehghah, N., Almahmoud, S., Delpech, B., Chauhan, A., & Tassou, S. A. (2018). Waste heat recovery technologies and applications. *Thermal Science and Engineering Progress*, 6, 268–289. doi: 10.1016/j.tsep.2018.04.017
- Kandylas, I., & Stamatelos, A. (1999). Engine exhaust system design based on heat transfer computation. *Energy Conversion and Management*, 40(10), 1057–1072. doi: 10.1016/s0196-8904(99)00008-4
- Kobayashi, H., Yoshimura, K., & Hirayama, T. (1984). A study on dual circuit cooling for higher compression ratio. *SAE Technical Paper Series*. doi:10.4271/841294
- Kusnetz, N. (2020). U.S. Emissions Dropped in 2019: Here's Why in 6 Charts. <https://insideclimatenews.org/>
- Lan, S., Smith, A., Stobart, R., & Chen, R. (2019). Feasibility study on a vehicular thermoelectric generator for both waste heat recovery and engine oil warm-up. *Applied Energy*, 242, 273–284. doi: 10.1016/j.apenergy.2019.03.056
- Lee, S., Bae, C., Lee, Y., & Han, T. (2002). Effects of Engine Operating Conditions on Catalytic Converter Temperature in an SI Engine. *SAE Technical Paper Series*. doi: 10.4271/2002-01-1677
- Lindsey, R. (2020). Climate Change: Atmospheric Carbon Dioxide. Climate.gov
- Lodi, F. S. (2008). Reducing cold start fuel consumption through improved thermal management. *Masters Research thesis, Faculty of Engineering, Mechanical and Manufacturing Engineering, The University of Melbourne*.
- Mitchell, T., Salah, M., Wagner, J., & Dawson, D. (2009). Automotive Thermostat Valve Configurations: Enhanced Warm-Up Performance. *Journal of Dynamic Systems, Measurement, and Control*, 131(4), 044501. doi:10.1115/1.3117183
- Mohamed, E. S. (2016). Development and analysis of a variable position thermostat for smart cooling system of a light duty diesel vehicles and engine emissions assessment during NEDC. *Applied Thermal Engineering*, 99, 358-372. doi:10.1016/j.applthermaleng.2015.12.099
- Motorcycles data. (2019). World Motorcycles Market. Despite growing, the industry is 5 million below the record. [motorcyclesdata.com/2019/03/25/world-motorcycles-market/](https://motorcyclesdata.com/2019/03/25/world-motorcycles-market/)
- Neumeister, D., Heckenberger, T., Brehm, H. (2008). Heat recovery from exhaust gas [ThermorekuperationausdemAbgas], *VDI Berichte* 2033:259-274.

- Orr, B., Akbarzadeh, A., Mochizuki, M., & Singh, R. (2016). A review of car waste heat recovery systems utilising thermoelectric generators and heat pipes. *Applied Thermal Engineering*, 101, 490–495. doi: 10.1016/j.applthermaleng.2015.10.081
- Osman, A. (2009). Feasibility Study of a Novel Combustion Cycle Involving Oxygen and Water. *SAE Technical Paper Series*. doi: 10.4271/2009-01-2808
- Osman, A. (2012). Design Concept and Manufacturing Method of a Lightweight Deep Skirt Cylinder Block. *SAE Technical Paper Series*. doi: 10.4271/2012-01-0406
- Osman, A., Sabrudin, A. S., Hussin, M. A., & Bakri, Z. A. (2013). Design and Simulations of an Enhanced and Cost Effective Engine Split Cooling Concept. *SAE Technical Paper Series*. doi:10.4271/2013-01-1640
- Osman, A. (2014). Design and Development of a Compact and Lightweight Oil Pan for High Performance Vehicle Applications. *SAE Technical Paper Series*. doi: 10.4271/2014-01-1640
- Osman, A., Hussin, M. A., & Abidin, S. F. (2015). Testing and Development of an Enhanced and Cost Effective Engine Split Cooling Circuit. *SAE Technical Paper Series*. doi:10.4271/2015-01-1650
- Osman, A., Yusof, M. K., & Rafi, M. (2016). Vehicle Testing and Development Involving a Simplified Split Cooling with Integrated Exhaust Heat Recovery and Reuse. *SAE Technical Paper Series*. doi:10.4271/2016-01-0647
- Osman, A., Razali, R. M., & Nurdin, N. (2018). Powertrain Warm-Up Optimization Involving Simplified Split Cooling with Integrated Exhaust Heat Recovery and Reuse. *SAE Technical Paper Series*. doi:10.4271/2018-01-0086
- Pang, H. H., & Brace, C. J. (2004). Review of engine cooling technologies for modern engines. *Proceedings of the Institution of Mechanical Engineers, Part D: Journal of Automobile Engineering*, 218(11), 1209-1215. doi:10.1243/0954407042580110
- Park, M., Jung, D., Kim, M., & Min, K. (2013). Study on the improvement in continuously variable transmission efficiency with a thermal management system. *Applied Thermal Engineering*, 61(2), 11-19. doi:10.1016/j.applthermaleng.2013.07.032
- Qasemian, A. & Keshavarz, A. (2016). Experimental and numerical study of an internal combustion engine coolant flow distribution. *Tehnicki Vjesnik - Technical Gazette*, 23(1). doi: 10.17559/tv-20150124180113
- Quaiyum, M.A., (2012). Experimental investigation of automatic transmission fluid (ATF) in an air cooled mini channel heat exchanger, Master of Science thesis, University of Windsor
- Quoilin, S., Declaye, S., Tchanche, B. F., & Lemort, V. (2011). Thermo-economic optimization of waste heat recovery Organic Rankine Cycles. *Applied Thermal Engineering*, 31(14-15), 2885–2893. doi: 10.1016/j.applthermaleng.2011.05.014

- Roberts, A., Brooks, R., & Shipway, P. (2014). Internal combustion engine cold-start efficiency: A review of the problem, causes and potential solutions. *Energy Conversion and Management*, 82, 327-350. doi:10.1016/j.enconman.2014.03.002
- Robinson K. (2001). IC engine coolant heat transfer studies. *PhD Thesis, Department of Mechanical Engineering, University of Bath, Bath, UK.*
- Saidur, R., Rezaei, M., Muzammil, W., Hassan, M., Paria, S., & Hasanuzzaman, M. (2012). Technologies to recover exhaust heat from internal combustion engines. *Renewable and Sustainable Energy Reviews*, 16(8), 5649–5659. doi: 10.1016/j.rser.2012.05.018
- Talom, H. L., & Beyene, A. (2009). Heat recovery from automotive engine. *Applied Thermal Engineering*, 29(2-3), 439-444. doi:10.1016/j.applthermaleng.2008.03.021
- Torregrosa, A. J., Broatch, A., Olmeda, P., & Romero, C. (2008). Assessment of the influence of different cooling system configurations on engine warm-up, emissions and fuel consumption. *International Journal of Automotive Technology*, 9(4), 447–458. doi: 10.1007/s12239-008-0054-1
- Verem, A. (2016). Physically Based Models for Predicting Exhaust Temperatures in SI Engine, Master of science thesis, Linkoping
- Vittorini, D., Battista, D. D., & Cipollone, R. (2018). Engine oil warm-up through heat recovery on exhaust gases – Emissions reduction assessment during homologation cycles. *Thermal Science and Engineering Progress*, 5, 412–421. doi: 10.1016/j.tsep.2018.01.010
- Wang, T., Zhang, Y., Zhang, J., Shu, G., & Peng, Z. (2013). Analysis of recoverable exhaust energy from a light-duty gasoline engine. *Applied Thermal Engineering*, 53(2), 414–419. doi: 10.1016/j.applthermaleng.2012.03.025
- Will, F., & Boretti, A. (2011). A New Method to Warm Up Lubricating Oil to Improve the Fuel Efficiency During Cold Start. *SAE International Journal of Engines*, 4(1), 175–187. doi: 10.4271/2011-01-0318
- Wrenick, S., Sutor, P., Pangilinan, H., & Schwarz, E. E. (2005). Heat Transfer Properties of Engine Oils. *World Tribology Congress III, Volume 1*. doi: 10.1115/wtc2005-64316

## LIST OF PUBLICATIONS AND PAPERS PRESENTED

i. Journal paper

**Osman, A., Zulkifli, N., Said, M. A., & Tuan Kamaruddin, T. N. A.** (2021). Experimental study on recoverable thermal energy from low thermal inertia exhaust heat recovery unit. *Advances in Mechanical Engineering*, 13(6), 168781402110260. <https://doi.org/10.1177/16878140211026069>. (ISI indexed)

ii. Paper presented

**Osman, A.**, (2019, 8-9 May). Recent progress in simplified split cooling with integrated exhaust heat recovery and reuse. Keynote speaker at International Conference on Turbocharger and Turbocharging Asia Pacific organised by Institution of Mechanical Engineers, UK. Parkroyal, Singapore.